BioMed Research International

Advances in Confocal Microscopy of the Eye

Guest Editors: Paolo Fogagnolo, Michele Iester, Hong Liang, and Dipika V. Patel

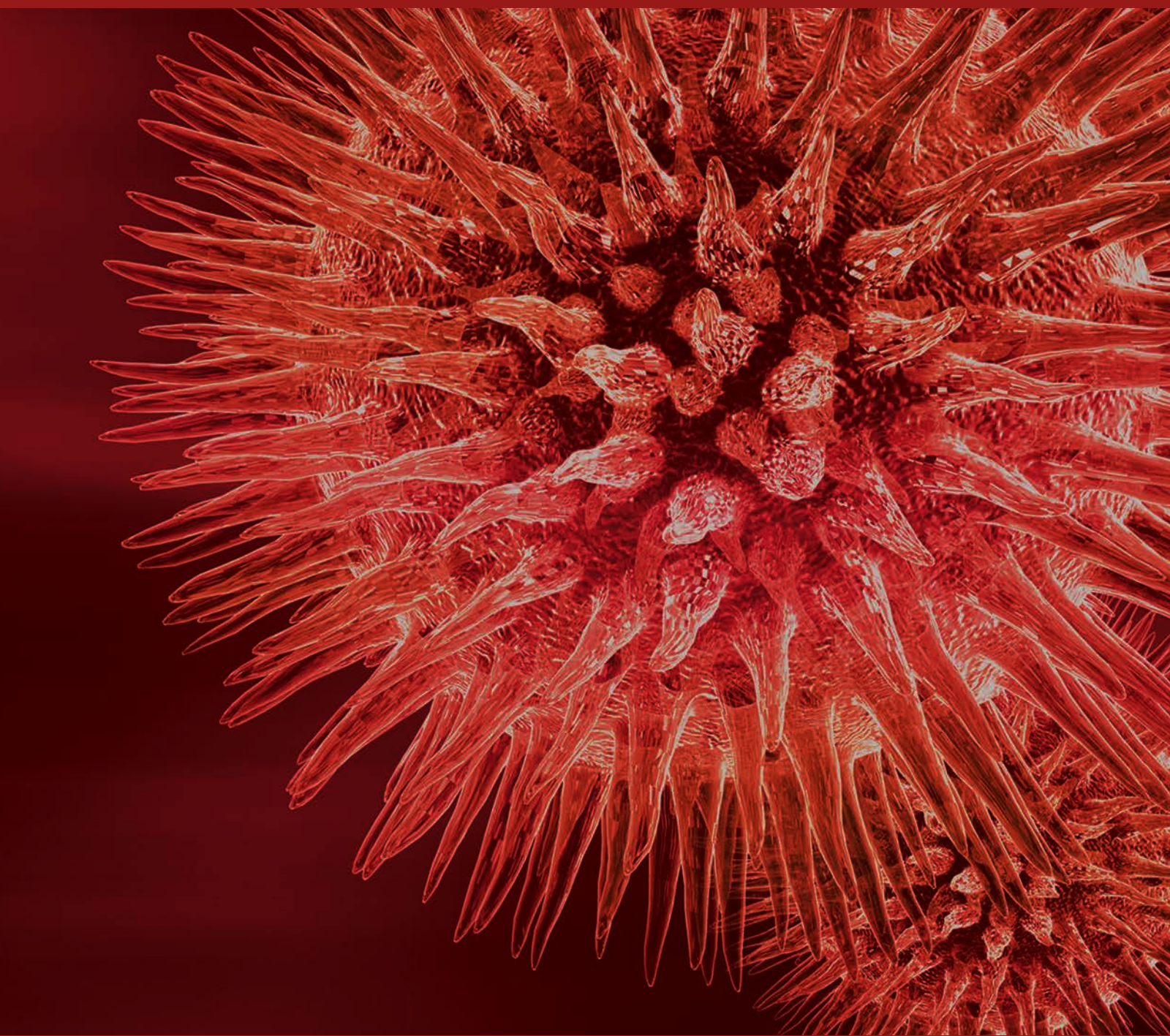

Advances in Confocal Microscopy of the Eye

BioMed Research International

Advances in Confocal Microscopy of the Eye

Guest Editors: Paolo Fogagnolo, Michele Iester, Hong Liang, and Dipika V. Patel

Contents

Hindawi Publishing Corporation
BioMed Research International
Volume 2016, Article ID 1794240, 2 pages
http://dx.doi.org/10.1155/2016/1794240

Editorial

Advances in Confocal Microscopy of the Eye

Paolo Fogagnolo,[1] Michele Iester,[2] Hong Liang,[3] and Dipika V. Patel[4]

[1]*Eye Clinic, Ospedale San Paolo, Dipartimento Testa-Collo, Università degli Studi, Milan, Italy*
[2]*Anatomical-Clinical Laboratory for Functional Diagnosis and Treatment of Glaucoma and Neuroophthalmology, Eye Clinic, DiNOGMI, University of Genoa, Genoa, Italy*
[3]*Department of Ophthalmology III, Quinze-Vingts National Ophthalmology Hospital, Paris, France*
[4]*Department of Ophthalmology, New Zealand National Eye Centre, Faculty of Medical and Health Sciences, University of Auckland, Auckland, New Zealand*

Correspondence should be addressed to Paolo Fogagnolo; fogagnolopaolo@googlemail.com

Received 6 April 2016; Accepted 6 April 2016

This special issue focuses on the recent advances on *in vivo* confocal microscopy (IVCM), a technique used to investigate eye structures at the cellular level without tissue damage.

In 1985 Lemp and coworkers were the first to study *ex vivo* corneas by confocal microscopy and to suggest a possible *in vivo* use [1]. In the early 1990s, the groups directed by Cavanagh and Kaufman published the first IVCM in humans; thereafter the scientific interest in ocular IVCM rapidly increased. In the last decade, IVCM progressively gained a relevant role in the clinical setting, being of help in the diagnosis and management of a number of conditions such as toxicity induced by preservatives [2, 3] and different eye treatments [4, 5], iatrogenic damage [6], infections [7], and dystrophies [8], pathology of the conjunctiva [9–11] and limbus [12], ocular surface tumors [13], and corneal deposits [14, 15].

IVCM is a valuable tool for enhancing our understanding of anterior segment physiology and pathology, as pointed out by Dr. V. Fasanella et al. in their paper investigating meibomian gland changes occurring with aging and a number of ocular surface diseases.

Examples of the usefulness of IVCM in detecting early corneal changes can be found in the paper by Dr. D. Wang et al., who highlighted that a higher-than-normal immune activity may be observed in a subgroup of patients with clear corneal grafts in the absence of any other clinical signs. Dr. P. Song et al. studied the confocal and histopathological features of the stromal scar in keratoconus and suggested that IVCM is capable of detecting subtle keratocyte activation associated with fibrosis.

In recent years, IVCM has become increasingly useful in evaluating corneal innervation (which is of key importance in regulating ocular surface homeostasis) [16] and corneal immune and inflammatory responses [17]. In this special issue, three papers explored the changes occurring in corneal innervation in both local and systemic diseases. The paper by Dr. E. F. Wang et al. reviewed the impact of various systemic diseases on corneal innervation and discussed the potential use of IVCM as a noninvasive marker of peripheral neuropathy. The reports by Dr. R. Shetty et al. and Dr. N. K. Pahuja et al. investigated nerve changes occurring, respectively, in dry eye disease and keratoconus.

Finally, IVCM plays a role in studying the therapeutic effects of topical eye treatments, as shown in this issue by the paper of Dr. A. M. Fea et al.

This special issue provides a useful update on the advances in the rapidly evolving field of IVCM and highlights the contribution of this technology to our understanding of the anterior segment in health and disease.

Paolo Fogagnolo
Michele Iester
Hong Liang
Dipika V. Patel

References

[1] M. A. Lemp, P. N. Dilly, and A. Boyde, "Tandem-scanning (confocal) microscopy of the full-thickness cornea," *Cornea*, vol. 4, no. 4, pp. 205–209, 1985.

[2] M. Iester, F. Oddone, P. Fogagnolo, P. Frezzotti, and M. Figus, "Changes in the morphological and functional patterns of the ocular surface in patients treated with prostaglandin analogues after the use of TSP 0.5%® preservative-free eyedrops: a prospective, multicenter study," *Ophthalmic Research*, vol. 51, no. 3, pp. 146–152, 2014.

[3] M. Iester, S. Telani, P. Frezzotti et al., "Ocular surface changes in glaucomatous patients treated with and without preservatives beta-blockers," *Journal of Ocular Pharmacology and Therapeutics*, vol. 30, no. 6, pp. 476–481, 2014.

[4] P. Fogagnolo, A. Dipinto, E. Vanzulli et al., "A 1-year randomized study of the clinical and confocal effects of tafluprost and latanoprost in newly diagnosed glaucoma patients," *Advances in Therapy*, vol. 32, no. 4, pp. 356–369, 2015.

[5] P. Fogagnolo, M. Sacchi, G. Ceresara et al., "The effects of topical coenzyme Q10 and vitamin e d-α-tocopheryl polyethylene glycol 1000 succinate after cataract surgery: a clinical and in vivo confocal study," *Ophthalmologica*, vol. 229, no. 1, pp. 26–31, 2013.

[6] S. De Cillà, P. Fogagnolo, M. Sacchi et al., "Corneal involvement in uneventful cataract surgery: an in vivo confocal microscopy study," *Ophthalmologica*, vol. 231, no. 2, pp. 103–110, 2014.

[7] M. Randon, H. Liang, M. El Hamdaoui et al., "In vivo confocal microscopy as a novel and reliable tool for the diagnosis of Demodex eyelid infestation," *British Journal of Ophthalmology*, vol. 99, no. 3, pp. 336–341, 2015.

[8] D. V. Patel, C. N. Grupcheva, and C. N. J. McGhee, "Imaging the microstructural abnormalities of Meesmann corneal dystrophy by in vivo confocal microscopy," *Cornea*, vol. 24, no. 6, pp. 669–673, 2005.

[9] P. Frezzotti, P. Fogagnolo, G. Haka et al., "In vivo confocal microscopy of conjunctiva in preservative-free timolol 0.1% gel formulation therapy for glaucoma," *Acta Ophthalmologica*, vol. 92, no. 2, pp. e133–e140, 2014.

[10] A. Labbé, B. Dupas, P. Hamard, and C. Baudouin, "In vivo confocal microscopy study of blebs after filtering surgery," *Ophthalmology*, vol. 112, no. 11, article 1979, 2005.

[11] A. Labbé, L. Gheck, V. Iordanidou, C. Mehanna, F. Brignole-Baudouin, and C. Baudouin, "An in vivo confocal microscopy and impression cytology evaluation of pterygium activity," *Cornea*, vol. 29, no. 4, pp. 392–399, 2010.

[12] D. V. Patel, T. Sherwin, and C. N. J. McGhee, "Laser scanning in vivo confocal microscopy of the normal human corneoscleral limbus," *Investigative Ophthalmology and Visual Science*, vol. 47, no. 7, pp. 2823–2827, 2006.

[13] E. E. Gabison, A. Labbé, F. Brignole-Baudouin et al., "Confocal biomicroscopy of corneal intraepithelial neoplasia regression following interferon alpha 2b treatment," *British Journal of Ophthalmology*, vol. 94, no. 1, pp. 134–135, 2010.

[14] G. Ceresara, P. Fogagnolo, S. De Cillà et al., "Corneal involvement in crohn's disease: an in vivo confocal microscopy study," *Cornea*, vol. 30, no. 2, pp. 136–142, 2011.

[15] G. Ceresara, P. Fogagnolo, M. Zuin, S. Zatelli, J. Bovet, and L. Rossetti, "Study of corneal copper deposits in wilson's disease by in vivo confocal microscopy," *Ophthalmologica*, vol. 231, no. 3, pp. 147–152, 2014.

[16] S. Allgeier, A. Zhivov, F. Eberle et al., "Image reconstruction of the subbasal nerve plexus with in vivo confocal microscopy," *Investigative Ophthalmology & Visual Science*, vol. 52, no. 9, pp. 5022–5028, 2011.

[17] W. J. Mayer, M. J. Mackert, N. Kranebitter et al., "Distribution of antigen presenting cells in the human cornea: correlation of in vivo confocal microscopy and immunohistochemistry in different pathologic entities," *Current Eye Research*, vol. 37, no. 11, pp. 1012–1018, 2012.

Hindawi Publishing Corporation
BioMed Research International
Volume 2016, Article ID 8406832, 10 pages
http://dx.doi.org/10.1155/2016/8406832

Research Article

The Effect of Autologous Platelet Lysate Eye Drops: An In Vivo Confocal Microscopy Study

Antonio M. Fea,[1] Vittoria Aragno,[1] Valeria Testa,[1] Federica Machetta,[1] Simone Parisi,[2] Sergio D'Antico,[3] Roberta Spinetta,[1] Enrico Fusaro,[2] and Federico M. Grignolo[1]

[1]*Department of Clinical Sciences, Ophthalmology Institute, University of Turin, 10122 Turin, Italy*
[2]*Rheumatology Department, AOU Città della Salute e della Scienza di Torino, 10134 Turin, Italy*
[3]*Blood Bank, AOU Città della Salute e della Scienza di Torino, 10134 Turin, Italy*

Correspondence should be addressed to Vittoria Aragno; vittoria.aragno@hotmail.it

Received 13 November 2015; Revised 7 March 2016; Accepted 29 March 2016

Academic Editor: Hong Liang

Purpose. To determine the effectiveness of autologous platelet lysate (APL) eye drops in patients with primary Sjögren syndrome (SS) dry eye, refractory to standard therapy, in comparison with patients treated with artificial tears. We focused on the effect of APL on cornea morphology with the in vivo confocal microscopy (IVCM). *Methods.* Patients were assigned to two groups: group A used autologous platelet lysate QID, and group B used preservative-free artificial tears QID, for 90 days. Ophthalmological assessments included ocular surface disease index (OSDI), best corrected visual acuity (BCVA), Schirmer test, fluorescein score, and breakup time (BUT). A subgroup of patients in group A underwent IVCM: corneal basal epithelium, subbasal nerves, Langerhans cells, anterior stroma activated keratocytes, and reflectivity were evaluated. *Results.* 60 eyes of 30 patients were enrolled; in group A ($n = 20$ patients) mean OSDI, fluorescein score, and BUT showed significant improvement compared with group B ($n = 10$ patients). The IVCM showed a significant increase in basal epithelium cells density and subbasal nerve plexus density and number and a decrease in Langerhans cells density ($p < 0.05$). *Conclusion.* APL was found effective in the treatment of SS dry eye. IVCM seems to be a useful tool to visualize cornea morphologic modifications.

1. Introduction

Sjögren syndrome (SS) is a chronic multisystem autoimmune disease characterized by hypofunction of salivary and lacrimal glands [1]. The pathogenesis of the dysfunction is due to a T-lymphocyte mediated destruction of the exocrine glands [2].

The result of the immune-mediate infiltration of the lacrimal gland is the development of a severe dry eye syndrome (DES).

The mainstay of conventional therapy for dry eye is the application of preservative-free artificial eye drops, which provide lubrication of the surface of the eye. Based on the concept that inflammation has a key role in the pathogenesis of dry eye, different treatment options, such as corticosteroids and cyclosporine, are used as a second-line treatment in more severe dry eye [3, 4].

However, none of the commercially available artificial tear preparations and anti-inflammatory topical treatment have the properties of the human tears. They do not contain growth factors (GFs), such as transforming growth factor β (TGF-β), and other components, including vitamin A, fibronectin, and other cytokines, which are necessary for the maintenance of normal corneal epithelium [5]. In particular, GFs stimulate tissue healing by inducing mesenchymal and epithelial cells migration and proliferation in case of ocular surface damage [6].

Since some of these components are found in serum, and its composition is very similar to natural tears, the autologous serum (AS) has been used since 1984 [7] as a second-line therapy for dry eye. Nevertheless, its potential benefits have been questioned by a recent meta-analysis [8].

Platelet alfa granules are a major source of GFs and are rich in platelet derived growth factor (PDGF), which

plays an important role in the maintenance of ocular surface and tear film stability. PDGF promotes the chemotaxis of fibroblasts, monocytes, and macrophages and stimulates the expression of TGF-β that inhibits metalloproteases and decreases inflammation [9]. These findings prompted the use of platelet rich plasma (PRP), platelet rich plasma in growth factors (PRGF), and autologous plasma rich in PDGFs eye drops (PRGD); indeed, recent studies on PRP [10], PRGF [11], and PRGD [12] have reported an improvement in both the objective and subjective outcomes in DES patients.

The use of in vivo confocal microscopy (IVCM) offers a completely new approach in the study of the ocular surface, with a noninvasive high resolution analysis [13, 14] that allows both a quantitative histopathological assessment of cornea damage and a qualitative evaluation of cellular and nerve properties [15–17].

IVCM has been used to analyze the morphology of cornea in DES and to study its relationship with the clinical evaluation. The morphological abnormalities that appear in patients with SS were first demonstrated in 2003 by Tuominen et al. [18] and then confirmed by other authors [19, 20]. A patchy corneal epithelium, an activation of anterior keratocytes, and an abnormal subbasal nerve plexus have been described. Some studies reported that these abnormalities are reversible by a topical treatment with hemocomponents that are able to restore epithelial integrity [21, 22].

In this study, we evaluated the efficacy of autologous platelet lysate (APL) eye drops in patients with primary SS refractory dry eye in comparison to artificial free preservatives tears. We focused on the histological effect that APL could have on corneal morphological modifications with a layer-by- layer analysis of the corneal ultrastructure in a sample of patients treated with APL.

2. Methods

This prospective case-control study was conducted from July 2014 to May 2015 at the University Eye Clinic of Turin. The study was conducted in accordance with the Declaration of Helsinki (1964) and approved by our Ethics Committee.

2.1. Patients Selection. We included patients with a diagnosis of SS according to the classification criteria of the American-European Consensus [1], a dry eye severity level ≥2 (Dry Eye Severity Grading Scheme, Workshop 2007), an ocular surface disease index (OSDI) ≥23, and a corneal fluorescein staining score ≥1 on Oxford scale. All patients were refractory for more than 2 months to previous conventional therapy (artificial tears, steroids, cyclosporine A, or autologous serum).

We excluded patients with ocular infections, previous corneal surgery (refractive surgery or corneal transplantation), positive tests for HBV, HCV, HIV, and fever, or sepsis. Platelet count had to be higher than $100 \times 10^3/\mu$L and Hb >10 g/dL.

Patients were enrolled and assigned to two groups, according to the randomization criteria 2 : 1. Group A patients were treated with eye drops and group B with preservative-free artificial tears (0.2% hyaluronic acid and TS-polysaccharide 0.2%). Both groups were treated for 90 days, 1 drop 4 QID.

Both eyes were examined in all subjects, and, for statistical analysis, both eyes were selected if responding to inclusion criteria and separately analyzed.

2.2. Autologous Platelet Lysate Eye Drops Preparation. The withdrawal and the APL eye drops preparation were conducted at the Blood Bank, AOU Città della Salute e della Scienza di Torino. A volume of 250 to 350 mL of venous peripheral blood was sampled from each patient, depending on platelet count, Hb value, total blood volume, and clinical condition; the autologous packed red blood cells separated from whole blood could be reinfused in patients having mild anemia (Hb < 11 g/dL). CompoFlow® T & B Fresenius Kabi bags, containing CPD anticoagulant, were used for the collection of blood. The blood was left for 60 min at room temperature and then centrifuged at 1580 rpm × 8 minutes (centrifuge Cryofuge 6000i) to obtain the PRP (platelet rich plasma) that underwent a second centrifugation (4000 rpm × 8 min). The PPP (platelet poor plasma) supernatant was partially removed to obtain a platelet concentration of $1.000 \times 10^3/\mu$L ± 10%. PRP was left at room temperature for 30 minutes, and then it was diluted by addition of 0.9% NaCl saline solution until a final concentration of 50% and platelets were lysed by three consecutive thermal shocks. Platelet lysate (PL) was centrifuged (4000 rpm × 8 min) and the supernatant PL was poured into a collection bag. The bag was connected to a COL.C30 (Biomed Device) kit and then aliquoted into 30 sterile vials (following Biomed Device instructions) and kept frozen at −80°C. A sample of the final preparation was used for bacterial culture (BacT/ALERT®) that had to be negative before the delivery to the patient.

Patients were instructed to keep APL frozen, to thaw the single daily dose the night before, and to store it at 4°C during the day. Thirty single doses of platelet lysate were delivered to group A subjects every 30 days. The schedule of use was two drops QID for 90 days.

2.3. Ophthalmological Assessment. Before and after 90 days of therapy, patients underwent an ophthalmologic assessment comprehensive of subjective symptoms evaluation by ocular surface disease index (OSDI), Schirmer test type I, breakup time (BUT), and corneal fluorescein staining (Oxford scale). Moreover, best corrected visual acuity (BCVA) was evaluated in Snellen lines and eyelid malposition or squamous metaplasia as well as anterior and posterior blepharitis (Efron Scale) [23], conjunctival folds (LIPCOF) [24], and Ocular Protection Index (OPI) were checked. Patients were then classified according to the Dry Eye Severity Grading Scheme and only those with grade ≥2 were enrolled in the study.

Patient's examination was always conducted by the same observer (AV).

In case of suspected conjunctivitis, the treatment was suspended and a microbial culture was performed to prescribe an appropriate local therapy, and patients took on again their original treatment after resolution.

2.4. In Vivo Corneal Confocal Microscopy Assessment. In vivo confocal microscopy was performed before and after 90 days of therapy with APL, on a sample of patients (subgroup 2)

randomized from subjects treated with APL (group A), with Heidelberg Retina Tomograph (HRT II) in combination with Rostock Cornea Module (RCM, 63x/0.9 W. 670 nm, ∞/0; Zeiss, Jena, Germany) and CCD camera.

The microscopy was performed on both eyes of each patient after a topical instillation of anesthetic (0.4% oxybuprocaine hydrochloride). A drop of an ophthalmic gel (2.0 g hydroxypropyl methylcellulose) was applied on the ocular surface, as coupling medium, to improve the adhesion of the contact cap objective to the cornea. Proper alignment and positioning of the head were maintained with the help of a dedicated target mobile red fixation light for the contralateral eye.

After the exam, the integrity of the corneal surface was controlled at the slit lamp and patients were medicated with antibiotic eye drops (tobramycin ophthalmic solution 0.3%).

We examined the central corneal areas, where images of intermediate and deep epithelial layers and anterior stroma were acquired and analyzed.

Patient's examination was always conducted by the same observer (TV).

All images were reviewed, and three well-focused micrographs for each corneal scan were manually selected. The micrographs were assessed in a masked way by one observer; the mean value of series of three readings was recorded for each parameter.

Evaluated parameters included the following:

(i) Basal epithelium cell density (cells/mm^2): basal epithelial layer was considered 10 μm above the membrane of Bowman. The counting was carried out within a region of interest of standardized size (region of interest [ROI] = 100 × 100 μm) using the manual cell counting system offered with the software. The system automatically calculated the density by the function "cell count."

(ii) Number of subbasal nerve fibers (between Bowman's membrane and the basal layer of epithelial, where nerve fibers run parallel to the corneal surface): it is defined as the sum of nerve branches in each frame; images with the greatest number of visible nerve fibers were chosen for each series of acquisitions. Only fibers longer than 50 μm were considered and counted as a separated branch.

(iii) Nerve fiber density (μm/160000 μm^2): it is defined as the sum of nerve fibers length (>50 μm), considered in the area of 400 × 400 μm (0.1589 mm^2, defined as the widest area possible); it was performed using the function MEASUREMENTS > J GROUP MEASUREMENTS of NeuronJ, plugin software ImageJ (available at http://rsb.info.nih.gov/ij/) (Figure 1).

(iv) Activated keratocytes density of the anterior stroma (number of activated keratocytes/mm^2): number of activated keratocytes in the stroma of the Central Front is defined as hyperreflective and with cytoplasm extensions, 20 μm under the Bowman layer. The counting was carried out using the manual cell counting system offered with the software in the region of interest (ROI) of 400 × 400 μm (0.1589 mm^2, defined as the widest area possible).

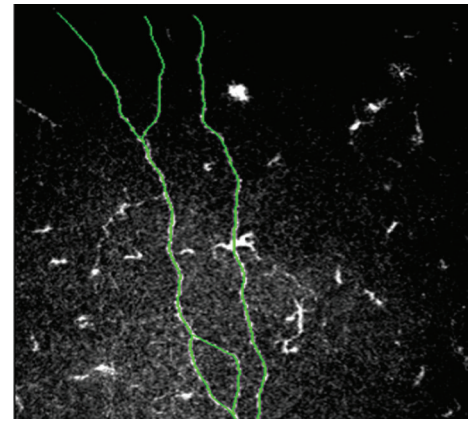

Figure 1: An example of neuron tracing with NeuronJ software. The plugin facilitates the tracing and quantification of nerves.

(v) Anterior stroma mean gray value: it is expressed with a value referred to as gray scale from 0 (black) to 255 (white) in Optical Units (OU), in relation to the anterior stroma reflectivity, with ImageJ software [25].

(vi) Langerhans cells (LCs) density (LCs/mm^2): dendritic cells number was manually counted in each corneal section at the level of subbasal nerves, selecting the images in which there was a greater density of LCs. The counting was carried out using the manual cell counting system offered with the software in the region of interest (ROI) of 400 × 400 μm (0.1589 mm^2, defined as the widest area possible).

2.5. Statistical Analysis. Descriptive statistics were produced for demographic, clinical, and laboratory variables. Mean and standard deviation were calculated for quantitative variables normally distributed; median and IQR were presented for not normally distributed quantitative variables and ordinal variables. Categorical variables were presented with frequencies and percentages.

A sample size of 50 eyes was calculated to detect a difference in OSDI between interventions of 50%, defining significance level of 0.05 and power of 70%.

The Wilcoxon test ($k = 2$) was used for quantitative continuous variables and for ordinal variables in order to assess statistically significant changes from the baseline. The nonparametric Mann-Whitney U test was chosen to compare the continuous quantitative variables and ordinal variables between the two groups; Fisher's exact test was used to compare the nominal categorical variables where appropriate. Performed tests were bilateral and the level of significance was set at 5%. The data were analyzed using the statistical software R.

3. Results

From July 2014 to May 2015, we enrolled 30 patients (mean age 59.5 ± 12.2 years) with primary Sjögren syndrome

Table 1: Patients characteristics at baseline. Group A = patients assigned to APL; group B = patients assigned to artificial tears.

	Group A	Group B	p value
Female, n (%)	19.0 (95)	10.0 (100.0)	1.00
Age, mean (SD) years	60.4 (11.68)	59.5 (13.34)	0.758
Dry eye, mean (SD) years	7.6 (6.5)	7.5 (6.2)	0.767

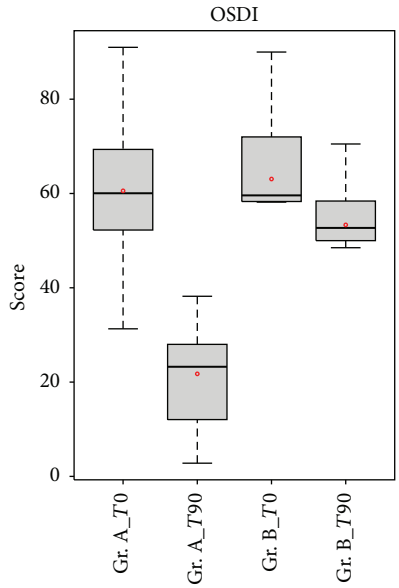

Figure 2: Comparison of OSDI score between patients in group A (APL) and patients in group B (artificial tears). OSDI score was significantly lower in group A patients compared with the group B patients after treatment ($p < 0.05$).

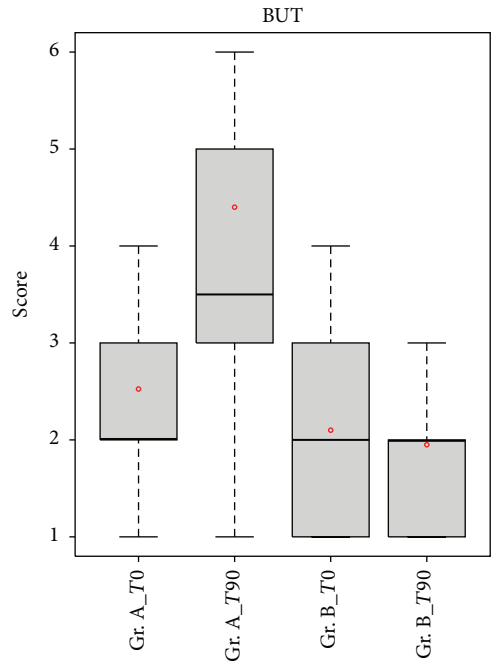

Figure 3: Comparison of BUT values between patients in group A (APL) and patients in group B (artificial tear). BUT increased significantly in group A patients compared with the group B patients after treatment ($p < 0.05$).

(selected from a starting group of 164 patients with primary SS followed up by the Rheumatology Department, the AOU Città della Salute e della Scienza di Torino, Turin). Group A consisted of 20 patients (40 eyes) and group B of 10 patients (20 eyes); demographic characteristics are summarized in Table 1. Dry eye duration was considered from the diagnosis of SS. The groups at baseline did not have significant differences ($p > 0.05$).

3.1. Ophthalmological Assessment. The ophthalmological parameters assessed are reported in Table 2.

None of the subjects presented eyelid abnormalities and squamous metaplasia.

Mean OSDI score statistically decreased in group A from 60, 56 ± 17, and 69 to 21, 75 ± 9, and 86 after 90 days with APL therapy (Δ = 38, 82, p value = 0.00438). In group B, it slightly decreased from 60, 67 ± 16, and 19 to 53, 60 ± 14, and 91 (Δ = 7, 07). The differences between the two groups after 90 days were statistically significant (p value = $1.007e-05$) (Figure 2).

Schirmer test values did not change significantly after 90 days of treatment between the two groups (p value: 0.544); however, in group A, there was an increase in BUT value after treatment, compared to group B (p value < 0.001) (Figure 3).

Concerning the fluorescein score, the differences in the mean ocular surface staining scores between the two groups after treatment were statistically significant ($p < 0.05$). After 90 days of treatment, 80% of the examined eyes showed an Oxford score ≤1 (Figure 4).

The OPI value was significantly higher at the end of the treatment in group A compared to group B ($p < 0.05$) and a significant decrease in the mean values of posterior blepharitis ($p < 0.05$) was observed in group A compared to group B.

The BCVA significantly increased after 90 days in group A, but the improvement is not statistically significant in comparison with the treatment of group B (p value = 0.100).

3.2. In Vivo Confocal Microscopy. In vivo confocal microscopy was performed at baseline and after 90 days of treatment on 10 patients of group A (20 eyes analyzed); this subgroup (subgroup 2) was randomized from group A. Excluded patients are defined as subgroup 1. Table 3 shows that there are not statistically significant differences between the two subgroups at baseline.

After treatment, a statistically significant increase in basal epithelium cells density (p value = 0.005) was detected; moreover, an increase in number of subbasal nerve fibers (p value = 0.005) as well as an increase in the density of innervation (p value = 0.003) was found (Figure 5).

The assessment of gray value of the anterior stroma did not show any statistically significant changes after 90 days of treatment (p value = 0.222), and no differences were found in activated keratocytes density at the end of the treatment period (p value = 0.976).

Table 2: Ophthalmological assessment.

		Group A	Group B	p value Gr. A versus Gr. B
		OSDI		
$T0$	Media (SD)	60.56 (17.69)	60.67 (16.19)	0.821
$T90$	Media (SD)	21.75 (9.86)	53.60 (14.91)	<0.001*
p value		0.000438*	0.059336	
		Fluorescein score (0–5)		
$T0$	Median (IQR)	2 (2)	3 (2.5)	0.17
$T90$	Median (IQR)	1 (2)	3 (2)	<0.001*
p value		<0.001*	0.463	
		FBUT (sec)		
$T0$	Median (IQR)	2 (1)	2 (2)	0.18
$T90$	Median (IQR)	3.5 (2)	2 (1)	<0.001*
p value		0.005*	0.463	
		BCVA		
$T0$	Median (IQR)	8 (4)	6 (3.5)	0.218
$T90$	Median (IQR)	8 (3.5)	6 (3.5)	0.100
p value		0.008*	0.317	
		Schirmer test (mm)		
$T0$	Median (IQR)	3 (2)	3 (2)	0.989
$T90$	Median (IQR)	3 (1)	3 (0.5)	0.544
p value		0.0611	0.328065	
		Anterior blepharitis (grades 0–4)		
$T0$	Median (IQR)	1 (1)	2 (1.5)	0.092
$T90$	Median (IQR)	1 (0.5)	2 (1.5)	0.778
p value		0.055	0.109	
		Posterior blepharitis (grades 0–4)		
$T0$	Median (IQR)	1 (1)	1.5 (1)	0.748
$T90$	Median (IQR)	1 (1)	1.5 (1.5)	0.036*
p value		0.011*	0.310	
		Lipcof (grades 0–3)		
$T0$	Median (IQR)	3 (2)	3 (1)	0.419
$T90$	Median (IQR)	3 (2)	3 (1)	0.994
p value		1.000	1.000	
		OPI (>/<1)		
$T0$	Median (IQR)	0.29	0.23	0.778
$T90$	Median (IQR)	0.53	0.25	<0.001
p value		<0.001*	0.245	

$T0$ = time 0; $T90$ = time 90 days; SD = standard deviation; IQR = interquartile range; OSDI = ocular surface disease index; OPI = ocular protection index; FBUT = breakup time; BCVA = best corrected visual acuity.
*Statistically significant results.

Table 3: Basal characteristics of subgroup 1 (nonevaluated by IVCM) and subgroup 2 (evaluated by IVCM).

		Subgroup 1	Subgroup 2	p value
Age	Media (SD)	63.67 (8.73)	57.6 (11.76)	0.692
Sex	Female : male (%)	9 : 10 (90)	10 : 0 (100)	1.000
OSDI	Media (SD)	63.73 (21.74)	56.07 (19.3)	0.397
Fluorescein score	Median (IQR)	2 (1)	1.5 (1.5)	0.744
BUT	Median (IQR)	2 (1.5)	3 (1)	0.287
Schirmer test	Median (IQR)	3 (1)	4 (1)	0.055

Table 4: Confocal microscopy assessments, subgroup 2.

	*T*0	*T*90	*p* value
Basal epithelial cell density (cell/mm^2)			
Media	5810.52	6680.16	0.005*
SD	859.78	739.91	
Nerve number (*n*/frame)			
Media	5.11	7.72	0.005*
SD	2.60	3.62	
Nerve density (μm/frame)			
Median	1070.25	1655.0	0.003*
IQR	906.46	1631.67	
Gray value anterior stroma (OU)			
Median	50.33	52.00	0.222
IQR	11	5.65	
Activated keratocyte (cell/mm^2)			
Media	42.04	39.08	0.976
SD	20.72	20.64	
Langerhans cells (cell/mm^2)			
Median	34.50	31.33	0.024*
IQR	127.33	93.34	

*Statistically significant results.

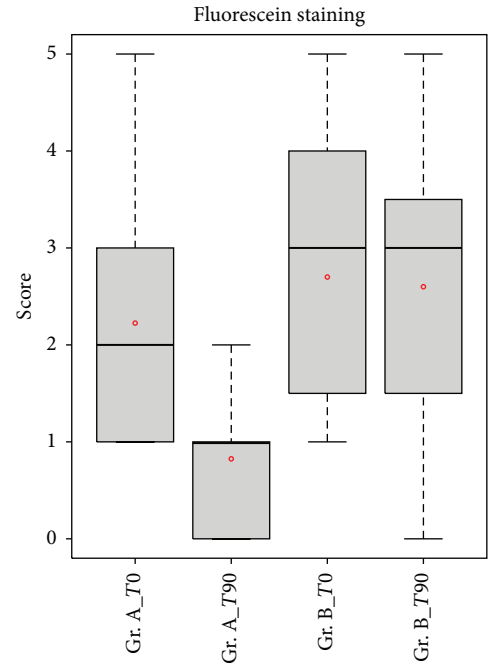

Figure 4: Comparison of fluorescein score between patients in group A (APL) and patients in group B (artificial tear). Fluorescein score was significantly lower in group A patients compared with the group B patients after treatment ($p < 0.05$).

Finally, a statistically significant decrease of Langerhans cell density (p value = 0.024) was detected. These results are presented in Table 4.

4. Discussion

Although there has been a relevant increase in knowledge regarding pathophysiology and therapeutic strategies of dry eye, severe dry eye constitutes a major management challenge. In fact, there is a large cohort of severe dry eye patients having persistent signs and symptoms despite maximal conventional therapies.

The critical role of inflammation in the pathogenesis of dry eye has suggested treatment options other than artificial tears. Topical administration of corticosteroids has been reported to improve signs and symptoms in patients with KCS [26], but these treatments cannot be used as long-term therapy and need careful monitoring, due to steroid-related complications (increased intraocular pressure and cataract). Clinical trials have shown topical cyclosporine to be effective in patients with moderate to severe dry eye, because of its ability to decrease inflammation and increase goblet cells density [27–29]. However, topical cyclosporine is correlated with several side effects, such as intolerable irritation, limiting its use [30].

It has been demonstrated that a reduction in epitheliotropic factors can lead to a loss of epithelial integrity and a delay in healing process; since standard therapy for DES such as artificial tears, corticosteroid, and cyclosporine is not able to restore the natural composition in GF of human tears, the use of hemoderivatives has gained popularity.

The autologous serum therapy is worldwide accepted [31–33], but the practicalities and published evidence were recently reviewed with the evidence that the use of AS was not associated with effects based on objective measurements. This result could be due to the presence of a high level of proinflammatory cytokine in the serum [34].

Based on the concept that platelet α granules are a major source of GFs, the research interest has moved to platelet-enriched plasma [9, 35]. Vitamin A, Endothelial Growth Factor (EGF), fibronectin, TGF-β, and nerve growth factor (NGF) are necessary for maintaining the integrity of conjunctival and corneal integrity and it has been demonstrated that LPA is rich in these GFs. A critical role seems to be played by TGF-β, in relation to the balance T regulatory (Treg)/Thelper 17 (Th17). TGF-β is a pleiotropic cytokine that can have pro- or anti-inflammatory effects depending on the context. It has been demonstrated that the correct Treg/Th17 ratio normally contributes to the maintenance of immune tolerance. Inflammatory interleukins, such as IL-6 or IL-27, can alter the balance in favor of Th17, promoting the production of interleukin-17 (IL-17) [36]. TGF-β, in appropriate concentrations, inhibits the priming of Th17, converting the naive T cell in Treg suppressor [37, 38].

Uncontrolled clinical studies have provided evidence of symptoms decrease and objective parameters improvement, such as impression cytology and BUT, after PRP and APL treatment in different pathologies and with a different posology or timing [10–12].

To our knowledge, this is the first randomized prospective study evaluating the effectiveness of APL. We used the standardized OSDI survey and objective clinical measures to evaluate its efficacy. Moreover, for the first time, we assessed

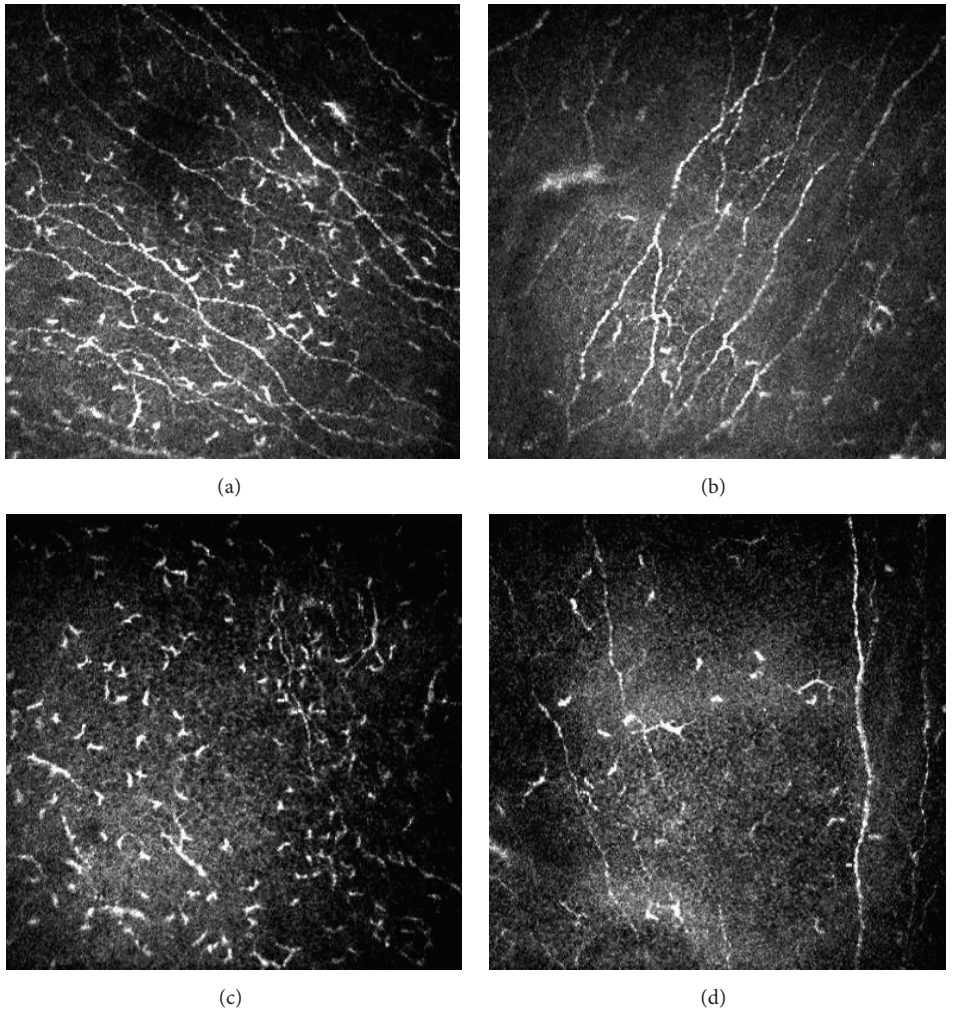

Figure 5: Confocal images of subbasal nerves, in central corneal sectors. At baseline (a–c), many Langerhans cells can be observed at this level; after 3-month-long treatment (b–d), a decreased number of inflammatory cells and an increased number of nerves were found. Figures show the improvement in corneal subbasal nerve plexus for two representative patients treated with APL.

the corneal morphological modifications after APL treatment by IVCM.

In our study, subjects without a satisfactory control of the disease with conventional topical therapy achieved improvement in symptoms after APL treatment. This improvement was significantly higher compared to patients treated with tear substitutes.

FBUT average and, in consequence, the mean value of OPI increased in patients treated with LPA, indicating greater stability and an improvement in quality of the tear film. The corneal staining score improved significantly and after 90 days of treatment 80% of patients showed an Oxford score ≤ 1.

BCVA did not increase significantly compared with group B, but an improvement was found in group A from the baseline. It must be considered that the decrease in visual acuity in these patients is probably due to other causes (conditioning regimen, topical and systemic steroids, and cataract) than tear film instability and therefore not reversible by platelet lysate. It has been demonstrated that the visual acuity measured by Snellen charts is not a good indicator of visual disturbances in patients suffering from dry eye. The Hartmann-Shack aberrometry and the double-pass aberrometry with OQAS (Optical Quality Analysis System) were found to be much more sensitive in quantifying visual disturbances in these patients [39].

Regarding side effects, there was only one reported conjunctivitis case during the treatment with LPA; the patient was temporarily excluded and resumed in group A after appropriate antibiotic therapy. The APL has bacteriostatic factors (β-lysine, lactoferrin, antibodies IgG and IgA, and lysozyme), which make superfluous addition of preservatives; however, all preparations underwent a bacterial culture before delivering.

Previous IVCM studies found morphological abnormalities in SS corneas. They described abnormal epithelial and stromal cells, decreased corneal thickness, and alterations of nerves number, density, and tortuosity as well as increased density of LCs [18, 19, 40–42].

After 3 months of treatment with APL, an increase in cell density of basal layer was found; such finding may be due to the migration of stem cells in division [43], attempting to reepithelize corneal central sectors. We observed complete resolution of corneal epithelial defect in 40% of treated eyes and an improvement in 90% of eyes.

The neuronal morphometric analysis of images captured with IVCM and processed with NeuronJ showed an increased number and density of subbasal nerves after 3 months. This improvement could be due to the direct or indirect action of nerve growth factor (NGF), present in APL. NGF in a neurotrophin has a role in nerve sprouting and damaged neurons restoring. Even if its use has shown encouraging results in few works that state its efficacy in neurite sprouting by neural cells [44–46], the chance that the APL could determine the regeneration of corneal nerves is currently discussed in literature [47]. A number of authors have recently observed that autologous serum is effective in restoring nerve topography through nerve regeneration in patients with corneal neuropathy [21, 22]. Our study showed similar results, but the limited sample and the not comparative nature of the evaluation do not allow more in-depth analyses on factors favoring this response. However, the leading mechanism for the actual nerve regeneration remains to be determined. It is possible that an improvement in epithelial healing, inflammatory response, and tear film changes could have a main role.

It is widely known that Langerhans cells migration is influenced by cytokines and chemokines [48] and that a significant increase of LCs density has been observed in the subbasal nerve plexus in patients with SS [41]. In group A patients, the density of Langerhans cells in central areas of the cornea underwent a significant reduction, suggesting the anti-inflammatory activity of platelet lysate. In support of this evidence, it has been shown that TGF-β, in suitable concentrations, can suppress resident DC maturation [49].

Activated stromal keratocytes density and anterior stroma gray values (Optical Units), which correspond to stromal reflectivity, did not change significantly after the treatment; this finding is probably due to the bioavailability of platelet lysate at this level, which is not known, but it could be reasonably expected to be very low (below 5%).

The main limitation of this study was the absence of evaluation of repeatability for confocal microscopy parameters. In literature, an inter- and intraobserver variance inferior to 5% [25, 50] is reported. Based on this data showing a high repeatability of IVCM, we decided not to undergo this type of analysis in our study.

The quantity of blood extraction required for the APL preparation is clearly higher than the one for AS preparation [51], in order to obtain the desired platelets concentration. However, the blood sample collection was conducted in safe conditions at the Transfusional Center of the Città della Salute e della Scienza by skilled nurses and Hb values were strictly evaluated before and after the procedure to exclude the potential risk of anemia. The blood sample was drawn once at the beginning of the study to increase patient's comfort and compliance. The optimal concentration of growth factors in the APL has not been established yet. The high interpatient variability of growth factor can potentially be responsible for differences in the efficacy of this treatment [12]. However, the preparation of any blood derivate is not standardized and the concentration of growth factors in any blood derivate is not completely clear. As a matter of fact, even the AS has been used in different studies with concentrations ranging from 20 to 100%. The minimal effective concentration of autologous hemoderivatives is still unknown and further studies should be addressed to define this value.

5. Conclusions

In conclusion, this study supports the hypothesis that autologous platelet lysate eye drops are effective on both subjective symptoms and objective findings, in the treatment of significant dry eye, in patients with primary Sjögren syndrome. The IVCM images added objectiveness to the evaluation suggesting that APL could be effective in restoring corneal damage by promoting epithelial and nerve regeneration and decreasing Langerhans cells. Our results encourage the use of morphological evaluations as a useful tool in the diagnosis and management of dry eye.

Additional Points

Protocol number is 00098937, 20/9/2013.

Ethical Approval

Ethics Committee approval date was 15/09/2014.

Competing Interests

The authors declare that they have no competing interests.

References

[1] C. Vitali, S. Bombardieri, R. Jonsson et al., "Classification criteria for Sjögren's syndrome: a revised version of the European criteria proposed by the American-European Consensus Group," *Annals of the Rheumatic Diseases*, vol. 61, no. 6, pp. 554–558, 2002.

[2] T. G. Coursey and C. S. de Paiva, "Managing Sjögren's syndrome and non-Sjögren syndrome dry eye with anti-inflammatory therapy," *Clinical Ophthalmology*, vol. 8, pp. 1447–1458, 2014.

[3] M. Dogru, M. Nakamura, J. Shimazaki, and K. Tsubota, "Changing trends in the treatment of dry-eye disease," *Expert Opinion on Investigational Drugs*, vol. 22, no. 12, pp. 1581–1601, 2013.

[4] T. Subcommittee, "Management and therapy of dry eye disease: report of the Management and Therapy Subcommittee of the International Dry Eye WorkShop (2007)," *The Ocular Surface*, vol. 5, no. 2, pp. 163–178, 2007.

[5] Y. Ohashi, M. Motokura, Y. Kinoshita et al., "Presence of epidermal growth factor in human tears," *Investigative Ophthalmology & Visual Science*, vol. 30, no. 8, pp. 1879–1882, 1989.

[6] V. Freire, N. Andollo, J. Etxebarria, J. A. Durán, and M.-C. Morales, "In vitro effects of three blood derivatives on human corneal epithelial cells," *Investigative Ophthalmology and Visual Science*, vol. 53, no. 9, pp. 5571–5578, 2012.

[7] R. I. Fox, R. Chan, J. B. Michelson, J. B. Belmont, and P. E. Michelson, "Beneficial effect of artificial tears made with autologous serum in patients with keratoconjunctivitis sicca," *Arthritis and Rheumatism*, vol. 27, no. 4, pp. 459–461, 1984.

[8] Q. Pan, A. Angelina, M. Marrone et al., "Autologous serum eye drops for dry eye syndrome," *Cochrane Database of Systematic Reviews*, no. 9, Article ID CD009327, 2011.

[9] E. Anitua, F. Muruzabal, A. Tayebba et al., "Autologous serum and plasma rich in growth factors in ophthalmology: preclinical and clinical studies," *Acta Ophthalmologica*, vol. 93, no. 8, pp. e605–e614, 2015.

[10] J. L. Alio, J. R. Colecha, S. Pastor, A. Rodriguez, and A. Artola, "Symptomatic dry eye treatment with autologous platelet-rich plasma," *Ophthalmic Research*, vol. 39, no. 3, pp. 124–129, 2007.

[11] S. López-Plandolit, M.-C. Morales, V. Freire, A. E. Grau, and J. A. Durán, "Efficacy of plasma rich in growth factors for the treatment of dry eye," *Cornea*, vol. 30, no. 12, pp. 1312–1317, 2011.

[12] S. Pezzotta, C. Del Fante, L. Scudeller, M. Cervio, E. R. Antoniazzi, and C. Perotti, "Autologous platelet lysate for treatment of refractory ocular GVHD," *Bone Marrow Transplantation*, vol. 47, no. 12, pp. 1558–1563, 2012.

[13] B. R. Masters and M. Böhnke, "Confocal microscopy of the human cornea in vivo," *International Ophthalmology*, vol. 23, no. 4–6, pp. 199–206, 2001.

[14] R. F. Guthoff, A. Zhivov, and O. Stachs, "In vivo confocal microscopy, an inner vision of the cornea—a major review," *Clinical and Experimental Ophthalmology*, vol. 37, no. 1, pp. 100–117, 2009.

[15] G. Martone, P. Frezzotti, G. M. Tosi et al., "An in vivo confocal microscopy analysis of effects of topical antiglaucoma therapy with preservative on corneal innervation and morphology," *American Journal of Ophthalmology*, vol. 147, no. 4, pp. 725.e1–735.e1, 2009.

[16] L. Oliveira-Soto and N. Efron, "Morphology of corneal nerves using confocal microscopy," *Cornea*, vol. 20, no. 4, pp. 374–384, 2001.

[17] N. Efron, G. Lee, R. N. Lim et al., "Development and validation of the QUT corneal nerve grading scale," *Cornea*, vol. 33, no. 4, pp. 376–381, 2014.

[18] I. S. J. Tuominen, Y. T. Konttinen, M. H. Vesaluoma, J. A. O. Moilanen, M. Helintö, and T. M. T. Tervo, "Corneal innervation and morphology in primary Sjögren's syndrome," *Investigative Ophthalmology and Visual Science*, vol. 44, no. 6, pp. 2545–2549, 2003.

[19] E. Villani, D. Galimberti, F. Viola, C. Mapelli, and R. Ratiglia, "The cornea in Sjögren's syndrome: an in vivo confocal study," *Investigative Ophthalmology and Visual Science*, vol. 48, no. 5, pp. 2017–2022, 2007.

[20] M. Zhang, J. Chen, L. Luo, Q. Xiao, M. Sun, and Z. Liu, "Altered corneal nerves in aqueous tear deficiency viewed by in vivo confocal microscopy," *Cornea*, vol. 24, no. 7, pp. 818–824, 2005.

[21] K. Rao, C. Leveque, and S. C. Pflugfelder, "Corneal nerve regeneration in neurotrophic keratopathy following autologous plasma therapy," *British Journal of Ophthalmology*, vol. 94, no. 5, pp. 584–591, 2010.

[22] S. Aggarwal, A. Kheirkhah, B. M. Cavalcanti et al., "Autologous serum tears for treatment of photoallodynia in patients with corneal neuropathy: efficacy and evaluation with in vivo confocal microscopy," *Ocular Surface*, vol. 13, no. 3, pp. 250–262, 2015.

[23] N. Efron, P. B. Morgan, and S. S. Katsara, "Validation of grading scales for contact lens complications," *Ophthalmic and Physiological Optics*, vol. 21, no. 1, pp. 17–29, 2001.

[24] "Methodologies to diagnose and monitor dry eye disease: report of the Diagnostic Methodology Subcommittee of the International Dry Eye WorkShop (2007)," *The Ocular Surface*, vol. 5, no. 2, pp. 108–152, 2007.

[25] P. Aragona, L. Rania, A. M. Roszkowska et al., "Effects of amino acids enriched tears substitutes on the cornea of patients with dysfunctional tear syndrome," *Acta Ophthalmologica*, vol. 91, no. 6, pp. e437–e444, 2013.

[26] P. Marsh and S. C. Pflugfelder, "Topical nonpreserved methylprednisolone therapy for keratoconjunctivitis sicca in Sjögren syndrome," *Ophthalmology*, vol. 106, no. 4, pp. 811–816, 1999.

[27] K. Sall, O. D. Stevenson, T. K. Mundorf, and B. L. Reis, "Two multicenter, randomized studies of the efficacy and safety of cyclosporine ophthalmic emulsion in moderate to severe dry eye disease," *Ophthalmology*, vol. 107, no. 4, pp. 631–639, 2000.

[28] D. Stevenson, J. Tauber, and B. L. Reis, "Efficacy and safety of cyclosporin A ophthalmic emulsion in the treatment of moderate-to-servere dry eye disease: a dose-ranging, randomized trial. The cyclosporin A phase 2 study group," *Ophthalmology*, vol. 107, no. 5, pp. 967–974, 2000.

[29] L. D. Barber, S. C. Pflugfelder, J. Tauber, and G. N. Foulks, "Phase III safety evaluation of cyclosporine 0.1% ophthalmic emulsion administered twice daily to dry eye disease patients for up to 3 years," *Ophthalmology*, vol. 112, no. 10, pp. 1790–1794, 2005.

[30] Y. Wang, Y. Ogawa, M. Dogru et al., "Ocular surface and tear functions after topical cyclosporine treatment in dry eye patients with chronic graft-versus-host disease," *Bone Marrow Transplantation*, vol. 41, no. 3, pp. 293–302, 2008.

[31] C. A. Urzua, D. H. Vasquez, A. Huidobro, H. Hernandez, and J. Alfaro, "Randomized double-blind clinical trial of autologous serum versus artificial tears in dry eye syndrome," *Current Eye Research*, vol. 37, no. 8, pp. 684–688, 2012.

[32] T. Kojima, R. Ishida, M. Dogru et al., "The effect of autologous serum eyedrops in the treatment of severe dry eye disease: a prospective randomized case-control study," *American Journal of Ophthalmology*, vol. 139, no. 2, pp. 242–246, 2005.

[33] A. R. C. Celebi, C. Ulusoy, and G. E. Mirza, "The efficacy of autologous serum eye drops for severe dry eye syndrome: a randomized double-blind crossover study," *Graefe's Archive for Clinical and Experimental Ophthalmology*, vol. 252, no. 4, pp. 619–626, 2014.

[34] J. Hwang, S.-H. Chung, S. Jeon, S.-K. Kwok, S.-H. Park, and M.-S. Kim, "Comparison of clinical efficacies of autologous serum eye drops in patients with primary and secondary Sjögren syndrome," *Cornea*, vol. 33, no. 7, pp. 663–667, 2014.

[35] J. L. Alio, A. E. Rodriguez, and D. WróbelDudzińska, "Eye platelet-rich plasma in the treatment of ocular surface disorders," *Current Opinion in Ophthalmology*, vol. 26, no. 4, pp. 325–332, 2015.

[36] B. Afzali, G. Lombardi, R. I. Lechler, and G. M. Lord, "The role of T helper 17 (Th17) and regulatory T cells (Treg) in human organ transplantation and autoimmune disease," *Clinical and Experimental Immunology*, vol. 148, no. 1, pp. 32–46, 2007.

[37] L. Zhou, J. E. Lopes, M. M. W. Chong et al., "TGF-β-induced Foxp3 inhibits TH17 cell differentiation by antagonizing RORγt function," *Nature*, vol. 453, no. 7192, pp. 236–240, 2008.

[38] S. Q. Crome, A. Y. Wang, and M. K. Levings, "Translational mini-review series on Th17 cells: function and regulation of

human T helper 17 cells in health and disease," *Clinical & Experimental Immunology*, vol. 159, no. 2, pp. 109–119, 2010.

[39] T. Habay, S. Majzoub, O. Perrault, C. Rousseau, and P. J. Pisella, "Objective assessment of the functional impact of dry eye severity on the quality of vision by double-pass aberrometry," *Journal Francais d'Ophtalmologie*, vol. 37, no. 3, pp. 188–194, 2014.

[40] H. Lin, W. Li, N. Dong et al., "Changes in corneal epithelial layer inflammatory cells in aqueous tear-deficient dry eye," *Investigative Ophthalmology and Visual Science*, vol. 51, no. 1, pp. 122–128, 2010.

[41] F. Machetta, A. M. Fea, A. G. Actis, U. de Sanctis, P. Dalmasso, and F. M. Grignolo, "In vivo confocal microscopic evaluation of corneal langerhans cells in dry eye patients," *Open Ophthalmology Journal*, vol. 8, pp. 51–59, 2014.

[42] A. Alhatem, B. Cavalcanti, and P. Hamrah, "In vivo confocal microscopy in dry eye disease and related conditions," *Seminars in Ophthalmology*, vol. 27, no. 5-6, pp. 138–148, 2012.

[43] S. C. G. Tseng, "Concept and application of limbal stem cells," *Eye*, vol. 3, no. 2, pp. 141–157, 1989.

[44] W. Yu, J. Wang, and J. Yin, "Platelet-rich plasma: a promising product for treatment of peripheral nerve regeneration after nerve injury," *International Journal of Neuroscience*, vol. 121, no. 4, pp. 176–180, 2011.

[45] E. Emel, S. S. Ergün, D. Kotan et al., "Effects of insulin-like growth factor-I and platelet-rich plasma on sciatic nerve crush injury in a rat model: laboratory investigation," *Journal of Neurosurgery*, vol. 114, no. 2, pp. 522–528, 2011.

[46] T. Y. Farrag, M. Lehar, P. Verhaegen, K. A. Carson, and P. J. Byrne, "Effect of platelet rich plasma and fibrin sealant on facial nerve regeneration in a rat model," *Laryngoscope*, vol. 117, no. 1, pp. 157–165, 2007.

[47] J. Javaloy, J. L. Alió, A. E. Rodriguez, A. Vega, and G. Muñoz, "Effect of platelet-rich plasma in nerve regeneration after LASIK," *Journal of Refractive Surgery*, vol. 29, no. 3, pp. 213–219, 2013.

[48] S. Yamagami, P. Hamrah, K. Miyamoto et al., "CCR5 chemokine receptor mediates recruitment of MHC class II-positive Langerhans cells in the mouse corneal epithelium," *Investigative Ophthalmology and Visual Science*, vol. 46, no. 4, pp. 1201–1207, 2005.

[49] L. Shen, S. Barabino, A. W. Taylor, and M. R. Dana, "Effect of the ocular microenvironment in regulating corneal dendritic cell maturation," *Archives of Ophthalmology*, vol. 125, no. 7, pp. 908–915, 2007.

[50] E. Villani, D. Galimberti, F. Viola, C. Mapelli, N. D. Papa, and R. Ratiglia, "Corneal involvement in rheumatoid arthritis: an in vivo confocal study," *Investigative Ophthalmology and Visual Science*, vol. 49, no. 2, pp. 560–564, 2008.

[51] J. S. López-García, I. García-Lozano, L. Rivas, and J. Martínez-Garchitorena, "Use of autologous serum in ophthalmic practice," *Archivos de la Sociedad Espanola de Oftalmologia*, vol. 82, no. 1, pp. 9–20, 2007.

Hindawi Publishing Corporation
BioMed Research International
Volume 2016, Article ID 7432131, 8 pages
http://dx.doi.org/10.1155/2016/7432131

Review Article

In Vivo Laser Scanning Confocal Microscopy of Human Meibomian Glands in Aging and Ocular Surface Diseases

Vincenzo Fasanella,[1] Luca Agnifili,[1] Rodolfo Mastropasqua,[2] Lorenza Brescia,[1] Federico Di Staso,[3] Marco Ciancaglini,[3] and Leonardo Mastropasqua[1]

[1]*Ophthalmology Clinic, Department of Medicine and Aging Science, "G. d'Annunzio" University of Chieti-Pescara, 66100 Chieti, Italy*
[2]*Ophthalmology Unit, Department of Neurological, Neuropsychological, Morphological and Movement Sciences, University of Verona, 37126 Verona, Italy*
[3]*Ophthalmic Clinic, Department of Life, Health and Environmental Sciences, University of L'Aquila, 67100 L'Aquila, Italy*

Correspondence should be addressed to Luca Agnifili; l.agnifili@unich.it

Received 13 November 2015; Revised 8 February 2016; Accepted 17 February 2016

Academic Editor: Dipika V. Patel

Meibomian glands (MGs) play a crucial role in the ocular surface homeostasis by providing lipids to the superficial tear film. Their dysfunction destabilizes the tear film leading to a progressive loss of the ocular surface equilibrium and increasing the risk for dry eye. In fact, nowadays, the meibomian gland dysfunction is one of the leading causes of dry eye. Over the past decades, MGs have been mainly studied by using meibography, which, however, cannot image the glandular structure at a cellular level. The diffusion of the *in vivo* laser scanning confocal microscopy (LSCM) provided a new approach for the structural assessment of MGs permitting a major step in the noninvasive evaluation of these structures. LSCM is capable of showing MGs modifications during aging and in the most diffuse ocular surface diseases such as dry eye, allergy, and autoimmune conditions and in the drug-induced ocular surface disease. On the other hand, LSCM may help clinicians in monitoring the tissue response to therapy. In this review, we summarized the current knowledge about the role of *in vivo* LSCM in the assessment of MGs during aging and in the most diffuse ocular surface diseases.

1. Introduction

Meibomian glands (MGs) are holocrine glands embedded in the tarsal plate of the eyelids. Each gland comprises multiple acini connected by a long common central duct running throughout the entire length of the gland [1]. The functional unit of a meibomian gland is the meibocyte, which synthesizes the meibum, a lipoid complex forming the superficial layer of the tear film. Meibum permeates the tear surface where it serves several important functions: it prevents tear evaporation and desiccation of the ocular surface, acts as a physical and hydrophobic barrier to the inward movement of environmental and organic agents, lubricates the ocular surface preventing irritation, and promotes clear ocular vision due to its optic properties. Thus, tear physiology is dependent upon the proper functioning of the MGs [2, 3].

Meibography represented for many years the only diagnostic approach to observe the MGs morphology *in vivo* [4].

With the recent diffusion of the laser scanning confocal microscopy (LSCM) (HRT I–III Rostok Cornea Module (RCM), Heidelberg Engineering, Heidelberg, Germany), it was possible to study the microscopic anatomy of several adnexal and ocular surface structures such as eyelid, conjunctiva, cornea, limbus, tarsal plate, and MGs [5–12]. LSCM allows integrated high-resolution evaluation of the morpho-functional ocular surface unit in normal and pathological conditions [13]. Several conditions may affect the anatomy and function of MGs, such as the primary meibomian gland dysfunction, dry eye, ocular allergy, the use of contact lenses, and the long-term application of topical medications in chronic ocular surface diseases and in glaucoma. In this review, we discuss the main MGs modifications during aging

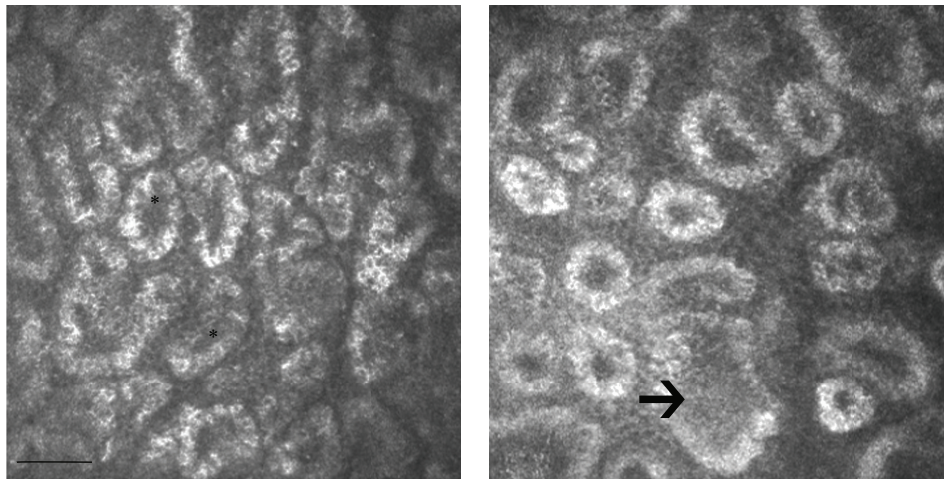

(a) (b)

Figure 1: LSCM of MGs in two healthy Caucasian subjects. (a) A 26-year-old male with a normal feature and density of the acini (asterisks); (b) a 73-year-old male with decreased MG acinar density and increased acinar size (arrow), indicative of atrophic age-related changes. Bar represents 50 μm.

and during the course of the most diffuse ocular surface diseases.

2. Methodology and Results

PubMed searches were performed on September 20, 2015, using the following phrases: "*in vivo* confocal microscopy" and "meibomian glands", which identified thirty-four unique publications. Six were excluded, since they did not concern the use of IVCM to study MGs.

Three of the considered publications were not published in English; however, they provided enough information in the English abstract to warrant inclusion.

2.1. Meibomian Glands in the Healthy and Aging Human Eye. The confocal images are captured from a coronal scan through a mass of acini posterior to a central, vertically oriented MG duct [14]. LSCM provides structural and functional information of the glandular status: MGs acini appear to be constituted by convoluted borders with large cells lining the acini and fine cellular material within the lumen [14].

The main structural modifications induced by aging were evidenced for the first time by Wei et al. [15] and afterwards confirmed by Villani et al. [16] in a heterogeneous population study, which revealed significant negative correlations between age and meibomian glandular acinar unit density [1]. LSCM permits indirect functional evaluation of MGs, by assessing the secretion reflectivity [4].

Besides the acinar density reduction, the normal aging induces also an evident decrease of the acinar diameter (Figure 1) and an increase of the acinar wall inhomogeneity, without significant modifications of the glandular orifice diameter. The overall interpretation of the structural modification suggests glandular dropout with qualitative changes of the meibum. Therefore, the authors speculated that acinar atrophy leads to a decrease in the MGs secretion with aging. These results are in accordance with the main clinical changes observed during aging, represented by tear film break-up time (BUT) and Schirmer test scores reduction.

Even though several studies reported likely hormone-dependent changes of MGs structure [17–19], LSCM did not document significant structural and functional differences between genders during aging [19, 20]. Further studies are warranted to elucidate the clinical implications of the hormonal action on MGs age-related changes.

In summary, LSCM in healthy subjects provides information of the normal modifications of glands with aging. Normal aging induces atrophic involution of the glandular unit along with progressive dysfunction of the secretive activity (Table 1). This appears to be in line with the involution of most parts of secretive structures, such as exocrine glands and lymphatics, observed in several tissues of the human body during aging [21–23]. In the eye, the glandular unit involution may take part in the increased risk of dry eye related conditions observed in the elderly.

2.2. Primary and Secondary Meibomian Glands Dysfunction. The primary meibomian gland dysfunction (MGD), characterized by inflammatory changes of the lid margin structures and in the anatomy of the MG orifices, is one of the most common ocular surface disorders: Hom et al. [20] reported prevalence of 38.9%, whereas Stanek [41] reported prevalence of 71.7% in individuals above 60 years old. MGD is a major cause of dry eye and results in a qualitative alteration and/or a quantitative reduction of the lipid secretion, which leads to decreased tear stability, increased tear evaporation, loss of lubrication, and damage to the ocular surface epithelia. LSCM, which currently has a primary role in the ocular surface analysis [26, 27], allows studying MG at cellular level. In MGD, LSCM permits the analysis of the cellular density of the superficial and basal epithelium of the eyelid and the assessment of the mean acinar area and density of MGs,

Table 1: Summary of the most important confocal signs for each disease affecting MGs.

Conditions	LSCM characteristics	References
Aging	MG acinar unit density and diameter reduction; increase of the acinar wall inhomogeneity	[13, 15, 16, 24, 25]
MGD	MG acinar unit density reduction; larger acinar unit diameter; duct dilation	[26–31]
Dry eye	MG acinar unit density and diameter reduction; inhomogeneous appearance of the MG walls and interstices; extensive periglandular Langerhans cell infiltration	[13, 16, 24, 25, 32–35]
Ocular allergy	Eosinophils and multinucleated granulocytes in the superficial conjunctival epithelium; periglandular lymphocytic cell infiltration; glandular atrophy and acinar and ductal dilatation	[13, 16, 24, 25, 36–39]
Glaucoma	MG acinar unit density and area reduction; increased reflectivity of the acinar secretion; ductal orifice dilation; inhomogeneity of MG interstice and wall	[9, 40]

the glandular orifice area, the meibum secretion reflectivity, and the inflammatory features of periglandular interstices and acinar unit wall (patterns of inhomogeneity) [40]. In the first confocal study on MG diseases, Messmer et al. [28] showed dilatation and obstruction of the meibomian gland ducts in twelve patients with blepharitis/meibomitis or MGD. On the other hand, in fifteen out of 19 patients with blepharitis/meibomitis, but not in MGD, intense inflammation was observed in the tarsal conjunctival epithelium and in the stroma. The inflammatory reaction was defined by an increase of hyperreflective roundish elements corresponding to immune cells. Matsumoto et al. [29] reported that the mean acinar unit density was significantly lower in MGD patients than in control subjects, whereas the mean acinar unit diameter was significantly larger in MGD patients than in controls. Both the density and diameter of MGs acinar units significantly correlated with the severity of MGs dropout and expression grades (Figure 3).

Other confocal parameters that presented acceptable sensitivity and specificity for the diagnosis of MGD were the longest and shortest MG diameters: in the study of Ibrahim et al., these parameters resulted to be significantly worse than those observed in the controls [30]. As stated above, LSCM can also provide information about the inflammatory status of MG during MGD. Matsumoto et al. [42] measured the mean inflammatory cell density (cells/mm^2) from the periglandular site of the entire lower and upper eyelid, reporting inflammatory cell numbers approximately ten to thirty times higher than those found in healthy controls. Interestingly, these cells markedly reduced after medical therapy: the combination of lid hygiene, topical nonpreserved artificial tears with 0.1% sodium hyaluronate, topical 0.5% levofloxacin and 0.1% fluorometholone, and oral minocycline (100 mg twice a day for 12 weeks) significantly improved the tear stability, the fluorescein staining scores, and the lid injection and cleared periglandular inflammatory infiltrates.

In a very recent study, LSCM revealed an increased immune cell number in the palpebral conjunctiva of patients with refractory MGD, compared to patients with therapy-responding MGD [43]. In the therapy-responding group, the mean inflammatory cell density in the periglandular area reduced from baseline values of 1216 ± 328 to 700 ± 436 cells/mm^2 at the last follow-up. No statistically significantly difference was found in the group that did not receive any therapy, 882 ± 301 cells/mm^2 before the initiation of trial and 843 ± 321 cells/mm^2 at the final follow-up.

Interestingly, OSDI scores correlated with epithelial immune cells infiltrating the palpebral conjunctiva, suggesting that the inflammation of the palpebral conjunctiva may contribute to explaining the MGD-associated refractory symptoms.

Secondary MGD can develop as a complication of the use of topical medications in patients with glaucoma [44–46] and in contact lens wearers (CLWs) (Figure 2) [32].

In CLWs, a decreased basal epithelium cell density, reduced acinar unit diameters, higher glandular orifice diameters, greater secretion reflectivity, and greater inhomogeneity of the periglandular interstices were the main observed findings. Morphologic changes in the MGs shown by LSCM were interpreted by the authors as signs of MGs dropout, duct obstruction, and glandular inflammation caused by chronic mechanical contact lens irritation.

In summary, MGD has a huge impact on the daily clinical practice since it plays a major role in the development of dry eye related conditions. Confocal microscopy precisely depicts, at a cellular level, the main macroscopic and microscopic MGs changes in patients affected with both primary and secondary MGD. The main features are represented by the MGs dropout, which is the glandular unit loss, the increase of the acinar surface (except for glaucoma), which, along with the increased meibum viscosity, is the hallmark of the glandular malfunction, and the inflammation of the periglandular interstice and acinar wall. The dilation of the duct orifice and the increased acinar diameter are the compensatory mechanism adopted by the glands to overcome the meibum stagnation (Table 1). All these changes lead to a

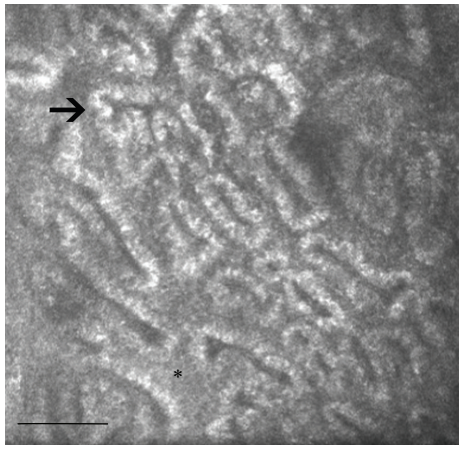

Figure 2: LSCM of MGs in a contact lens wearer. The most evident modifications are represented by the inhomogeneity of periglandular interstices (asterisk) and MG wall (arrow), periglandular inflammation, and the reduction of MG duct diameters. Bar represents 50 μm.

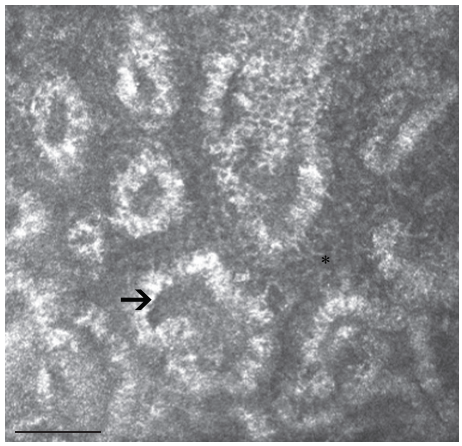

Figure 3: Confocal microscopy features in a 47-year-old male patient with MGD: inhomogeneity of periglandular interstices (asterisk) and MG wall (arrow), dilation and obstruction of the MG ducts, and reduction of the density of MG acinar units are the most significant alterations. Bar represents 50 μm.

decrease of the meibum production, which negatively affect the tear film stability and induce dry eye.

Therefore, MGD could be in part intended as accelerated aging of the glands, in which there is a marked inflammatory and immune component. Also, these aspects are shared by other exocrine glands' dysfunction in the human body, such as salivary glands [21–23].

In this field, confocal microscopy may provide a significant advancement in the daily clinical practice since it helps clinicians in the early diagnosis of primary or secondary MGD and in monitoring the response to therapy and the side effects of drugs.

In fact, as recently reported in a study that evaluated the efficacy of wet chamber warming goggles (Blephasteam®) in MGD patients unresponsive to warm compress treatment,

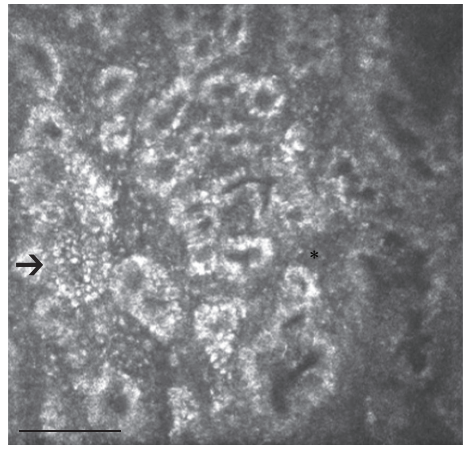

Figure 4: LSCM of MGs in a patient with dry eye: the image shows a decreased diameter of meibomian gland ducts, along with marked inhomogeneous appearance of the MG walls and interstices. Several punctate hyperreflective elements, which reflect a high degree of local inflammation, are recognizable in the interstice and within the MG wall (arrow and asterisk). Bar represents 50 μm.

LSCM documented a decreased acinar diameter and area, which was associated with an increased OSDI score [38].

2.3. Meibomian Glands in Dry Eye. Dry eye syndrome (DES) is one of the most common disorders of the eye, with prevalence of 10% to 20% in the adult population. The International Dry Eye Workshop (2007) [47] defined DES as a "multifactorial disease of the tears and ocular surface that results in symptoms of discomfort, visual disturbance, and tear film instability with potential damage to the ocular surface. It is accompanied by increased osmolarity of the tear film and inflammation of the ocular surface." In this field, LSCM documented the fine and peculiar microscopic findings of the target tissues including the cornea, conjunctiva, and meibomian glands. While several reports studied the confocal corneal and conjunctival changes in DES, MGs were only partially studied. In patients with primary DES and MGD, Villani et al. [33] reported increased acinar dilatation compared to primary DES and healthy controls, higher meibum reflectivity, and decreased diameters of gland orifices. Moreover, very interestingly, the authors showed increased acinar density in primary DES (Figure 4). The reduced lipid amount induces tear film hyperosmolarity, which leads to tear film instability, increased evaporation, and ocular surface inflammation [46]. A new integrated laser scanning confocal microscopy approach recently found some differences in the MGs features in patients with primary Sjogren syndrome, non-Sjogren syndrome dry eye, and MGD [32]. The pattern of inhomogeneity of the MGs walls and interstices was markedly higher in all groups of patients than in controls, with features more pronounced in primary Sjogren syndrome compared to non-Sjogren syndrome dry eye. The inhomogeneous appearance varies with the level of inflammation that is significantly higher in eyes with Sjogren syndrome, because of the autoimmune pathogenesis of this

condition. The presence of confocal signs of inflammation with the absence of dilative morphologic changes supports the occurrence of an inflammatory/atrophic nonobstructive MGD in the primary Sjogren syndrome [24, 33, 48].

Ban et al. [34] studied the morphological changes of MGs in patients with dry eye due to chronic graft-versus-host disease (GVHD), a major cause of morbidity and mortality in patients undergoing allogeneic hematopoietic stem cell transplantation for hematologic malignancies. They showed that the acinar unit density and the longest and shortest diameters of MGs acini are significantly decreased. Patients with severe DES after chronic GVHD show glandular fibrosis with MGs atrophy.

LSCM was also used to evaluate MGs modification in allergic keratoconjunctival diseases, such as vernal and atopic keratoconjunctivitis (VKC, AKC), which may frequently lead to secondary dry eye [VZ, VW]. In VKC, extensive periglandular Langerhans cell infiltration, with blurred lumen contours and hyperreflective solid matter in the lumen, was described [35, 39]. Ibrahim et al. [36] reported severe MGs changes in patients with AKC, with extensive fibrotic changes much more evident than that observed in MGD. These patients present shrunken MGs with extensive periglandular fibrosis, which does not allow gland enlargement as what occurs in obstructive MGD [25].

In conclusion, in patients with dry eye, confocal microscopy revealed that the inflammation is the first and most important pathogenetic mechanism involved in the development of the MG alterations. The main findings were the increased acinar density and the reduced orifice diameter, which differentiated DES from primary or secondary MGD (Table 1). In this way, DES seems to lead to an incomplete inflammatory-induced MGD. Other particular conditions potentially leading to dry eye, such as VK, AK, and GHVD, present also various degree of periglandular fibrotic reaction, which finally causes MGs atrophy. In this wide scenario of dry eye syndromes, LSCM may help clinicians in the early diagnosis of each type of disease leading to dry eye and in monitoring the response to therapy.

2.4. Meibomian Glands in Ocular Allergy. AKC and VKC are two of the most common and important ocular allergies. AKC is a bilateral chronic hypersensitivity disease characterized by conjunctival papillary hypertrophy, acute and chronic conjunctivitis, keratitis and corneal ulceration, eyelid eczema, and blepharitis [49–53]. Tears proinflammatory cytokines are responsible for the conjunctival and corneal damage and also for the MG alterations. MG changes play a critical role in the development of the allergy-related dry eye [29].

VKC is a recurring seasonally inflammatory condition of the cornea and conjunctiva, characterized by giant tarsal papillae and pathological changes of the conjunctival epithelium and MGs. LSCM documented intense infiltration of eosinophils and multinucleated granulocytes in the superficial conjunctival epithelium, extensive periglandular lymphocytic cells infiltration. These inflammatory alterations lead to macroscopic modifications of MGs, represented by glandular atrophy, and ductal dilation (Figure 5). The same morphofunctional changes were described in ACK patients,

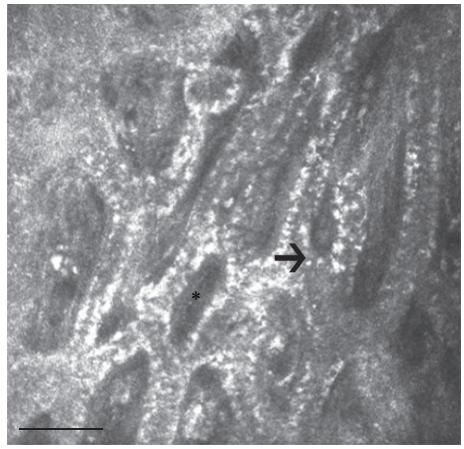

Figure 5: Morphological changes of MGs in a 38-year-old female patient with VKC: confocal microscopy shows extensive periglandular mononucleate cell infiltration (arrow), acinar atrophy, and ductal dilation, along with increased reflectivity of the acinar wall (asterisk). Bar represents 50 μm.

where there is an important decrease in size and density of MG acinar units. MGs appear small and irregular with periglandular fibrosis and a restricted and not well-defined lumen, occluded by hyperreflective and dense meibum [16, 31, 37, 54].

In allergic patients, the fibrotic involution of MG acinar units is more extensive than that observed in obstructive MGD, where the pressure induced by the stagnating meibum induces enlargement of MG acini [29].

In summary, MG modifications in patients with ocular allergy diseases are in part different from those observed in MGD and dry eye, since the periacinar fibrosis, along with the inflammatory infiltration and the meibum stagnation, represents the main finding (Table 1). In these ocular surface diseases, probably because of the periglandular compression induced by the fibrosis and the intense inflammation, MGs seem to be unable to activate adaptive mechanisms and develop a progressive atrophy. At present, the small sample size of research studies and poor standardization of examination and interpretation are the most challenging issues.

2.5. Meibomian Glands in Glaucoma. In the last years, LSCM was also used to evaluate the impact of glaucoma therapy on ocular surface structures [5–7, 55], including MGs [40]. In these studies, the modifications induced by the different classes of topical medications, the impact of the preservative and active compounds, and the role of the number of daily instillations in patients in multitherapy have been investigated.

MGs presented a reduction of glandular density and area and increased reflectivity of the acinar secretion, more evident in patients treated with two or more drugs compared to patients in monotherapy. The reduced density and area were expressions of glandular loss and reduced meibum production, respectively. Higher secretion reflectivity indicated increased secretion viscosity.

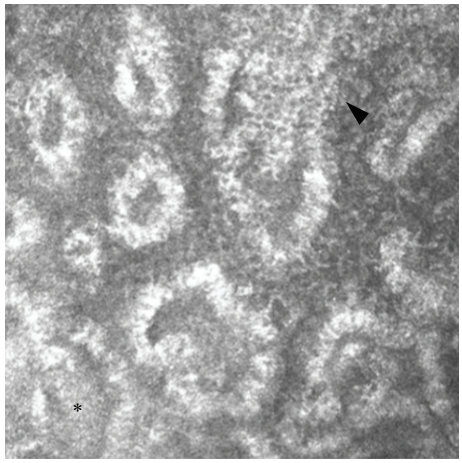

Figure 6: LSCM of MGs in a glaucomatous patient in multitherapy. The acinar unit density and area appeared to be reduced; MG wall and periglandular interstice presented inhomogeneous appearance, with some scattered hyperreflective punctate elements (arrowhead), and increased density of the meibum (asterisk). Bar represents 50 μm.

These modifications were similar to those observed in patients with MGD, with the exception of the glandular area that appeared to be reduced in glaucoma (Figure 6). Higher secretion reflectivity could indicate increased meibum secretion viscosity.

Other aspects characterizing MGs in glaucoma are the ductal orifice dilation and the inflammation of the glandular wall and interstice, which confocal microscopy documented with the presence of punctate hyperreflective elements. The ductal orifice dilation was probably an adaptive mechanism to overcome the high secretion density and duct blockage induced by treatment.

The potential induction mechanisms are the toxicity and an inflammatory or immune-mediated response, with the inflammation probably being the first step in the cascade of glandular modifications [7, 12].

In patients in monotherapy LSCM contributed to clarifying the role of preservatives (benzalkonium chloride (BAK)) and active compounds in the acinar modifications: preserved drugs were more toxic than preservative-free (PF) formulations, with preserved prostaglandin analogues (PGA) being more toxic than preserved β-blockers. Therefore, BAK and PGA, with their toxic and inflammatory stimuli, play the most crucial role in the induction of glaucoma therapy-related MGD.

Very interestingly, all the microscopic modifications of MGs significantly correlated with the ocular surface disease index (OSDI) score, break-up time (BUT), and Schirmer test I (STI). These correlations indicated that MGs alterations, as assessed with LSCM, were indicators of dry eye and have a main role in development of the therapy-related ocular surface disease in patients with glaucoma. Thus, the preservation of the structural and functional integrity of MGs represents a critical challenge during medical management of glaucoma.

In conclusion, the long-term antiglaucoma therapy has a strong negative impact on MGs functionality: the iatrogenic changes of MGs, in fact, lead to meibomian gland dysfunction very similar to primary MGD, with the exception of the reduced acinar area (Table 1). It is hypothesizable that toxicity induces secondary meibomian gland dysfunction in which glands are unable to activate processes that attempt to overcome the secretion blockage. As a consequence, the acinar size decreases and MGs progressively drop out. These features are shared with CLWs, in which the mechanical trauma leads to a secondary MGD, with the exception of the reduced acinar area. One may suppose that when the inflammation plays the main role, MGs modify their features as in primary MGD, whereas when toxic or mechanic stimuli play the main role, MGs reduce also their size.

These modifications present evident clinical implications since they could strongly affect adherence and persistence of treatment.

3. Summary and Conclusions

Until recently, the microanatomy evaluation of the ocular surface structures was limited to the impression cytology, which is based on sampling the superficial epithelial layers. This methodology, despite being highly reproducible, does not allow exploring deep tissues and induces discomfort to patients.

The rapid diffusion of LSCM in the last decades permitted an *in vivo* biopsy of all ocular surface tissues, at different depths, and the tissue analysis at cellular and subcellular level. The meibomian gland is one of the ocular surface structures that mostly benefited from the confocal assessment, since the standard meibography can only give a macroscopic analysis of the entire gland. The possibility of imaging MGs at cellular level, *in vivo*, and in a noninvasive way permit studying these structures in the most diffuse and important ocular surface diseases such as dry eye, ocular allergy, and drug toxicity.

In this way, LSCM may allow a preclinical diagnosis of MG conditions, potentially before glands begin to malfunction. In addition, since confocal microscopy does not produce significant discomfort for patients, this technique offers the advantage to strictly monitor the disease over time, to anticipate the treatment when required, to follow the response to therapy, and to modify the therapy regimen accordingly.

Moreover, the fine microscopic assessment could also clarify the pathophysiology of these conditions. This is even more important considering that the incidence of ocular surface diseases is exponentially growing in the last years.

Conflict of Interests

The authors declare that there is no conflict of interests regarding the publication of this paper.

Authors' Contribution

Vincenzo Fasanella and Luca Agnifili equally contributed to this work and share primary authorship.

References

[1] E. Knop, N. Knop, T. Millar, H. Obata, and D. A. Sullivan, "The international workshop on meibomian gland dysfunction: report of the subcommittee on anatomy, physiology, and pathophysiology of the meibomian gland," *Investigative Ophthalmology and Visual Science*, vol. 52, no. 4, pp. 1938–1978, 2011.

[2] S. Mishima and D. M. Maurice, "The oily layer of the tear film and evaporation from the corneal surface," *Experimental Eye Research*, vol. 1, pp. 39–45, 1961.

[3] J. M. Tiffany, "The lipid secretion of the meibomian glands," *Advances in Lipid Research*, vol. 22, pp. 1–62, 1987.

[4] J. V. Jester, L. Rife, D. Nii, J. K. Luttrull, L. Wilson, and R. E. Smith, "In vivo biomicroscopy and photography of meibomian glands in a rabbit model of meibomian gland dysfunction," *Investigative Ophthalmology and Visual Science*, vol. 22, no. 5, pp. 660–677, 1982.

[5] R. Mastropasqua, V. Fasanella, E. Pedrotti et al., "Trans-conjunctival aqueous humor outflow in glaucomatous patients treated with prostaglandin analogues: an in vivo confocal microscopy study," *Graefe's Archive for Clinical and Experimental Ophthalmology*, vol. 252, no. 9, pp. 1469–1479, 2014.

[6] L. Agnifili, P. Carpineto, V. Fasanella et al., "Conjunctival findings in hyperbaric and low-tension glaucoma: an in vivo confocal microscopy study," *Acta Ophthalmologica*, vol. 90, no. 2, pp. e132–e137, 2012.

[7] L. Mastropasqua, L. Agnifili, V. Fasanella et al., "Conjunctival goblet cells density and preservative-free tafluprost therapy for glaucoma: an in vivo confocal microscopy and impression cytology study," *Acta Ophthalmologica*, vol. 91, no. 5, pp. e397–e405, 2013.

[8] L. Mastropasqua, M. Nubile, M. Lanzini et al., "Morphological modification of the cornea after standard and transepithelial corneal cross-linking as imaged by anterior segment optical coherence tomography and laser scanning in vivo confocal microscopy," *Cornea*, vol. 32, no. 6, pp. 855–861, 2013.

[9] L. Agnifili, V. Fasanella, S. D'Aguanno et al., "Shotgun proteomics reveals specific modulated protein patterns in tears of patients with primary open angle glaucoma naïve to therapy," *Molecular BioSystems*, vol. 9, no. 6, pp. 1108–1116, 2013.

[10] R. Mastropasqua, L. Agnifili, V. Fasanella et al., "Corneoscleral limbus in glaucoma patients: in vivo confocal microscopy and immunocytological study," *Investigative Opthalmology & Visual Science*, vol. 56, no. 3, pp. 2050–2058, 2015.

[11] P. Carpineto, L. Agnifili, M. Nubile et al., "Conjunctival and corneal findings in bleb-associated endophthalmitis: an in vivo confocal microscopy study," *Acta Ophthalmologica*, vol. 89, no. 4, pp. 388–395, 2011.

[12] L. Mastropasqua, L. Agnifili, R. Mastropasqua et al., "In vivo laser scanning confocal microscopy of the ocular surface in glaucoma," *Microscopy and Microanalysis*, vol. 20, no. 3, pp. 879–894, 2014.

[13] E. Villani, C. Baudouin, N. Efron et al., "In vivo confocal microscopy of the ocular surface: from bench to bedside," *Current Eye Research*, vol. 39, no. 3, pp. 213–231, 2014.

[14] N. Efron, M. Al-Dossari, and N. Pritchard, "In vivo confocal microscopy of the palpebral conjunctiva and tarsal plate," *Optometry and Vision Science*, vol. 86, no. 11, pp. E1303–E1308, 2009.

[15] A. Wei, J. Hong, X. Sun, and J. Xu, "Evaluation of age-related changes in human palpebral conjunctiva and meibomian glands by in vivo confocal microscopy," *Cornea*, vol. 30, no. 9, pp. 1007–1012, 2011.

[16] E. Villani, V. Canton, F. Magnani, F. Viola, P. Nucci, and R. Ratiglia, "The aging meibomian gland: an in vivo confocal study," *Investigative Ophthalmology and Visual Science*, vol. 54, no. 7, pp. 4735–4740, 2013.

[17] D. A. Sullivan, B. D. Sullivan, M. D. Ullman et al., "Androgen influence on the meibomian gland," *Investigative Ophthalmology and Visual Science*, vol. 41, no. 12, pp. 3732–3742, 2000.

[18] B. D. Sullivan, J. E. Evans, J. M. Cermak, K. L. Krenzer, M. R. Dana, and D. A. Sullivan, "Complete androgen insensitivity syndrome: effect on human meibomian gland secretions," *Archives of Ophthalmology*, vol. 120, no. 12, pp. 1689–1699, 2002.

[19] C. Auw-Haedrich and N. Feltgen, "Estrogen receptor expression in meibomian glands and its correlation with age and dry-eye parameters," *Graefe's Archive for Clinical and Experimental Ophthalmology*, vol. 241, no. 9, pp. 705–709, 2003.

[20] M. M. Hom, J. R. Martinson, L. L. Knapp, and J. R. Paugh, "Prevalence of meibomian gland dysfunction," *Optometry and Vision Science*, vol. 67, no. 9, pp. 710–712, 1990.

[21] A. Bodineau, M. Folliguet, and S. Séguier, "Tissular senescence and modifications of oral ecosystem in the elderly: risk factors for mucosal pathologies," *Current Aging Science*, vol. 2, no. 2, pp. 109–120, 2009.

[22] E. M. Rocha, M. Alves, J. D. Rios, and D. A. Dartt, "The aging lacrimal gland: changes in structure and function," *Ocular Surface*, vol. 6, no. 4, pp. 162–174, 2008.

[23] L. Agnifili, R. Mastropasqua, V. Fasanella et al., "In vivo confocal microscopy of conjunctiva-associated lymphoid tissue in healthy humans," *Investigative Ophthalmology and Visual Science*, vol. 55, no. 8, pp. 5254–5262, 2014.

[24] E. Villani, F. Magnani, F. Viola et al., "In vivo confocal evaluation of the ocular surface morpho-functional unit in dry eye," *Optometry and Vision Science*, vol. 90, no. 6, pp. 576–586, 2013.

[25] E. Villani, F. Mantelli, and P. Nucci, "In-vivo confocal microscopy of the ocular surface: ocular allergy and dry eye," *Current Opinion in Allergy and Clinical Immunology*, vol. 13, no. 5, pp. 569–576, 2013.

[26] A. Kobayashi, T. Yoshita, and K. Sugiyama, "In vivo findings of the bulbar/palpebral conjunctiva and presumed meibomian glands by laser scanning confocal microscopy," *Cornea*, vol. 24, no. 8, pp. 985–988, 2005.

[27] E. M. Messmer, M. J. Mackert, D. M. Zapp, and A. Kampik, "In vivo confocal microscopy of normal conjunctiva and conjunctivitis," *Cornea*, vol. 25, no. 7, pp. 781–788, 2006.

[28] E. M. Messmer, E. Torres Suárez, M. I. Mackert, D. M. Zapp, and A. Kampik, "In vivo confocal microscopy in blepharitis," *Klinische Monatsblatter fur Augenheilkunde*, vol. 222, no. 11, pp. 894–900, 2005.

[29] Y. Matsumoto, E. A. Sato, O. M. A. Ibrahim, M. Dogru, and K. Tsubota, "The application of in vivo laser confocal microscopy to the diagnosis and evaluation of meibomian gland dysfunction," *Molecular Vision*, vol. 14, pp. 1263–1271, 2008.

[30] O. M. A. Ibrahim, Y. Matsumoto, M. Dogru et al., "The efficacy, sensitivity, and specificity of in vivo laser confocal microscopy in the diagnosis of meibomian gland dysfunction," *Ophthalmology*, vol. 117, no. 4, pp. 665–672, 2010.

[31] O. M. A. Ibrahim, Y. Matsumoto, M. Dogru et al., "In vivo confocal microscopy evaluation of meibomian gland dysfunction in atopic-keratoconjunctivitis patients," in *Proceedings of the 64th Congress of Clinical Ophthalmology of Japan*, Kobe, Japan, November 2010.

[32] E. Villani, G. Ceresara, S. Beretta, F. Magnani, F. Viola, and R. Ratiglia, "In vivo confocal microscopy of meibomian glands in contact lens wearers," *Investigative Ophthalmology and Visual Science*, vol. 52, no. 8, pp. 5215–5219, 2011.

[33] E. Villani, S. Beretta, M. De Capitani, D. Galimberti, F. Viola, and R. Ratiglia, "In vivo confocal microscopy of meibomian glands in Sjögren's syndrome," *Investigative Ophthalmology and Visual Science*, vol. 52, no. 2, pp. 933–939, 2011.

[34] Y. Ban, Y. Ogawa, O. M. A. Ibrahim et al., "Morphologic evaluation of Meibomian glands in chronic graft-versus-host disease using in vivo laser confocal microscopy," *Molecular Vision*, vol. 17, pp. 2533–2543, 2011.

[35] Q. Le, J. Hong, W. Zhu, X. Sun, and J. Xu, "In vivo laser scanning confocal microscopy of vernal keratoconjunctivitis," *Clinical and Experimental Ophthalmology*, vol. 39, no. 1, pp. 53–60, 2011.

[36] O. M. A. Ibrahim, Y. Matsumoto, M. Dogru et al., "In vivo confocal microscopy evaluation of meibomian gland dysfunction in atopic-keratoconjunctivitis patients," *Ophthalmology*, vol. 119, no. 10, pp. 1961–1968, 2012.

[37] E. Villani, M. D. Strologo, F. Pichi et al., "Dry eye in vernal keratoconjunctivitis: a cross-sectional comparative study," *Medicine (Baltimore)*, vol. 94, no. 42, article e1648, 2015.

[38] E. Villani, E. Garoli, V. Canton, F. Pichi, P. Nucci, and R. Ratiglia, "Evaluation of a novel eyelid-warming device in meibomian gland dysfunction unresponsive to traditional warm compress treatment: an in vivo confocal study," *International Ophthalmology*, vol. 35, no. 3, pp. 319–323, 2014.

[39] Q. Wei, Q. Le, J. Hong, J. Xiang, A. Wei, and J. Xu, "In vivo confocal microscopy of meibomian glands and palpebral conjunctiva in vernal keratoconjunctivitis," *Indian Journal of Ophthalmology*, vol. 63, no. 4, pp. 327–330, 2015.

[40] L. Agnifili, V. Fasanella, C. Costagliola et al., "In vivo confocal microscopy of meibomian glands in glaucoma," *British Journal of Ophthalmology*, vol. 97, no. 3, pp. 343–349, 2013.

[41] S. Stanek, "Meibomian gland status comparison between active duty personnel and U.S. veterans," *Military Medicine*, vol. 165, no. 8, pp. 591–593, 2000.

[42] Y. Matsumoto, Y. Shigeno, E. A. Sato et al., "The evaluation of the treatment response in obstructive meibomian gland disease by in vivo laser confocal microscopy," *Graefe's Archive for Clinical and Experimental Ophthalmology*, vol. 247, no. 6, pp. 821–829, 2009.

[43] Y. Qazi, A. Kheirkhah, C. Blackie et al., "In vivo detection of clinically non-apparent ocular surface inflammation in patients with meibomian gland dysfunction-associated refractory dry eye symptoms: a pilot study," *Eye*, vol. 29, no. 8, pp. 1099–1110, 2015.

[44] M. G. Cunniffe, R. Medel-Jiménez, and M. González-Candial, "Topical antiglaucoma treatment with prostaglandin analogues may precipitate meibomian gland disease," *Ophthalmic Plastic and Reconstructive Surgery*, vol. 27, no. 5, pp. 128–129, 2011.

[45] R. Arita, K. Itoh, S. Maeda et al., "Comparison of the long-term effects of various topical antiglaucoma medications on meibomian glands," *Cornea*, vol. 31, no. 11, pp. 1229–1234, 2012.

[46] R. Arita, K. Itoh, S. Maeda et al., "Effects of long-term topical anti-glaucoma medications on meibomian glands," *Graefe's Archive for Clinical and Experimental Ophthalmology*, vol. 250, no. 8, pp. 1181–1185, 2012.

[47] International Dry Eye WorkShop, "The definition and classification of dry eye disease: report of the definition and classification subcommittee of the international dry eye workshop," *The Ocular Surface*, vol. 5, pp. 75–92, 2007.

[48] A. Alhatem, B. Cavalcanti, and P. Hamrah, "In vivo confocal microscopy in dry eye disease and related conditions," *Seminars in Ophthalmology*, vol. 27, no. 5-6, pp. 138–148, 2012.

[49] A. S. Bacon, S. J. Tuft, D. M. Metz et al., "The origin of keratopathy in chronic allergic eye disease: a histopathological study," *Eye*, vol. 7, supplement, pp. 21–25, 1993.

[50] M. Dogru, C. Katakami, N. Nakagawa, K. Tetsumoto, and M. Yamamoto, "Impression cytology in atopic dermatitis," *Ophthalmology*, vol. 105, no. 8, pp. 1478–1484, 1998.

[51] S. J. Tuft, D. M. Kemeny, J. K. G. Dart, and R. J. Buckley, "Clinical features of atopic keratoconjunctivitis," *Ophthalmology*, vol. 98, no. 2, pp. 150–158, 1991.

[52] C. S. Forster and M. Calonge, "Atopic keratoconjunctivitis," *Ophthalmology*, vol. 97, no. 8, pp. 992–1000, 1990.

[53] M. J. Hogan, "Atopic keratoconjunctivitis," *Transactions of the American Ophthalmological Society*, vol. 50, pp. 265–281, 1952.

[54] M. Dogru, N. Okada, N. Asano-Kato et al., "Atopic ocular surface disease: implications on tear function and ocular surface mucins," *Cornea*, vol. 24, no. 8, supplement, pp. S18–S23, 2005.

[55] L. Mastropasqua, L. Agnifili, R. Mastropasqua, and V. Fasanella, "Conjunctival modifications induced by medical and surgical therapies in patients with glaucoma," *Current Opinion in Pharmacology*, vol. 13, no. 1, pp. 56–64, 2013.

Hindawi Publishing Corporation
BioMed Research International
Volume 2016, Article ID 5159746, 6 pages
http://dx.doi.org/10.1155/2016/5159746

Research Article

Laser Scanning In Vivo Confocal Microscopy of Clear Grafts after Penetrating Keratoplasty

Dai Wang,[1] Peng Song,[2] Shuting Wang,[1] Dapeng Sun,[2] Yuexin Wang,[1] Yangyang Zhang,[2] and Hua Gao[1]

[1]*Shandong Eye Hospital, Shandong Eye Institute, Shandong Academy of Medical Sciences, Jinan 250012, China*
[2]*Qingdao Eye Hospital, Shandong Eye Institute, Shandong Academy of Medical Sciences, Qingdao 266071, China*

Correspondence should be addressed to Hua Gao; gaohua100@126.com

Received 13 November 2015; Revised 29 January 2016; Accepted 1 February 2016

Academic Editor: Paolo Fogagnolo

Purpose. To evaluate the changes of keratocytes and dendritic cells in the central clear graft by laser scanning in vivo confocal microscopy after penetrating keratoplasty (PK). *Methods.* Thirty adult subjects receiving PK at Shandong Eye Institute and with clear grafts and no sign of immune rejection after surgery were recruited into this study, and 10 healthy adults were controls. The keratocytes and dendritic cells in the central graft were evaluated by laser scanning confocal microscopy, as well as epithelium cells, keratocytes, corneal endothelium cells, and corneal nerves (especially subepithelial plexus nerves). *Results.* Median density of subepithelial plexus nerves, keratocyte density in each layer of the stroma, and density of corneal endothelium cells were all lower in clear grafts than in controls. The dendritic cells of five (16.7%) patients were active in Bowman's membrane and stromal membrane of the graft after PK. *Conclusions.* Activated dendritic cells and Langerhans cells could be detected in some of the clear grafts, which indicated that the subclinical stress of immune reaction took part in the chronic injury of the clear graft after PK, even when there was no clinical rejection episode.

1. Introduction

Corneal transplantation has a long history of more than 100 years [1, 2]. Microscopic technology has greatly improved the success rate of keratoplasty [3]. Clinical application of immunosuppressive agents, such as cyclosporine A and FK506, significantly reduces the frequency of acute rejection [3–9]. Even so, clinically, the corneal grafts have been found to display gradual functional deterioration for months to years after transplantation. That is, with no history of rejection, the corneal grafts eventually become edematous and opaque. This behavior has been attributed to progressive late endothelium failure or chronic corneal allograft dysfunction [10, 11], which may represent the leading cause of poor long-term survival rates after penetrating keratoplasty (PK). It was reported that the loss rate of endothelial cells was 0.6% per year in normal human corneas. The loss rate of endothelial cells in the graft was up to 4.2% per year, even when there was no rejection episode after surgery [12].

To date, few studies have been reported about chronic damage to the graft because of lack of species of the clear allografts clinically. We have no idea whether the clear graft with no sign of immune rejection suffers chronic immune damage. It is also controversial whether immunosuppressive agents can be used in these patients. Confocal microscopy is a noninvasive technique for investigations of the cellular structure of corneal physiology and disease. It offers visualization of the living tissues and provides greyscale images with greatly increased resolutions over light biomicroscopy and biocytology, which can observe ultrastructure of the cornea [13–15]. Due to the advantage of in vivo confocal microscopy, it is possible to observe the graft in vivo and activation of keratocytes. In this study, we observed the clear graft without any sign of immune rejection after PK by confocal microscopy and investigated whether immune cells and other keratocytes were involved in the chronic damage to corneal grafts.

2. Methods

2.1. Subjects. Patients who underwent PK at Shandong Eye Institute between November 1, 1997, and December 21, 2013, were examined by using slit-lamp biomicroscopy to determine whether the graft was clear. Grafts suffering any clinical immune rejection episode were excluded from the study. Thirty patients (30 eyes) were included. The mean age was 47.56 ± 13.10 years (range, 16 to 65 years). The mean preoperative uncorrected visual acuity (Log MAR) was 1.736 ± 0.48 (range, 1.00 to 3.00).

2.2. Groups. Thirty clear grafts were examined at 12.8 ± 8.7 years (range, 1–17 years) after surgery. Preoperative indications for keratoplasty were corneal ulcer (18 eyes), granular corneal dystrophy (three eyes), pseudophakic bullous keratopathy due to the anterior chamber lens (two eyes), corneal scar due to eye injury (two eyes), keratoconus (two eyes), and others (three eyes). Ten normal corneas of 10 subjects who were examined between 2009 and 2014 were used as concurrent controls for keratocyte density and subbasal nerve density. The mean age was 30 ± 4.8 years (range, 24 to 34 years). The mean uncorrected visual acuity was 1.776 ± 0.67 (range, 0.52 to 3.00).

2.3. In Vivo Scanning Confocal Microscopy of Corneas. Laser scanning in vivo confocal microscopy was performed in all subjects with the Heidelberg Retina Tomograph II Rostock Corneal Module (Heidelberg Engineering GmBH, Heidelberg, Germany). All eyes were anesthetized with a drop of 0.4% benoxinate hydrochloride (Chauvin Pharmaceuticals, Surrey, UK). Viscotears (Carbomer 980, 0.2%; Novartis, North Ryde, NSW, Australia) was used as a coupling agent between the applanate lens cap and the cornea. During the examination, all subjects were asked to fixate on a distance target aligned to enable examination of the central cornea. The central corneal thickness may increase with time after PK [16, 17]. For brevity, we referred to this variable as "the number of keratocytes." Three randomly chosen images per subject were analyzed and statistically compared.

2.4. Records of Digital Images. The objective was adjusted to provide an en face view of the central cornea. The patient fixated on a target with the contralateral eye to minimize eye movements. Digital images of the central cornea were recorded with the optical section advancing through the full-thickness cornea. Each image represented a coronal section of the cornea that was approximately 380 μm (horizontal) × 380 μm (vertical) [18, 19]. The full thickness of the central cornea or the area within the central 2 mm diameter was scanned using the "section mode" of the device. This mode enables instantaneous imaging of a single area of the cornea at a desired depth. A "through focus" series of images of one cornea constituted one "scan" with more than 450 video frames, depending on the thickness of the cornea. Two to four scans which contained the clearest images of the central basal epithelium were acquired per eye.

2.5. Image Analysis. For each confocal microscopic examination, three images were taken from each of the following levels: subepithelial nerve plexus, anterior stroma, posterior stroma, and endothelium. The best-quality scan without motion artifact was selected for each cornea by an experienced observer (SW). For the density measurement, the cornea was divided into 3 layers: epithelium, stroma (anterior corneal stromal cells and posterior corneal stromal cells), and endothelium. The nuclei of the keratocytes sharply demarcated only the highly reflective ones, and the reflective keratocytes were visualized on examination of the stroma. Confocal microscopy permitted in vivo evaluation of Langerhans cells (LCs) and other immune cells within the human cornea, with a particular emphasis on cell morphology distribution in Bowman's membrane and stroma. The density of subepithelial plexus nerves was evaluated using NeuronJ, a free semiautomatic image analysis program, and ImageJ (http://www.imagescience.org/meijering/software/neuronj/; accessed November 2012), a plug-in to the program. Images of keratocytes were analyzed using a custom automated program, which objectively identified bright objects (presumed to represent keratocyte nuclei) and calculated keratocyte density [10, 20]. Ten percent of all images were recounted by one of the examiners (DS) to determine the interexaminer limit of agreement.

2.6. Statistical Analysis. Mean keratocyte density of the full-thickness stroma, keratocyte density for each layer of the stroma, number of keratocytes, and subbasal nerve density were compared between clear grafts after PK and controls. Differences were analyzed using unpaired t-tests if the data were distributed normally or using Wilcoxon rank sum tests if the data were not distributed normally. $P \leq 0.05$ was considered statistically significant. Correlations between keratocyte density or subbasal nerve density and time after keratoplasty were assessed using Pearson correlation coefficients if the data were distributed normally or using Spearman tests if the data were not distributed normally. The annual rate of keratocyte loss (percentage of decrease per year) was calculated from the number of keratocytes at each examination and the interval between examinations by assuming that the number of keratocytes decreased as a simple first-order loss.

2.7. Medical Ethics. The research adhered to the tenets of the Declaration of Helsinki. Informed, written consent was obtained from all subjects after explanation of the nature and possible consequences of the study. The protocol used was approved by the ethics committee of Shandong Eye Institute.

3. Results

3.1. Evaluation of Corneal Nerves. Mean density of subepithelial plexus nerves was lower in clear grafts (1506 μm/mm^2; range, 782–5846 μm/mm^2) ($n = 30$) than in controls (7020 μm/mm^2; range, 2371–12448 μm/mm^2; $P \leq 0.001$) ($n = 10$). The subepithelial nerves regenerated smaller and shorter than the normal after PK in a random and disordered pattern (Figure 1).

3.2. Evaluation of Keratocytes. Keratocyte density in each layer of the stroma was lower in clear grafts compared with

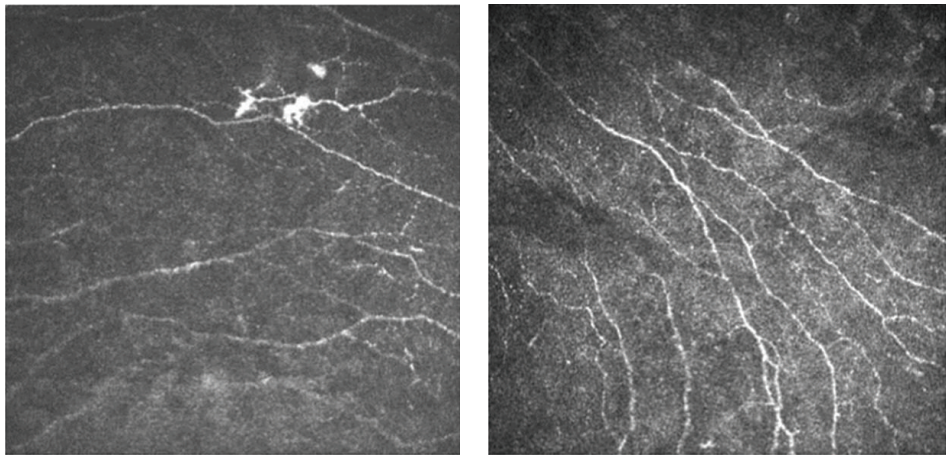

(a) (b)

Figure 1: Laser scanning in vivo confocal microscopy images of (a) the subepithelial nerves in the patient after penetrating keratoplasty (regenerated in a random and disordered pattern) and (b) the subepithelial nerves of the healthy cornea (parallel neural contorts and regular morphology). (a) Scanning-depth: 45 μm; age: 43 years. (b) Scanning-depth: 50 μm; age: 29 years.

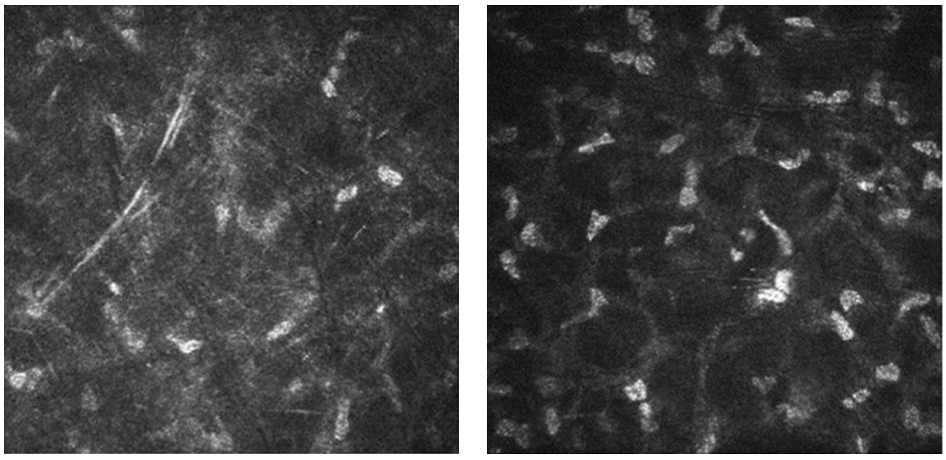

(a) (b)

Figure 2: Laser scanning in vivo confocal microscopy images of (a) the stromal cells (disorderly and unsystematic) in the patient after penetrating keratoplasty and (b) the stromal cells in the healthy cornea. (a) Scanning-depth: 379 μm; age: 44 years. (b) Scanning-depth: 401 μm; age: 35 years.

controls. The anterior stromal cell density was 860.6 ± 299 cells/mm^2 (range, 493–1404 cells/mm^2) in clear grafts, while it was 1099 ± 164.9 cells/mm^2 (range, 798–1380 cells/mm^2) in normal corneas ($P = 0.018$). The posterior stromal cell density was 607.6 ± 263 cells/mm^2 (range, 295–1203 cells/mm^2) in clear grafts, significantly lower than that in normal corneas (754.9 ± 90.37 cells/mm^2; range, 587–1380 cells/mm^2; $P = 0.024$). The shape of a few nuclei transformed from the ellipse to the irregular spindle. The stromal cells were disorderly and unsystematic in patients after PK, and some cells became scars (Figure 2).

3.3. Evaluation of Endothelium Cells. Corneal endothelium cell density was 1561 ± 864 cells/mm^2 (range, 480–3371 cells/mm^2) in clear grafts, significantly lower than that in normal corneas (3099 ± 489 cells/mm^2; range, 2798–3972 cells/mm^2; $P = 0.003$). The endothelium cells changed from the hexagon shape into the heptagon or even more, with a bigger size. Some of the nuclei had high reflection and a few multinuclear cells. Endothelial cell nuclei of the PKs affected the brighter refraction of light than the normal (Figure 3).

3.4. Evaluation of Inflammatory Cells. Mean keratocyte density correlated weakly with time after surgery ($r = -0.20$; $P = 0.05$). The dentritic cells of five (16.7%) adults were active in Bowman's membrane and stromal membrane of the graft after PK. There were five or six activated LCs (white objects of split ends) in each scan of confocal microscopy (Figure 4).

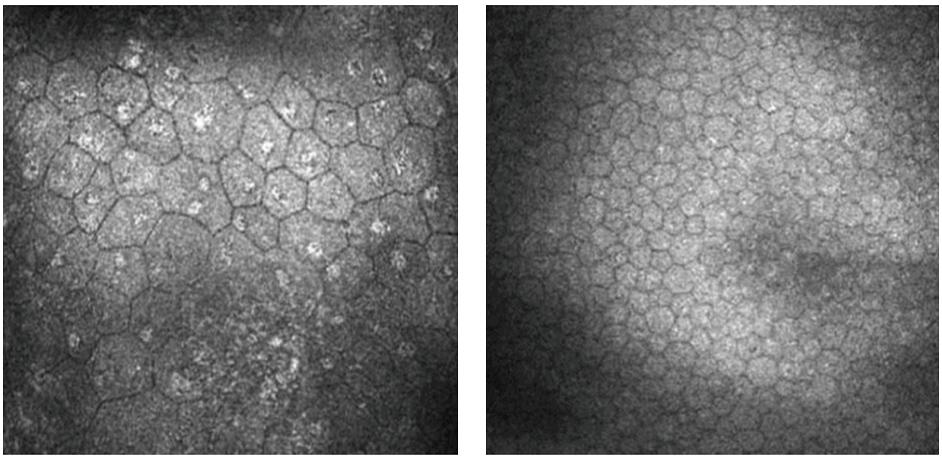

(a) (b)

Figure 3: Laser scanning in vivo confocal microscopy images of (a) the corneal endothelium cells (heptagon) in the patient after penetrating keratoplasty and (b) the corneal endothelium cells in the healthy cornea. (a) Scanning-depth: 453 μm; age: 39 years. (b) Scanning-depth: 460 μm; age: 35 years.

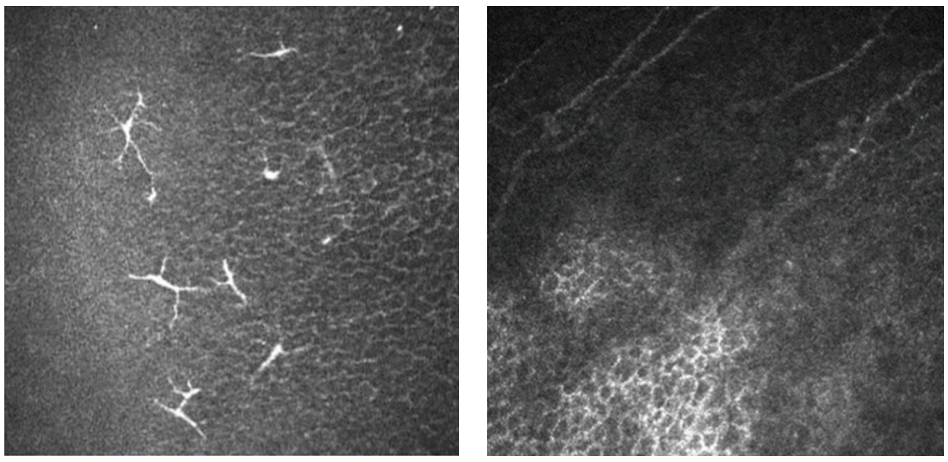

(a) (b)

Figure 4: Laser scanning in vivo confocal microscopy images of (a) the Langerhans cells (white objects of split ends) activated in Bowman's membrane and stromal membrane in the patient after penetrating keratoplasty and (b) the same position in the healthy cornea. (a) Scanning-depth: 53 μm; age: 51 years. (b) Scanning-depth: 49 μm; age: 29 years.

4. Discussion

PK is one of the most important treatments for corneal disease. Every year about 100,000 people around the world accept this surgery for vision rehabilitation. However, chronic corneal allograft dysfunction or late graft failure after PK is a great problem threatening the long-term graft survival. The half time for the component was 21 years after PK according to a recent report [20]. Transplants can maintain about 20 years of transparency [12]. Although the causes of chronic corneal dysfunction are not very clear at present, literature and experimental data show that it has a certain relationship with cellular immune. After the graft is observed to be clear without any sign of immune rejection by slit-lamp microscopy, the results of confocal microscopy may be ignored. Confocal microscopy was used in our study to observe pathomorphological changes of clear central corneal grafts after PK for objective evaluation of graft changes.

Considering the neurological aspect, we mainly focused on subepithelial plexus nerves. Corneal nerves have an important function of ocular surface feeling and can also release all kinds of nutrients, like substance P and pituitary adenylate cyclase activating polypeptide, which promote the steady state of epithelium, and activation of tear secretion and blink reflex, so as to maintain the integrity of the structure and functional role of the ocular surface [21, 22]. Moreover, corneal nerves can promote corneal epithelial cell proliferation and migration and adjust the differentiation and proliferation of stem cells of corneal limbus by conducting the growth factor signals-β and completing repair of the graft

[23]. It has been proved that nerve regeneration is very slow after PK no matter in what species, and the sensation of the cornea is difficult to fully recover. The transplanted cornea nerve rupture may cause the slow regeneration. Regeneration of postoperative matrix is incomplete, and the sensitivity of the corneal central nerve is closely correlated with the morphology and density of the substrate nerve [24, 25]. The short nerves may produce fewer neuropeptides, leading to the random pattern.

Normal corneal stromal cells are stable and do not differentiate or proliferate. The number of stromal cells was remarkably decreased after keratoplasty in our series, suggesting an instable state. We supposed some stromal cells may be removed by the immune cells. Stromal haze may be an important phenomenon of keratocytes, corresponding to accumulation of amorphous acellular reflective structures and the results of fibrosis. Stromal cells are the main components of normal corneal stroma, responsible for the synthesis of collagens and extracellular matrix and playing a quite important role in maintaining corneal transparency [26]. When amorphous acellular reflective materials are reduced, the recognizable stromal cells are gradually increased. During the regenerative repair of cornea, stromal cells also can enter the corneal injury by proliferative migration instead of transforming to repair-type fibroblasts [27, 28]. The stromal scar and the changing shapes of nuclei may hint stromal cells in the "state of stress."

Corneal endothelium is the most important layer of the graft. In our study, when the number of endothelial cells declined, corneal edema and opacification occurred and affected the visual quality. This was consistent with the results of the study by Bourne [17]. Chronic corneal allograft dysfunction is mainly characterized by the loss of endothelial cells and changes in the morphology of endothelial cells. But no obvious immune rejection was found in our patients. Patel et al. [18] performed confocal microscopy to examine the cornea in 505 patients with different eye diseases. They found that among 17 patients treated by PK, reflection of endothelial nuclei can be observed in 9 patients (53%), and endothelial cells declined faster than the physiological speed [29]. It was reported that the defected cell area was mainly filled with migrated and enlarged cells from the surrounding area [29]. Some investigators speculated that the increased area of endothelial cells or stretching of the cells would lead to a thinner endothelial cell layer and fewer contents of cytoplasm per unit area. This is a kind of compensatory mechanism of cells. In endothelial cells with an increased area, reflection of dual cores and even multiple cores appeared in our series. This may be a phenomenon of cell fusion. Morphological changes of corneal endothelial cell nuclei may affect the refraction of light, making bright reflection of endothelial nucleus be directly observed under a confocal microscope [27, 30]. These phenomena may also hint the graft after PK in a state of stress.

Both the occurrence time of immune rejection after corneal transplantation and whether the immune cells are involved in the rejection remain controversial. Corneas are allosomes with good histocompatibility. It seems impossible if there is no presence of immune cells. However, we did not find a large number of immune cells or inflammatory cells in the patients at the end stage of retransplantation by ultrastructure observation of the corneal transplant. Therefore, detection of the immune cells in vivo had great significance in guiding the clinical medication. We noticed that not all grafts were adhered with activated immune cells (especially LCs). The results were roughly consistent with the previous reports [11, 28, 31]. Apparent immune cells were found in only 16% of the patients, suggesting that some patients were still affected. Immunosuppressants are routinely applied in our hospital after PK. Patients with a regular follow-up are given low concentrations of corticosteroid eye drops or immune inhibitors, which may reduce the number of immune cells in the grafts. Active immune cells invade the corneal graft bed from the vascular network of corneoscleral limbus and migrate to the corneal graft [32]. The decreasing number of corneal nerves and keratocytes indicates the graft may have chronic inflammation and be in the state of stress. These immune cells are not enough to cause a clinical visible immune rejection episode, but they may cause chronic damage to corneal grafts and gradually decrease the cell function. Adhesion mechanism of immune cells has not been clearly identified, and further investigations are needed. In our study, the patients were scheduled to follow-up every three months. But some patients failed to present in time. Therefore, data were not complete.

In summary, the subepithelial plexus nerves, keratocytes, and endothelial cells may significantly decline in number in the central clear graft after PK. The graft after PK is in a state of stress, affecting the normal physiological function of keratocytes and leading to the declination of graft function. Immune factors and other nonspecific factors are involved in the development of chronic dysfunction of the corneal graft.

Conflict of Interests

The authors declare that there is no conflict of interests regarding the publication of this paper.

Acknowledgments

This work is supported by National Natural Science Foundation of China (81370989, 81570821), National Basic Research Program of China (2013CB967004), Innovation Project of Shandong Academy of Medical Sciences, Taishan Scholar Program Phase II (20081148), and Shandong Provincial Excellent Innovation Team Program. The authors thank Ping Lin for her linguistic and editorial assistance.

References

[1] D. J. Coster and K. A. Williams, "Transplantation of the cornea," *The Medical Journal of Australia*, vol. 157, no. 6, pp. 405–408, 1992.

[2] A. J. T. George and D. F. P. Larkin, "Corneal transplantation: the forgotten graft," *American Journal of Transplantation*, vol. 4, no. 5, pp. 678–685, 2004.

[3] C. B. Cosar, P. R. Laibson, E. J. Cohen, and C. J. Rapuano, "Topical cyclosporine in pediatric keratoplasty," *Eye & Contact Lens*, vol. 29, no. 2, pp. 103–107, 2003.

[4] L. Xie, W. Shi, Z. Wang, J. Bei, and S. Wang, "Effect of a cyclosporine a delivery system in corneal transplantation," *Chinese Medical Journal*, vol. 115, no. 1, pp. 110–113, 2002.

[5] A. Reis, M. Megahed, T. Reinhard, E. Godehardt, C. Braunstein, and R. Sundmacher, "Synergism of RAD and cyclosporin A in prevention of acute rat corneal allograft rejection," *Cornea*, vol. 21, no. 1, pp. 81–84, 2002.

[6] R. A. Mills, D. B. Jones, C. R. Winkler, G. W. Wallace, and K. R. Wilhelmus, "Topical FK-506 prevents experimental corneal allograft rejection," *Cornea*, vol. 14, no. 2, pp. 157–160, 1995.

[7] W. Shi, T. Liu, L. Xie, and S. Wang, "FK506 in a biodegradable glycolide-co-clatide-co-caprolactone polymer for prolongation of corneal allograft survival," *Current Eye Research*, vol. 30, no. 11, pp. 969–976, 2005.

[8] W. Shi, H. Gao, L. Xie, and S. Wang, "Sustained intraocular rapamycin delivery effectively prevents high-risk corneal allograft rejection and neovascularization in rabbits," *Investigative Ophthalmology & Visual Science*, vol. 47, no. 8, pp. 3339–3344, 2006.

[9] T. Reinhard, A. Reis, D. Böhringer et al., "Systemic mycophenolate mofetil in comparison with systemic cyclosporin A in high-risk keratoplasty patients: 3 years' results of a randomized prospective clinical trial," *Graefe's Archive for Clinical and Experimental Ophthalmology*, vol. 239, no. 5, pp. 367–372, 2001.

[10] H.-Q. Gong, H. Gao, L.-X. Xie, and W.-Y. Shi, "Ultrastructure changes in chronic corneal allograft dysfunction after penetrating keratoplasty," *Chinese Journal of Ophthalmology*, vol. 43, no. 4, pp. 307–312, 2007.

[11] K. D. Bell, R. J. Campbell, and W. M. Bourne, "Pathology of late endothelial failure: late endothelial failure of penetrating keratoplasty: study with light and electron microscopy," *Cornea*, vol. 19, no. 1, pp. 40–46, 2000.

[12] R. F. Guthoff, H. Wienss, C. Hahnel, and A. Wree, "Epithelial innervation of human cornea: a three-dimensional study using confocal laser scanning fluorescence microscopy," *Cornea*, vol. 24, no. 5, pp. 608–613, 2005.

[13] R. F. Guthoff, A. Zhivov, and O. Stachs, "In vivo confocal microscopy, an inner vision of the cornea—a major review," *Clinical & Experimental Ophthalmology*, vol. 37, no. 1, pp. 100–117, 2009.

[14] R. Alzubaidi, M. S. Sharif, R. Qahwaji, S. Ipson, and A. Brahma, "In vivo confocal microscopic corneal images in health and disease with an emphasis on extracting features and visual signatures for corneal diseases: a review study," *The British Journal of Ophthalmology*, vol. 100, no. 1, pp. 41–55, 2016.

[15] E. Villani, C. Baudouin, N. Efron et al., "In vivo confocal microscopy of the ocular surface: from bench to bedside," *Current Eye Research*, vol. 39, no. 3, pp. 213–231, 2014.

[16] Y. Shao, J. Chen, Z. Wang, and S. Zhou, "A three years follow-up study on microkeratome associated deep lamellar endothelial keratoplasty," *Yan Ke Xue Bao*, vol. 22, no. 2, pp. 65–97, 2006.

[17] W. M. Bourne, "Cellular changes in transplanted human corneas," *Cornea*, vol. 20, no. 6, pp. 560–569, 2001.

[18] D. V. Patel, Y. S. Phua, and C. N. J. McGhee, "Clinical and microstructural analysis of patients with hyper-reflective corneal endothelial nuclei imaged by in vivo confocal microscopy," *Experimental Eye Research*, vol. 82, no. 4, pp. 682–687, 2006.

[19] H. Gao, W. Shi, H. Gong, Y. Wang, Y. Wang, and L. Xie, "Establishment of a murine model of chronic corneal allograft dysfunction," *Graefe's Archive for Clinical and Experimental Ophthalmology*, vol. 248, no. 10, pp. 1437–1445, 2010.

[20] W. J. Armitage, A. D. Dick, and W. M. Bourne, "Predicting endothelial cell loss and long-term corneal graft survival," *Investigative Ophthalmology & Visual Science*, vol. 44, no. 8, pp. 3326–3331, 2003.

[21] D.-Q. Li and S. C. G. Tseng, "Three patterns of cytokine expression potentially involved in epithelial-fibroblast interactions of human ocular surface," *Journal of Cellular Physiology*, vol. 163, no. 1, pp. 61–79, 1995.

[22] T. Møller-Pedersen, H. F. Li, W. M. Petroll, H. D. Cavanagh, and J. V. Jester, "Confocal microscopic characterization of wound repair after photorefractive keratectomy," *Investigative Ophthalmology & Visual Science*, vol. 39, no. 3, pp. 487–501, 1998.

[23] B. E. Frueh, R. Cadez, and M. Böhnke, "In vivo confocal microscopy after photorefractive keratectomy in humans. A prospective, long-term study," *Archives of Ophthalmology*, vol. 116, no. 11, pp. 1425–1431, 1998.

[24] M. P. Calvillo, J. W. McLaren, D. O. Hodge, and W. M. Bourne, "Corneal reinnervation after LASIK: prospective 3-year longitudinal study," *Investigative Ophthalmology & Visual Science*, vol. 45, no. 11, pp. 3991–3996, 2004.

[25] S. J. Lee, J. K. Kim, K. Y. Seo, E. K. Kim, and H. K. Lee, "Comparison of corneal nerve regeneration and sensitivity between LASIK and laser epithelial keratomileusis (LASEK)," *American Journal of Ophthalmology*, vol. 141, no. 6, pp. 1009–1015, 2006.

[26] K. Kawamoto and H. Matsuda, "Nerve growth factor and wound healing," *Progress in Brain Research*, vol. 146, pp. 369–384, 2004.

[27] T. Reinhard, A. Böcking, N. Pomjanski, and R. Sundmacher, "Immune cells in the anterior chamber of patients with immune reactions after penetrating keratoplasty," *Cornea*, vol. 21, no. 1, pp. 56–61, 2002.

[28] L. W. Hirst and W. J. Stark, "Clinical specular microscopy of corneal endothelial rejection," *Archives of Ophthalmology*, vol. 101, no. 9, pp. 1387–1391, 1983.

[29] M. Hara, N. Morishige, T.-I. Chikama, and T. Nishida, "Comparison of confocal biomicroscopy and noncontact specular microscopy for evaluation of the corneal endothelium," *Cornea*, vol. 22, no. 6, pp. 512–515, 2003.

[30] J. P. G. Bergmanson, T. M. Sheldon, and J. D. Goosey, "Fuchs' endothelial dystrophy: a fresh look at an aging disease," *Ophthalmic & Physiological Optics*, vol. 19, no. 3, pp. 210–222, 1999.

[31] L. J. Müller, C. F. Marfurt, F. Kruse, and T. M. T. Tervo, "Corneal nerves: structure, contents and function," *Experimental Eye Research*, vol. 76, no. 5, pp. 521–542, 2003.

[32] C. F. Marfurt and S. F. Echtenkamp, "The effect of diabetes on neuropeptide content in the rat cornea and iris," *Investigative Ophthalmology & Visual Science*, vol. 36, no. 6, pp. 1100–1106, 1995.

Hindawi Publishing Corporation
BioMed Research International
Volume 2016, Article ID 4369750, 10 pages
http://dx.doi.org/10.1155/2016/4369750

Research Article

Corneal Dendritic Cell Density Is Associated with Subbasal Nerve Plexus Features, Ocular Surface Disease Index, and Serum Vitamin D in Evaporative Dry Eye Disease

Rohit Shetty,[1] Swaminathan Sethu,[2] Rashmi Deshmukh,[1] Kalyani Deshpande,[1] Arkasubhra Ghosh,[2] Aarti Agrawal,[1] and Rushad Shroff[1]

[1]*Cornea and Refractive Services, Narayana Nethralaya, Bangalore 560 010, India*
[2]*GROW Research Laboratory, Narayana Nethralaya Foundation, Bangalore 560 099, India*

Correspondence should be addressed to Rushad Shroff; rushad09@gmail.com

Received 13 November 2015; Accepted 3 January 2016

Academic Editor: Michele Iester

Dry eye disease (DED) has evolved into a major public health concern with ocular discomfort and pain being responsible for significant morbidity associated with DED. However, the etiopathological factors contributing to ocular pain associated with DED are not well understood. The current IVCM based study investigated the association between corneal dendritic cell density (DCD), corneal subbasal nerve plexus (SBNP) features, and serum vitamin D and symptoms of evaporative dry eye (EDE). The study included age and sex matched 52 EDE patients and 43 heathy controls. A significant increase in the OSDI scores (discomfort subscale) was observed between EDE (median, 20.8) and control (median, 4.2) cohorts ($P < 0.001$). Similarly, an increase in DCD was observed between EDE (median, 48.1 cells/mm^2) patients and controls (median, 5.6 cells/mm^2) ($P < 0.001$). A significant decrease in SBNP features (corneal nerve fiber length, fiber density, fiber width, total branch density, nerve branch density, and fiber area) was observed in EDE patients with OSDI score >23 ($P < 0.05$). A positive correlation was observed between DCD and OSDI discomfort subscale ($r = 0.348$; $P < 0.0003$) and SBNP features. An inverse correlation was observed between vitamin D and OSDI scores ($r = -0.332$; $P = 0.0095$) and DCD with dendritic processes ($r = -0.322$; $P = 0.0122$). The findings implicate DCD, SBNP features, and vitamin D with EDE symptoms.

1. Introduction

Dry eye disease (DED) is one of the common disorders of the eye with an estimated prevalence of 5.5%–33.7% worldwide [1]. Due to its high prevalence it is a public health concern with a significant economic burden. The hallmarks of DED include discomfort, visual disturbance, and tear film instability with potential damage to the ocular surface. It is accompanied by increased tear film osmolarity and inflammation of the ocular surface [2]. There has been widespread interest in understanding the disease and developing new treatment modalities for combating the ocular morbidity caused by it, especially the pain and discomfort associated with DED. Furthermore, in a subset of patients with DED the standard therapeutic strategies failed to alleviate the symptoms [3, 4]. Despite the knowledge available on the pathophysiological mechanisms of DED, there is a lack of substantial understanding with relevance to the etiopathology of the symptoms and their association with other in vivo clinical findings. The source of ocular discomfort or pain in DED cannot solely be explained by tear film metrics suggesting the role of other factors in causation of symptoms. Pain associated with dry eye has been described as neuropathic pain [5–7] and there have been emerging reports regarding dysfunctional ocular somatosensory nerves including the subbasal nerve plexus in ocular pain [8].

In vivo confocal microscopy (IVCM) has been extensively used to image the cornea at a cellular level both in ophthalmic clinical practice and in research. IVCM is used to study corneal diseases such as ectasias, keratitis, DED, and dystrophies [9]. Corneal nerves, epithelial cells, keratocytes, endothelial cells, and immune cells have been

demonstrated on IVCM in different ocular and systemic diseases [8–11]. IVCM studies provide valuable insights into the etiology of DED and allow longitudinal imaging and quantification of cellular changes such as dendritic cells and subbasal nerve plexus morphology in the cornea of patients over time. Studies have demonstrated an increase in the corneal dendritic cell density in patients with DED [12–14]; however, its relevance to DED symptoms is yet to be investigated. Changes in corneal nerve morphology have been reported in keratoconus [15] and dry eye including those associated with systemic conditions such as chronic migraine, rheumatoid arthritis, chronic graft-versus-host disease, and Sjogrens syndrome [16–19].

Multiple etiologies including autoimmune diseases, aging, medications, refractive surgery, habits, diet, and environmental factors have been implicated in the pathophysiology of dry eye [20]. Recently, vitamin D, a fat-soluble prohormone with the ability to modulate calcium homeostasis and immune responses, has been associated with DED [21, 22]. Furthermore, there is also growing evidence regarding the potential role of vitamin D in chronic pain [23–25]. Similar to corneal nerve density and corneal nerve morphology, there is lack of evidence regarding the role of vitamin D and DED symptoms. Hence, in the current study the association between the severity of dry eye symptoms (pain and/or discomfort), corneal dendritic cell density, corneal subbasal nerve plexus features, and serum vitamin D was determined.

2. Materials and Methods

2.1. Study Population. The study was approved by the Ethics Committee of Narayana Nethralaya Hospital and was performed in accordance with the guidelines of the Declaration of Helsinki. Informed consent of study subjects was obtained at the time of enrollment. The subjects for this cross-sectional study to investigate the association between symptoms severity (pain or discomfort) and corneal dendritic cell density and corneal subbasal nerve plexus changes using in vivo confocal microscopy (IVCM) in evaporative dry eye (EDE) were selected from patients who presented to the Cornea Clinic at Narayana Nethralaya, Bangalore, India. A total of 52 patients (23 males and 29 females) who presented to our clinic with symptoms of EDE were included in the evaporative dry eye (EDE) group and 43 healthy volunteer subjects constituted the control group.

A thorough medical history was elicited to rule out any other ocular and systemic comorbidity, following which visual acuity, refraction, detailed slit-lamp and fundus evaluation, and DED investigations were performed. All the tests were performed under ambient conditions of temperature and humidity. A hanging drop of 1% fluorescein stain from fluorescein strip (ContaCare Ophthalmics and Diagnostics, India) was instilled in the cul-de-sac of the conjunctiva to measure the tear film break-up time (TBUT) in seconds and corneal and conjunctival epithelial staining, if present. Schirmer's test without anaesthetic was performed using sterile Schirmer's strips—Whatman filter paper (5×35-mm^2, ContaCare Ophthalmics and Diagnostics, India). Schirmer strips were placed in the lower conjunctival sac at the junction of the lateral and middle thirds, without instilling anaesthesia. All patients were seated at rest with their eyes closed. Meibomian gland status was examined using infrared meibography (Oculus, Wetzlar, Germany) and was scored based on the loss of meibomian glands for each eyelid [26]. Patient ocular pain or discomfort was graded using ocular surface disease index (OSDI) questionnaire and the total OSDI scores were further classified into discomfort- and vision-related subscales [27]. Based on OSDI scores, the severity of symptoms can be grouped as normal (OSDI score of 0–12), mild (OSDI score of 13–22), moderate (OSDI score of 23–32), or severe (OSDI score of 33–100) [28]. Patients with OSDI scores indicating symptoms of dry eye, normal Schirmer's test values, and low TBUT were categorized as EDE. The control group included age matched healthy volunteers with Schirmer's test values > 10 mm and TBUT > 5 seconds and no symptoms of dry eye and other ocular conditions. Exclusion criteria include the use of contact lenses, the presence of drug allergy or ocular or systemic diseases with ocular manifestations such as Sjogren's syndrome, rheumatoid arthritis, and diabetes mellitus. Patients with disorders involving the lacrimal gland (congenital alacrimia, Steven-Johnson syndrome) and lid disorders including clinically evident meibomian gland dysfunction along with patients using topical medication were also excluded.

2.2. In Vivo Confocal Microscopy. IVCM imaging was performed using Rostock Corneal Module/Heidelberg Retina Tomograph ll (RCM/HRT ll, Heidelberg Engineering GmBH, Dossenheim, Germany) [7]. The device uses a diode laser of 670 nm wavelength. 0.5% proparacaine drops were used to anaesthetize the cornea before the procedure. Study subjects were asked to fixate on a distant target such as to enable examination of the central cornea. The central cornea was scanned in a single area at a desired depth. A drop of 0.5% moxifloxacin was instilled after the procedure. Image acquisition time was approximately 2 minutes per eye, and none of the subjects experienced any visual symptoms or corneal complications as a result of this examination. Both eyes were included for IVCM based investigations in the subjects of EDE cohort, whereas only one eye (right) was included for the control group.

2.3. Corneal Subbasal Nerve Plexus and Dendritic Cell Density Assessments. An experienced masked observer selected five representative IVCM frames for corneal subbasal nerves and dendritic cells image based analyses. Images of the subbasal nerve plexus from the center of the cornea (Figure 1(a)) were assessed for each subject and for all the images the entire frame of 400×400 microns^2 was used for analysis. Quantitative analyses of the nerve fibers were performed using Automatic CCMetrics software, version 1.0 (University of Manchester, UK) [29–33]. The parameters quantified as shown in Figure 1(b) include corneal nerve fiber density (CNFD), the total number of major nerves per square millimeter; corneal nerve fiber length (CNFL), the total length of all nerve fibers and branches (millimeters per square millimeter); corneal nerve branch density (CNBD),

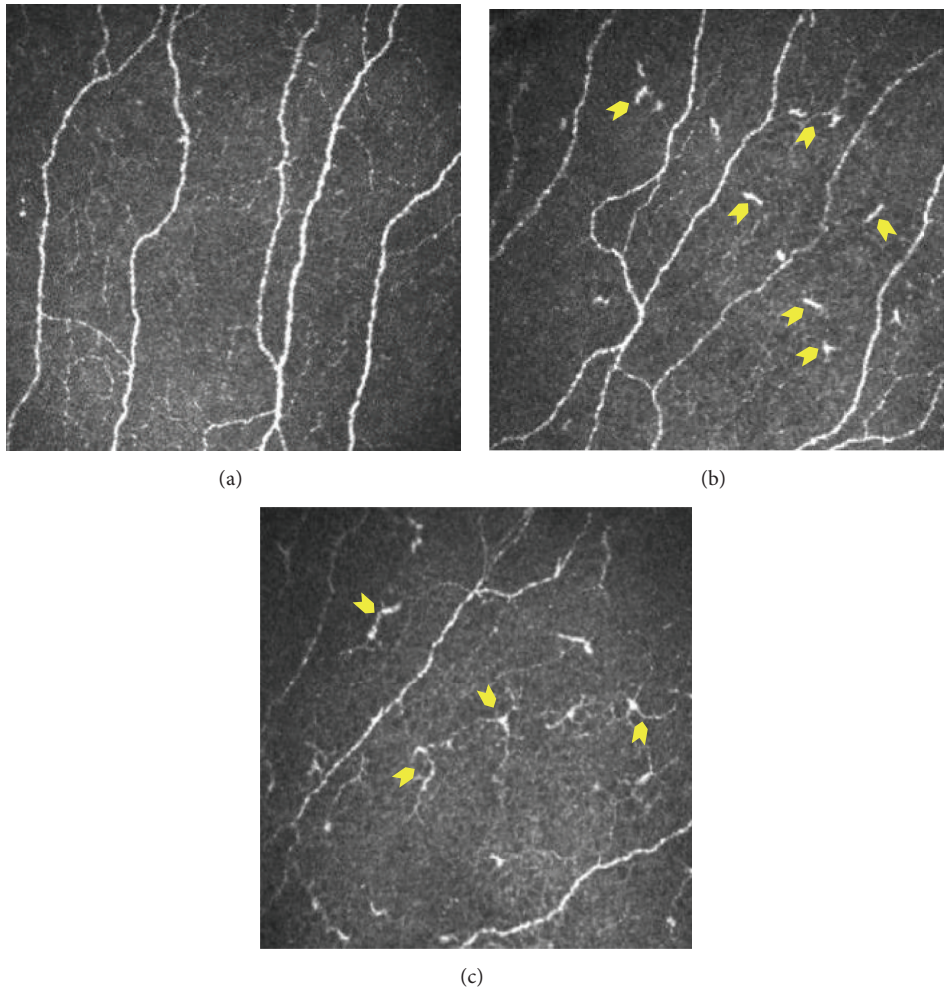

(a) (b) (c)

Figure 1: Dendritic cells at the level of subbasal nerve plexus in the cornea. Subbasal nerve plexus without dendritic cells (DCs) in a healthy control eye (a). DCs without dendritic process (b) and with dendritic processes (c) in dry eye patients. Panels shown are representative IVCM images with frame size 400 × 400 microns at a depth of 45 microns.

number of branches emanating from major nerve trunks per square millimeter; total branch density (CTBD), the total number of branch points per square millimeter; the nerve fiber area (CNFA) and the total nerve fiber area per square millimeter; and the corneal nerve fiber width (CNFW), the average nerve fiber width per square millimeter [29–31]. Dendritic cells (cells/mm^2) were quantified using Cell Count software (Heidelberg Engineering GmbH) by identifying bright individual dendriform structures with cell bodies in each image at the level of basal epithelium or at subbasal nerve plexus [34]. Cells were included after assessment of two sides of the image for cells that overlapped with the edge of the frame. Bright cell bodies with and without dendritic processes or extensions were also identified (Figure 2). The images were analyzed by two blinded observers and the average of the values was used for statistical analysis.

2.4. Measurement of Serum Vitamin D. Serum was isolated from peripheral venous blood by using BD Vacutainer® Plus Plastic Serum Tubes (BD, New Jersey, USA). Total vitamin D—25 (OH) vitamin D levels—in the serum was measured by direct competitive chemiluminescent enzyme linked immunoassay (Euroimmun, Medizinische Labordiagnostika AG, Germany) that detects both 25 (OH) vitamins D_2 and D_3. The measurements were performed according to manufacturer's instructions.

2.5. Statistical Analysis. All statistical analyses were performed with MedCalc® version 12.5 (MedCalc Software bvba, Belgium) and GraphPad Prism 6.0 (GraphPad Software, Inc., La Jolla, CA, USA). Shapiro-Wilk normality test was done to check the distribution of the data set following which Spearman correlations analysis and Mann-Whitney test were used for further analyses. $P < 0.05$ was considered to be statistically significant. Data are represented as both mean ± SEM and median with range.

3. Results

Parameters such as TBUT, ocular surface disease index, corneal dendritic cell density (DCD), and corneal subbasal

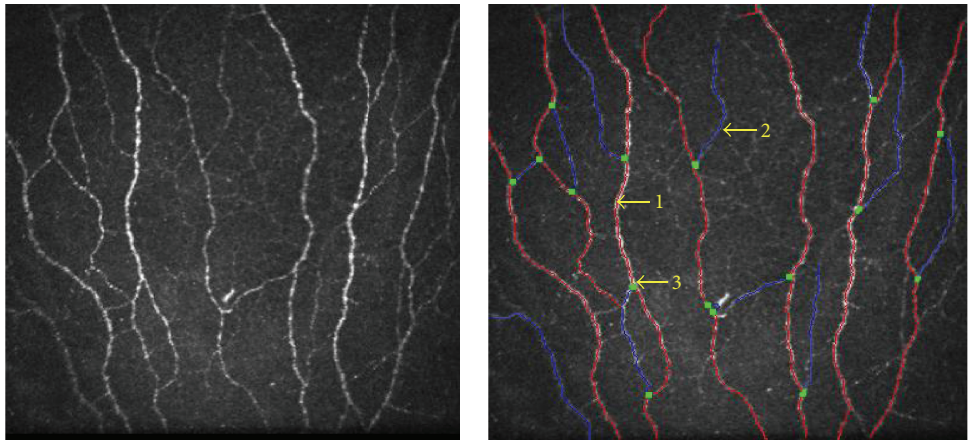

(a) (b)

Figure 2: Morphological assessment of corneal subbasal nerve plexus. (a) Subbasal nerve plexus morphology as seen in a raw IVCM image. (b) Automated analysis of (a) using CC metrics software version 1.0 (University of Manchester, UK). "1" indicates the main nerve fibers highlighted in red. "2" denotes nerve fiber branches in blue. "3" as shown as green dots indicates branch points. Panels shown are representative IVCM images with frame size 400 × 400 microns at a depth of 50 microns.

nerve plexus features were measured and analyzed in 43 (43 eyes) healthy controls and 52 (104 eyes) patients with EDE. The study subjects were age and gender matched. The ages between control (median 41 years; range 22–78 years) and EDE (median 44.5 years; range 19–73 years) cohort were not significantly different. Gender distribution (male/female) between the control and EDE cohort was 14M/29F and 23M/29F, respectively. TBUT was significantly lower in EDE subjects compared to controls (Table 1(a)). Total OSDI scores including discomfort- and vision-related OSDI subscales were observed to be significantly higher in the EDE cohort (Table 1(a)). An inverse correlation was observed between TBUT with total OSDI score ($r = -0.32$; $P = 0.0009$) and discomfort- ($r = -0.354$; $P = 0.0002$) and vision-related OSDI subscale ($r = -0.197$; $P = 0.04$).

IVCM investigations revealed the presence of corneal dendritic cells (DCs) in EDE (Figure 2). Image based analyses revealed a significant increase in corneal dendritic cell (DC) density and subsets (DCs with and without dendritic processes) in the eyes of EDE patients compared to controls (Table 1(a)). Analysis of subbasal nerve plexus features (as listed in Table 1(a)) from IVCM images revealed no significant difference between the study groups. However, significant decrease in nerve features such as nerve fiber length, branch points, and number of nerve branches was observed in EDE patients with moderate-to-severe OSDI scores (OSDI score > 23) compared to EDE patients with mild or normal OSDI scores (OSDI score < 23) and controls (Table 1(b)). In addition, number of major nerves and nerve fiber width were significantly lower in EDE patients with moderate-to-severe OSDI score compared to controls (Table 1(b)). OSDI score, specifically pain or discomfort-related subscale, exhibited a positive correlation with total corneal DC density, as well as density of DCs with and without dendritic process in EDE patients (Table 2). However, no correlation was observed between total OSDI score and vision-related OSDI subscale and corneal dendritic cell density in EDE patients (Table 2). Similarly, no association was observed between the various subbasal nerve plexus features and OSDI scores and subscale scores in EDE (Table 2). Nevertheless, a significant association between the corneal DC density (total, with and without dendritic process) and various subbasal nerve plexus features in EDE cohort was also observed as shown in Table 3. Furthermore, on many occasions a close proximity between DCs and the nerve fibers was observed in the EDE patients (Figure 3).

In addition, the relationship between serum vitamin D status and the various parameters studied was also investigated. The median serum vitamin D level in the EDE cohort ($n = 30$) was 16.4 ng/mL (range 5.8–61.9 ng/mL). Analyses demonstrated an inverse correlation between serum vitamin D level and OSDI scores—total and discomfort- and vision-related subscales (Table 4). The density of corneal DCs with dendritic process revealed an inverse correlation with serum vitamin D in EDE patients (Table 4). However, no associations were observed between serum vitamin D and total corneal DC density, DCs without dendritic process, or subbasal nerve plexus features in the EDE cohort (Table 4).

4. Discussion

The persistence of ocular pain and discomfort in a subset of patients with DED following standard therapeutic strategies as well as the lack of tear film metrics to predict this population poses a major challenge in the management of DED. It is therefore imperative to identify diagnostic modalities that can accurately predict patients whose symptoms may not resolve with conventional therapy or may require additional dietary or environmental interventions along with topical therapy to ensure a favourable prognosis. IVCM used to study architecture of the cornea in dry eye and other ocular conditions can provide additional predictive information

Table 1: (a) Study parameters between control and EDE cohort. (b) Subbasal nerve plexus feature differences based on severity of symptoms in EDE patients.

(a)

	Control (n = 43; 43 eyes)			EDE (n = 52; 104 eyes)			P value
	Mean	Median	Range	Mean	Median	Range	
OSDI							
Total	15.0 ± 1.5	14.9	0–38.5	28.1 ± 2.5	20.8	2.1–68.8	0.0005*
OSDI—discomfort	4.5 ± 0.5	4.2	0–12.5	32.6 ± 3.2	20.8	4.2–83.3	<0.0001*
OSDI—vision	6.4 ± 0.8	8.3	0–20.8	23.5 ± 2.4	20.8	0–70.8	<0.0001*
TBUT	10.7 ± 0.3	10	7–15	7.0 ± 0.2	7	1–12	<0.0001*
Dendritic cells							
Total cells (cells/mm^2)	9.1 ± 1.3	5.6	0–36.8	52.9 ± 4.0	48.1	7–261.2	<0.0001*
DCs with dendrites (cells/mm^2)	1.0 ± 0.2	0	0–4	13.0 ± 1.2	8.5	0–54.6	<0.0001*
DCs without dendrites (cells/mm^2)	8.1 ± 1.2	5.2	0–35.4	39.9 ± 3.2	29.8	7–235	<0.0001*
Subbasal nerve plexus							
CNFL (length in mm/mm^2)	17.0 ± 0.4	17.7	7.1–22.3	16.5 ± 0.3	16.27	8.09–22.98	ns
CNFD (major nerves/mm^2)	28.6 ± 0.8	29.7	12.5–40	27.2 ± 0.6	27.5	5–43.75	ns
CNFW (average nerve fiber width/mm^2)	0.0211 ± 0.0002	0.0209	0.0186–0.0254	0.0211 ± 0.00009	0.021	0.0184–0.0237	ns
CTBD (branch points/mm^2)	58.4 ± 3.2	58.75	3.7–103.7	56.8 ± 2.5	52.5	15–123.7	ns
CNBD (number of branches/mm^2)	40.9 ± 2.3	42.35	1.2–83.7	39.0 ± 1.7	37.5	3.75–81.24	ns
CNFA (total nerve fiber area/mm^2)	0.0066 ± 0.0002	0.0066	0.002–0.0111	0.0068 ± 0001	0.00665	0.0034–0.0134	ns

EDE: evaporative dry eye; OSDI: ocular surface disease index; TBUT: tear break-up time; DCs: dendritic cells; CNFL: corneal nerve fiber length; CNFD: corneal nerve fiber density; CNFW: corneal nerve fiber width; CTBD: corneal total branch density; CNBD: corneal nerve branch density; CNFA: corneal nerve fiber area; ns: not statistically significant; * P value compared to controls (Mann-Whitney test).

(b)

	EDE (OSDI score < 23) n = 58 eyes			P value	EDE (OSDI score > 23) n = 46 eyes			P value
	Mean	Median	Range		Mean	Median	Range	
Subbasal nerve plexus								
CNFL (length in mm/mm^2)	16.9 ± 0.3	17.7	7.1–22.3	ns*	15.9 ± 0.4	15.8	8.09–22.3	0.0165*; 0.04#
CNFD (major nerves/mm^2)	27.9 ± 0.7	28.7	15–42.5	ns*	26.2 ± 1.0	27.5	5–43.75	0.0447*; ns#
CNFW (average nerve fiber width/mm^2)	0.0210 ± 0.0001	0.021	0.0193–0.0233	ns*	0.0211 ± 0.0001	0.021	0.0184–0.0237	0.6107*; ns#
CTBD (branch points/mm^2)	61.5 ± 3.5	59.3	15–123.7	ns*	50.8 ± 3.4	48.7	15–111.2	0.0398*; 0.04#
CNBD (number of branches/mm^2)	42.7 ± 2.3	41.2	11.2–81.2	ns*	34.3 ± 2.6	32.5	3.75–78.7	0.0208*; 0.01#
CNFA (total nerve fiber area/mm^2)	0.0071 ± 0.0002	0.0069	0.0035–0.0134	ns*	0.0064 ± 0002	0.0063	0.0034–0.0119	0.4098*; ns#

EDE: evaporative dry eye; OSDI: ocular surface disease index; CNFL: corneal nerve fiber length; CNFD: corneal nerve fiber density; CNFW: corneal nerve fiber width; CTBD: corneal total branch density; CNBD: corneal nerve branch density; CNFA: corneal nerve fiber area; ns: not statistically significant; * P value compared to controls (Mann-Whitney test); # P value compared to EDE—OSDI score < 23 (Mann-Whitney test).

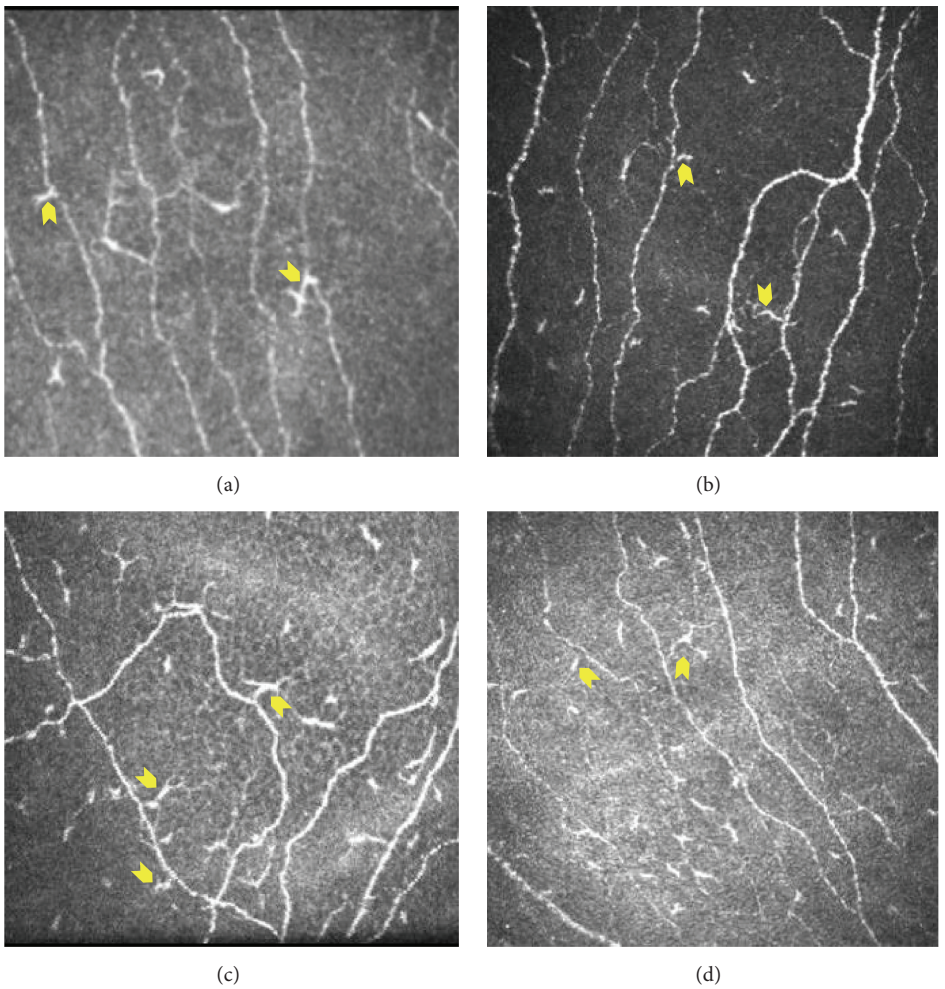

Figure 3: Anatomical localization of dendritic cells in relation to nerve fibers at the level of subbasal nerve plexus in the cornea of EDE patients. Yellow arrow indicates dendritic cells impinging or in close proximity to the nerve fibers. Panels shown are representative IVCM images from four EDE patients with frame size 400 × 400 microns at a depth of 50 microns.

Table 2: Correlation of OSDI scores with corneal dendritic cell density and corneal subbasal nerve plexus features in EDE patients.

	OSDI—discomfort		OSDI—vision		OSDI—total	
	r	P value	r	P value	r	P value
Dendritic cells						
Total cells (cells/mm^2)	**0.348**	**0.0003**	−0.104	0.2925	0.161	0.1028
DCs with dendrites (cells/mm^2)	**0.274**	**0.0048**	−0.039	0.6937	0.126	0.2016
DCs without dendrites (cells/mm^2)	**0.347**	**0.0003**	−0.118	0.2335	0.162	0.0999
Subbasal nerve plexus						
CNFL (length in mm/mm^2)	0.148	0.1342	0.079	0.427	0.157	0.112
CNFD (major nerves/mm^2)	0.097	0.3292	0.167	0.0897	0.153	0.1215
CNFW (average nerve fiber width/mm^2)	0.009	0.9247	0.009	0.9259	0.027	0.7824
CTBD (branch points/mm^2)	0.124	0.2101	0.009	0.9249	0.102	0.3027
CNBD (number of branches/mm^2)	0.094	0.3411	0.073	0.459	0.117	0.2352
CNFA (total nerve fiber area/mm^2)	0.18	0.067	−0.103	0.2991	0.07	0.4787

OSDI: ocular surface disease index; DCs: dendritic cells; CNFL: corneal nerve fiber length; CNFD: corneal nerve fiber density; CNFW: corneal nerve fiber width; CTBD: corneal total branch density; CNBD: corneal nerve branch density; CNFA: corneal nerve fiber area; r: Spearman correlation coefficient.

Table 3: Correlation between corneal dendritic cell density and corneal subbasal nerve plexus features in EDE patients.

Subbasal nerve plexus	Dendritic cells					
	DCs with dendrites		DCs without dendrites		Total DCs	
	r	*P* value	*r*	*P* value	*r*	*P* value
CNFL (length in mm/mm^2)	0.004	0.9705	0.036	0.7147	0.028	0.7752
CNFD (major nerves/mm^2)	**−0.223**	**0.0229**	−0.177	0.0723	**−0.213**	**0.03**
CNFW (average nerve fiber width/mm^2)	**0.277**	**0.0044**	0.169	0.0855	**0.228**	**0.0201**
CTBD (branch points/mm^2)	**0.213**	**0.0299**	**0.219**	**0.0254**	**0.244**	**0.0124**
CNBD (number of branches/mm^2)	0.066	0.505	0.109	0.272	0.108	0.2737
CNFA (total nerve fiber area/mm^2)	**0.419**	**<0.0001**	**0.427**	**<0.0001**	**0.463**	**<0.0001**

OSDI: ocular surface disease index; DCs: dendritic cells; CNFL: corneal nerve fiber length; CNFD: corneal nerve fiber density; CNFW: corneal nerve fiber width; CTBD: corneal total branch density; CNBD: corneal nerve branch density; CNFA: corneal nerve fiber area; *r*: Spearman correlation coefficient.

Table 4: Association of serum vitamin D with OSDI score, corneal dendritic cell density, and corneal subbasal nerve plexus features in EDE patients.

	Serum vitamin D level	
	r	*P* value
OSDI score		
OSDI—total	**−0.332**	**0.0095**
OSDI—discomfort	**−0.375**	**0.0032**
OSDI—vision	**−0.289**	**0.025**
Dendritic cells		
Total cells (cells/mm^2)	−0.184	0.1589
DCs with dendrites (cells/mm^2)	**−0.322**	**0.0122**
DCs without dendrites (cells/mm^2)	−0.099	0.45
Subbasal nerve plexus		
CNFL (length in mm/mm^2)	−0.004	0.9749
CNFD (major nerves/mm^2)	0.037	0.777
CNFW (average nerve fiber width/mm^2)	−0.083	0.5267
CTBD (branch points/mm^2)	−0.094	0.4742
CNBD (number of branches/mm^2)	−0.007	0.96
CNFA (total nerve fiber area/mm^2)	−0.011	0.9334

OSDI: ocular surface disease index; DCs: dendritic cells; CNFL: corneal nerve fiber length; CNFD: corneal nerve fiber density; CNFW: corneal nerve fiber width; CTBD: corneal total branch density; CNBD: corneal nerve branch density; CNFA: corneal nerve fiber area; *r* – Spearman correlation coefficient.

such as corneal DCD and SBNP features which are altered in DED. In our study, we observed a significant association between OSDI scores especially the discomfort subscale with corneal DCD. Despite the absence of correlation between the decreased SBNP features and OSDI in EDE patients, we did observe a significant decrease in a subset of EDE patients with moderate-to-severe OSDI. Furthermore, a significant different correlation was also observed between DCD and SBNP features. These observations implicate the changes in DCD and SBNP morphology with symptoms observed in EDE.

Reports on subbasal nerve plexus have revealed conflicting findings. Benítez-Del-Castillo et al. showed a significant decrease in the nerve density in patients with dry eye [19] which is similar to what we have observed in the current study. Similar observations were made in other studies on dry eye with relation to chronic migraine and chronic graft-versus-host disease [16, 17]. However, Hoçal et al. reported no difference in subbasal nerve density whereas Zhang et al. demonstrated increased corneal nerve density in patients with dry eye [35, 36]. The variations observed could be due to the influence of the underlying disease. A recent report demonstrated a positive correlation between changes in subbasal nerve morphology features (decrease in CNFL, CNFD, and CNBD) and pain in patients with diabetic neuropathy [37]. Similary, in our current study we have also observed a significant decrease in various nerve features in EDE patients with moderate-to-severe symptoms, thus suggesting the use of corneal nerve morphological features as a predictor of the presence of pain in EDE patients. The mechanistic basis of this association is necessary to validate this observation. Neuropathic pain such as dysesthesias and hyperalgesia in dry eye patients can be due to either peripheral sensitization of neurons or damage to free nerve endings that interdigitate between superficial epithelial cells and are exposed to environmental and/or inflammatory stimuli. The presence of inflammation has also been found to directly and indirectly affect the structure and function of peripheral

nerves resulting in altered nociception [38]. On the other hand excited nerve fibers can secrete neuropeptides which in turn trigger a neurogenic inflammatory response.

The role of dendritic cells in modulation of nociception and pain has been previously studied [39, 40]. Dendritic cells play a role in immunomodulation and in antigen presentation and may influence pain pathways through their effect on T helper cells. Studies have described a possible role for corneal dendritic cells in the etiopathogenesis of dry eye, keratoconjunctivitis sicca, and corneal allograft rejection [41, 42]. Inflammatory pathologies show an increase in the number of dendritic cells in the cornea [43]. Lin et al. demonstrated an increase in dendritic cells in the anterior stroma along with activation of epithelial dendritic cells as documented by the presence of more dendrites in the center of the cornea [44]. In our study the significant increase in the corneal dendritic cells observed in EDE patients was found to have positive association with the OSDI discomfort-related subscale scores and not vision-related OSDI scores. The current study also reports a differential association between corneal dendritic cells and SBNP features in EDE. Tuisku et al. demonstrated altered stromal corneal nerves and the presence of increased antigen presenting cells in patients with dry eye. They proposed that these changes were responsible for dysesthesia experienced by the patient in dry eye disease. In their study, however, they did not describe association between the dendritic cell density and changes in the corneal nerves [45]. We propose that an increase in inflammatory cells and the associated changes in subbasal nerve plexus may be responsible for ocular discomfort experienced by patients in our cohort. Furthermore, an increase in the number of dendritic cells in close proximity to the subbasal nerves was observed in patients with severe symptoms. Whether DC-mediated inflammatory or physical irritation of the nerve or changes in nerve physiology are responsible for pain in these patients needs to be determined. Therefore, this incidental observation warrants further investigation.

Vitamin D and its role in the etiopathogenesis of dry eye disease have been the subject of many recent research publications. Studies have demonstrated the association of vitamin D deficiency with DED [21, 22, 25]. In the current study we observed a strong inverse correlation between the OSDI scores and vitamin D levels in the EDE cohort. Earlier reports have suggested vitamin D deficiency to be associated with neuralgia and chronic pain [23, 25]. Vitamin D exhibits anti-inflammatory and immunoregulatory properties and its deficiency results in inflammatory or immune mediated dryness of the eyes. Apart from its effect on tear film indices, the impact of vitamin D levels on ocular pain or discomfort has not been explored in detail. Vitamin D can influence the severity of symptoms by modulating nociception by regulating nerve homeostasis and inflammatory responses. The exact mechanism linking vitamin D to pain remains elusive; however several theories have been put forward. Serotonin which can perpetuate chronic pain response was found to be high in patients with DED [46] and vitamin D is known to affect serotonin synthesis [47] indicating a role of vitamin D in nociception. Studies have shown that vitamin D decreases production of nitric oxide, a nociceptive neurotransmitter, thereby modulating pain [48, 49]. Vitamin D and its agonists have been found to inhibit maturation and induce tolerance in dendritic cells resulting in the arrest of inflammatory processes [50]. Lower vitamin D levels were associated with an increase in DCs with dendritic processes (mature phenotyple) in our cohort which supports the current understanding regarding the immunomodulatory role of vitamin D on DCs. Vitamin D also modulates the expression of various inflammatory cytokines in various cells, including corneal epithelial cells [51] substantiating the anti-inflammatory/immunomodulatory functions of vitamin D. Our observations suggest that the increased corneal dendritic cells density and its potential effect on the subbasal nerve plexus features could contribute to the severity of symptoms in EDE. Furthermore, low vitamin D level can result in severe symptoms by directly influencing nociception on nerve fibers and/or indirectly by lack of negative regulation on DCs activation/migration and inflammatory responses. However, a more detailed mechanistic investigation is necessary to validate it.

Conflict of Interests

The authors declare no conflict of interests.

Acknowledgments

The study was funded by the Narayana Nethralaya Foundation. The authors extend their gratitude to Dr. Rayaz Malik, University of Manchester, UK, for CCMetrics Corneal Nerve Fibre Quantification software. The authors would also like to thank Dr. Abhijit Sinha-Roy, Narayana Nethralaya Foundation, Bangalore, India, for assistance with statistical analysis.

References

[1] J. A. Smith, J. Albenz, C. Begley et al., "The epidemiology of dry eye disease: report of the epidemiology subcommittee of the international Dry Eye WorkShop (2007)," *Ocular Surface*, vol. 5, no. 2, pp. 93–107, 2007.

[2] M. A. Lemp, C. Baudouin, J. Baum et al., "The definition and classification of dry eye disease: report of the definition and classification subcommittee of the international Dry Eye WorkShop (2007)," *Ocular Surface*, vol. 5, no. 2, pp. 75–92, 2007.

[3] S. N. Rao, "Topical cyclosporine 0.05% for the prevention of dry eye disease progression," *Journal of Ocular Pharmacology and Therapeutics*, vol. 26, no. 2, pp. 157–164, 2010.

[4] A. Galor, H. Batawi, E. R. Felix et al., "Incomplete response to artificial tears is associated with features of neuropathic ocular pain," *British Journal of Ophthalmology*, 2015.

[5] A. Galor, L. Zlotcavitch, S. D. Walter et al., "Dry eye symptom severity and persistence are associated with symptoms of neuropathic pain," *British Journal of Ophthalmology*, vol. 99, no. 5, pp. 665–668, 2015.

[6] P. Rosenthal, I. Baran, and D. S. Jacobs, "Corneal pain without stain: is it real?" *Ocular Surface*, vol. 7, no. 1, pp. 28–40, 2009.

[7] A. Galor, R. C. Levitt, E. R. Felix, E. R. Martin, and C. D. Sarantopoulos, "Neuropathic ocular pain: an important yet

underevaluated feature of dry eye," *Eye*, vol. 29, no. 3, pp. 301–312, 2014.

[8] A. Alhatem, B. Cavalcanti, and P. Hamrah, "In vivo confocal microscopy in dry eye disease and related conditions," *Seminars in Ophthalmology*, vol. 27, no. 5-6, pp. 138–148, 2012.

[9] R. L. Niederer and C. N. J. McGhee, "Clinical in vivo confocal microscopy of the human cornea in health and disease," *Progress in Retinal and Eye Research*, vol. 29, no. 1, pp. 30–58, 2010.

[10] N. Pritchard, K. Edwards, A. M. Shahidi et al., "Corneal markers of diabetic neuropathy," *Ocular Surface*, vol. 9, no. 1, pp. 17–28, 2011.

[11] D. V. Patel and C. N. J. McGhee, "In vivo laser scanning confocal microscopy confirms that the human corneal sub-basal nerve plexus is a highly dynamic structure," *Investigative Ophthalmology & Visual Science*, vol. 49, no. 8, pp. 3409–3412, 2008.

[12] E. Villani, E. Garoli, V. Termine, F. Pichi, R. Ratiglia, and P. Nucci, "Corneal confocal microscopy in dry eye treated with corticosteroids," *Optometry and Vision Science*, vol. 92, no. 9, pp. e290–e295, 2015.

[13] A. Kheirkhah, R. Rahimi Darabad, A. Cruzat et al., "Corneal epithelial immune dendritic cell alterations in subtypes of dry eye disease: a pilot in vivo confocal microscopic study," *Investigative Opthalmology & Visual Science*, vol. 56, no. 12, pp. 7179–7185, 2015.

[14] F. Machetta, A. M. Fea, A. G. Actis, U. de Sanctis, P. Dalmasso, and F. M. Grignolo, "In vivo confocal microscopic evaluation of corneal langerhans cells in dry eye patients," *The Open Ophthalmology Journal*, vol. 8, pp. 51–59, 2014.

[15] D. V. Patel and C. N. J. McGhee, "Mapping the corneal sub-basal nerve plexus in keratoconus by in vivo laser scanning confocal microscopy," *Investigative Ophthalmology & Visual Science*, vol. 47, no. 4, pp. 1348–1351, 2006.

[16] K. I. Kinard, A. G. Smith, J. R. Singleton et al., "Chronic migraine is associated with reduced corneal nerve fiber density and symptoms of dry eye," *Headache*, vol. 55, no. 4, pp. 543–549, 2015.

[17] B. Steger, L. Speicher, W. Philipp, and N. E. Bechrakis, "In vivo confocal microscopic characterisation of the cornea in chronic graft-versus-host disease related severe dry eye disease," *British Journal of Ophthalmology*, vol. 99, no. 2, pp. 160–165, 2015.

[18] E. Villani, D. Galimberti, F. Viola, C. Mapelli, N. Del Papa, and R. Ratiglia, "Corneal involvement in rheumatoid arthritis: an in vivo confocal study," *Investigative Ophthalmology and Visual Science*, vol. 49, no. 2, pp. 560–564, 2008.

[19] J. M. Benítez-Del-Castillo, M. C. Acosta, M. A. Wassfi et al., "Relation between corneal innervation with confocal microscopy and corneal sensitivity with noncontact esthesiometry in patients with dry eye," *Investigative Ophthalmology and Visual Science*, vol. 48, no. 1, pp. 173–181, 2007.

[20] J. L. Gayton, "Etiology, prevalence, and treatment of dry eye disease," *Clinical Ophthalmology*, vol. 3, no. 1, pp. 405–412, 2009.

[21] A. Galor, H. Gardener, B. Pouyeh, W. Feuer, and H. Florez, "Effect of a mediterranean dietary pattern and vitamin D levels on dry eye syndrome," *Cornea*, vol. 33, no. 5, pp. 437–441, 2014.

[22] B. E. Kurtul, P. A. Özer, and M. S. Aydinli, "The association of vitamin D deficiency with tear break-up time and Schirmer testing in non-Sjögren dry eye," *Eye*, vol. 29, no. 8, pp. 1081–1084, 2015.

[23] E. E. Shipton and E. A. Shipton, "Vitamin D deficiency and pain: clinical evidence of low levels of vitamin D and supplementation in chronic pain states," *Pain and Therapy*, vol. 4, no. 1, pp. 67–87, 2015.

[24] S. Straube, S. Derry, R. A. Moore, and H. J. McQuay, "Vitamin D for the treatment of chronic painful conditions in adults," *Cochrane Database of Systematic Reviews*, vol. 5, no. 1, Article ID CD007771, 2010.

[25] E. L. Singman, D. Poon, and A. S. Jun, "Putative corneal neuralgia responding to vitamin D supplementation," *Case Reports in Ophthalmology*, vol. 4, no. 3, pp. 105–108, 2013.

[26] R. Arita, K. Itoh, K. Inoue, and S. Amano, "Noncontact infrared meibography to document age-related changes of the meibomian glands in a normal population," *Ophthalmology*, vol. 115, no. 5, pp. 911–915, 2008.

[27] R. M. Schiffman, M. D. Christianson, G. Jacobsen, J. D. Hirsch, and B. L. Reis, "Reliability and validity of the ocular surface disease index," *Archives of Ophthalmology*, vol. 118, no. 5, pp. 615–621, 2000.

[28] K. L. Miller, J. G. Walt, D. R. Mink et al., "Minimal clinically important difference for the ocular surface disease index," *Archives of Ophthalmology*, vol. 128, no. 1, pp. 94–101, 2010.

[29] M. A. Dabbah, J. Graham, I. N. Petropoulos, M. Tavakoli, and R. A. Malik, "Automatic analysis of diabetic peripheral neuropathy using multi-scale quantitative morphology of nerve fibres in corneal confocal microscopy imaging," *Medical Image Analysis*, vol. 15, no. 5, pp. 738–747, 2011.

[30] M. Tavakoli, C. Quattrini, C. Abbott et al., "Corneal confocal microscopy: a novel noninvasive test to diagnose and stratify the severity of human diabetic neuropathy," *Diabetes Care*, vol. 33, no. 8, pp. 1792–1797, 2010.

[31] G. Bitirgen, A. Ozkagnici, B. Bozkurt, and R. A. Malik, "*In vivo* corneal confocal microscopic analysis in patients with keratoconus," *International Journal of Ophthalmology*, vol. 8, no. 3, pp. 534–539, 2015.

[32] M. Ferdousi, S. Azmi, I. N. Petropoulos et al., "Corneal confocal microscopy detects small fibre neuropathy in patients with upper gastrointestinal cancer and nerve regeneration in chemotherapy induced peripheral neuropathy," *PLoS ONE*, vol. 10, no. 10, Article ID e0139394, 2015.

[33] I. N. Petropoulos, U. Alam, H. Fadavi et al., "Rapid automated diagnosis of diabetic peripheral neuropathy with in vivo corneal confocal microscopy," *Investigative Ophthalmology & Visual Science*, vol. 55, no. 4, pp. 2071–2078, 2014.

[34] A. Kheirkhah, R. Muller, J. Mikolajczak et al., "Comparison of standard versus wide-field composite images of the corneal subbasal layer by in vivo confocal microscopy," *Investigative Opthalmology & Visual Science*, vol. 56, no. 10, pp. 5801–5807, 2015.

[35] B. M. Hoçal, N. Örnek, G. Zilelioglu, and A. H. Elhan, "Morphology of corneal nerves and corneal sensation in dry eye: a preliminary study," *Eye*, vol. 19, no. 12, pp. 1276–1279, 2005.

[36] M. Zhang, J. Chen, L. Luo, Q. Xiao, M. Sun, and Z. Liu, "Altered corneal nerves in aqueous tear deficiency viewed by in vivo confocal microscopy," *Cornea*, vol. 24, no. 7, pp. 818–824, 2005.

[37] H. Wang, D. Fan, S. Zhang, and X. Wang, "Early diagnosis of painful diabetic neuropathy by corneal confocal microscopy," *Zhonghua Yi Xue Za Zhi*, vol. 94, no. 33, pp. 2602–2606, 2014.

[38] A. Ellis and D. L. H. Bennett, "Neuroinflammation and the generation of neuropathic pain," *British Journal of Anaesthesia*, vol. 111, no. 1, pp. 26–37, 2013.

[39] Y. T. Jeon, H. Na, H. Ryu, and Y. Chung, "Modulation of dendritic cell activation and subsequent Th1 cell polarization by lidocaine," *PLOS ONE*, vol. 10, no. 10, Article ID e0139845, 2015.

[40] J. Luo, J. Feng, S. Liu, E. T. Walters, and H. Hu, "Molecular and cellular mechanisms that initiate pain and itch," *Cellular and Molecular Life Sciences*, vol. 72, no. 17, pp. 3201–3223, 2015.

[41] T. Hattori, S. K. Chauhan, H. Lee et al., "Characterization of langerin-expressing dendritic cell subsets in the normal cornea," *Investigative Ophthalmology and Visual Science*, vol. 52, no. 7, pp. 4598–4604, 2011.

[42] N. Gao, J. Yin, G. S. Yoon, Q.-S. Mi, and F.-S. X. Yu, "Dendritic cell-epithelium interplay is a determinant factor for corneal epithelial wound repair," *The American Journal of Pathology*, vol. 179, no. 5, pp. 2243–2253, 2011.

[43] P. Hamrah, Y. Liu, Q. Zhang, and M. R. Dana, "Alterations in corneal stromal dendritic cell phenotype and distribution in inflammation," *Archives of Ophthalmology*, vol. 121, no. 8, pp. 1132–1140, 2003.

[44] H. Lin, W. Li, N. Dong et al., "Changes in corneal epithelial layer inflammatory cells in aqueous tear-deficient dry eye," *Investigative Ophthalmology and Visual Science*, vol. 51, no. 1, pp. 122–128, 2010.

[45] I. S. Tuisku, Y. T. Konttinen, L. M. Konttinen, and T. M. Tervo, "Alterations in corneal sensitivity and nerve morphology in patients with primary Sjögren's syndrome," *Experimental Eye Research*, vol. 86, no. 6, pp. 879–885, 2008.

[46] P. Chhadva, T. Lee, C. D. Sarantopoulos et al., "Human tear serotonin levels correlate with symptoms and signs of dry eye," *Ophthalmology*, vol. 122, no. 8, pp. 1675–1680, 2015.

[47] R. P. Patrick and B. N. Ames, "Vitamin D and the omega-3 fatty acids control serotonin synthesis and action, part 2: relevance for ADHD, bipolar disorder, schizophrenia, and impulsive behavior," *The FASEB Journal*, vol. 29, no. 6, pp. 2207–2222, 2015.

[48] J. Bartley, "Post herpetic neuralgia, schwann cell activation and vitamin D," *Medical Hypotheses*, vol. 73, no. 6, pp. 927–929, 2009.

[49] I. Tegeder, R. Scheving, I. Wittig, and G. Geisslinger, "SNO-ing at the nociceptive synapse?" *Pharmacological Reviews*, vol. 63, no. 2, pp. 366–389, 2011.

[50] M. Barragan, M. Good, and J. Kolls, "Regulation of dendritic cell function by vitamin D," *Nutrients*, vol. 7, no. 9, pp. 8127–8151, 2015.

[51] T. Suzuki, Y. Sano, C. Sotozono, and S. Kinoshita, "Regulatory effects of 1alpha,25-dihydroxyvitamin D(3) on cytokine production by human corneal epithelial cells," *Current Eye Research*, vol. 20, no. 2, pp. 127–130, 2000.

Hindawi Publishing Corporation
BioMed Research International
Volume 2016, Article ID 5067853, 5 pages
http://dx.doi.org/10.1155/2016/5067853

Research Article

An In Vivo Confocal Microscopic Study of Corneal Nerve Morphology in Unilateral Keratoconus

Natasha Kishore Pahuja,[1] Rohit Shetty,[1] Rudy M. M. A. Nuijts,[2] Aarti Agrawal,[1] Arkasubhra Ghosh,[1] Chaitra Jayadev,[1] and Harsha Nagaraja[1]

[1]*Narayana Nethralaya Eye Hospital, Bangalore 560010, India*
[2]*Academic Hospital, Maastricht University, P.O. Box 616, 6200 MD Maastricht, Netherlands*

Correspondence should be addressed to Harsha Nagaraja; harshdr@gmail.com

Received 12 November 2015; Accepted 6 January 2016

Academic Editor: Dipika V. Patel

Purpose. To study the corneal nerve morphology and its importance in unilateral keratoconus. *Materials and Methods.* In this prospective cross-sectional study, 33 eyes of 33 patients with keratoconus in one eye (Group 3) were compared with the other normal eye of the same patients (Group 2) and 30 eyes of healthy patients (Group 1). All patients underwent detailed ophthalmic examination followed by topography with Pentacam HR and in vivo confocal microscopy (IVCM). Five images obtained with IVCM were analyzed using an automated CCmetrics software version 1.0 for changes in subbasal plexus of nerves. *Results.* Intergroup comparison showed statistically significant reduction in corneal nerve fiber density (CNFD) and length (CNFL) in Group 3 as compared to Group 1 ($p < 0.001$ and $p = 0.001$, resp.) and Group 2 ($p = 0.01$ and $p = 0.02$, resp.). Though corneal nerve fiber length, diameter, area, width, corneal nerve branch density, and corneal total branch density were found to be higher in decentered cones, only the corneal nerve branch density (CNBD) was found to be statistically significant ($p < 0.01$) as compared to centered cones. *Conclusion.* Quantitative changes in the corneal nerve morphology can be used as an imaging marker for the early diagnosis of keratoconus before the onset of refractive or topography changes.

1. Introduction

Keratoconus (KC) is characterized by stromal thinning and protrusion that leads to irregular astigmatism and altered optical performance of the cornea [1]. It has traditionally been described as a bilateral asymmetric disorder of the cornea though there are some reports on unilateral keratoconus [1–5]. The estimated frequency of the unilateral disease has been reported to range from 14.3% to 41% [1, 3]. Studying unilateral KC provides a comparative insight into disease pathogenesis as the unaffected fellow eye acts as an ideal control for the affected one with other contributing factors like atopy, genetics, and environment remaining constant for both [4, 5]. There is significant data on the management of keratoconus [6–8], with scarce literature on the mechanistic model of the disease itself. Nonetheless, abnormalities have been documented in all layers of keratoconic corneas [9, 10].

Recently, a review by Shaheen et al. [11] has highlighted the role of corneal nerves in health and disease of the cornea. A loose plexus of nerves under the Bowman's layer, formed by branches arising from the trigeminal nerve, is perforated to form the subbasal nerve plexus, where fibers of which terminate within the superficial epithelial cells as free nerve endings [12, 13]. Corneal nerves are known to regulate multiple pathways, which play crucial roles in several conditions including KC [11]. Significant changes in the corneal subbasal nerve plexus such as increased tortuosity, reduced nerve fiber, and branch density have previously been demonstrated in several diseases involving the cornea [10, 14].

Etiopathogenesis of KC has so far been studied in corneal buttons excised during penetrating keratoplasty as there are currently no animal models to study these cellular and morphological changes in vivo [15]. Corneal buttons excised from keratoconus patients represent advanced disease. It is therefore not possible to elucidate vital information, which may be seen in early disease. In vivo confocal microscopy (IVCM), a noninvasive imaging modality, has overcome this limitation and allows in vivo examination of the human

cornea at a microstructure level [14, 16]. While there are studies of IVCM in bilateral KC [9, 16], there are none in patients with unilateral disease. We therefore evaluated the alterations in subbasal nerves with the IVCM in a cohort of unilateral KC patients. The aim of this study was to gain more insight into the role of corneal nerves in pathogenesis and diagnosis and as a marker for disease progression in KC.

2. Materials and Methods

The protocol of this prospective cross sectional study was approved by the hospital's ethics committee and was performed according to the tenets of the Declaration of Helsinki. Written informed consent was obtained from each patient after a detailed explanation about the nature of the study.

Thirty healthy subjects who did not show any evidence of KC on topography were taken as controls (Group 1). Sagittal curvature map on topography showing a localized area of increased keratometry, inferior-superior asymmetry, and skewed steep radial axis above and below the horizontal meridian were diagnosed to have KC. Thirty-three patients showing these changes in only one eye were included in the study. Group 2 included the normal eye (thirty-three eyes) and Group 3 included the keratoconic eye of these patients. Group 3 was further subdivided into centered cones (Group 3a) and decentered cones (Group 3b) based on whether the cones were located within the central 2 mm or beyond [17]. Patients with a history of contact lens use, ocular surgery, trauma, any coexisting corneal disease, evidence of corneal scarring, or bilateral keratoconus were excluded from the study.

All patients underwent a complete ophthalmic examination including refraction (uncorrected and corrected visual acuity), retinoscopy, detailed slit lamp evaluation, corneal topography using Pentacam HR Scheimpflug imaging system (Oculus Optikgerate GmBH, Wetzlar Germany), and laser-scanning IVCM using the Rostock Corneal Module/Heidelberg Retina Tomograph II (Heidelberg Engineering GmbH, Dossenheim, Germany). Both eyes of the unilateral keratoconus patients and only one eye of the control group underwent IVCM. The laser in vivo confocal microscope uses a diode laser of 670 nm wavelength. Proparacaine 0.5% drops were used to anesthetize the cornea. Patients were asked to fixate on a distance target aligned to enable examination of the central cornea. For each IVCM examination, five high quality clear images of the subbasal nerve plexus were chosen. A full 400 × 400 micron square frame was used for the analysis. After the procedure, one drop of 0.5% moxifloxacin eye drops was instilled to prevent any secondary infection.

The subbasal nerve plexus was quantitatively analyzed using an automated CCmetrics software version 1.0 (University of Manchester, UK) (Figure 1). A total of six parameters were quantified in all three groups for the analysis:

(i) corneal nerve fiber density (CNFD): the number of nerve fibers per mm^2,

(ii) corneal nerve branch density (CNBD): the number of branch points on the main nerve fibers per mm^2,

(iii) corneal nerve fiber length (CNFL): the total length of nerve per mm^2,

(iv) corneal total branch density (CTBD): the total number of branch points per mm^2,

(v) corneal nerve fiber area (CNFA): the total nerve fiber area per mm^2,

(vi) corneal nerve fiber width (CNFW), the average nerve fiber width per mm^2.

All images were acquired and analyzed by a single observer who was masked about the study groups. Data was analyzed and compared between the three groups and subgroups.

2.1. Statistical Analysis. Statistical analyses were performed using Stata version 12.1 (StataCorp, College Station, TX, USA) statistical software. The continuous variables were described using mean and standard deviation. The t test was used to compare the parameter values within the groups. p value < 0.05 was considered statistically significant.

3. Results

A total of 480 images of subbasal plexus were analyzed with hundred and fifty images of Group 1, 165 images of Group 2, and 165 images of Group 3. Mean age of Group 1 was 28.06 ± 2.41 years and for Groups 2 and 3 it was 22.21 ± 4.66 years. Within Group 3, 18 eyes in Group 3 had centered cones and 15 eyes had decentered cones.

Table 1 shows the IVCM findings of different subbasal nerve parameters and the comparison between each group. The CNFD was 30.51 ± 5.8 mm/mm^2 in Group 1, 28.48 ± 23.82 mm/mm^2 in Group 2, and 23.82 ± 8.02/mm^2 in Group 3. The lower density of nerves was statistically significant in eyes with KC when compared to Group 2 ($p < 0.001$) and Group 3 ($p = 0.01$). The CNFL also followed a similar pattern being 17.59 ± 3.16 mm/mm^2 in Group 1, 16.6 ± 2.42 mm/mm^2 in Group 2, and 14.82 ± 3.61 mm/mm^2 in Group 3. The reduction in the fiber length was significant in Group 3 when compared to Group 2 ($p = 0.02$) and controls ($p < 0.001$). The mean value of CNBD, CTBD, and CNFA did not differ significantly within the groups ($p = 0.14$), ($p = 0.23$), and ($p = 0.13$), respectively. The mean CNFW was unaffected.

Group 3 was further subclassified and analyzed based on the location of cones (Table 2). The CNBD was 29.6 ± 18.9 mm/mm^2 in Group 3a (centered cones) and 47.1 ± 16.7 mm/mm^2 in Group 3b (decentered cones), which was a statistically significant difference ($p < 0.01$). The CNFD, CNFL, CTBD, CNFA, and CNFW were higher in Group 3b, but this was not statistically significant.

4. Discussion

With KC being a progressive disease, the changes in refractive and topographic parameters that help us decide further management for our patients have been defined [18]. Progression has also been documented using ultra high-resolution optical coherence tomography to detect changes in the Bowman's

Table 1: The mean of subbasal nerve plexus parameters with the standard deviation. Group 1 is control eye, Group 2 is unaffected eye of unilateral keratoconus, and Group 3 is keratoconic eye of unilateral keratoconus.

	Group 1 ($n = 30$)	Group 2 ($n = 33$)	Group 3 ($n = 33$)	Group 1 versus Group 2	Group 1 versus Group 3	Group 2 versus Group 3
CNFD	30.51 ± 5.8	28.48 ± 23.82	23.82 ± 8.02	0.26	<0.001	0.01
CNBD	43.45 ± 15.29	34.7 ± 16.1	37.61 ± 19.82	0.05	0.2	0.51
CNFL	17.59 ± 3.16	16.6 ± 2.42	14.82 ± 3.61	0.2	0.001	0.02
CTBD	59.73 ± 20.75	49.05 ± 25.3	54.66 ± 27.15	0.09	0.41	0.36
CNFA	0.01 ± 0.002	0.006 ± 0.001	0.006 ± 0.002	0.13	0.06	0.68
CNFW	0.02 ± 0.001	0.021 ± 0.002	0.02 ± 0.002	0.29	0.13	0.63

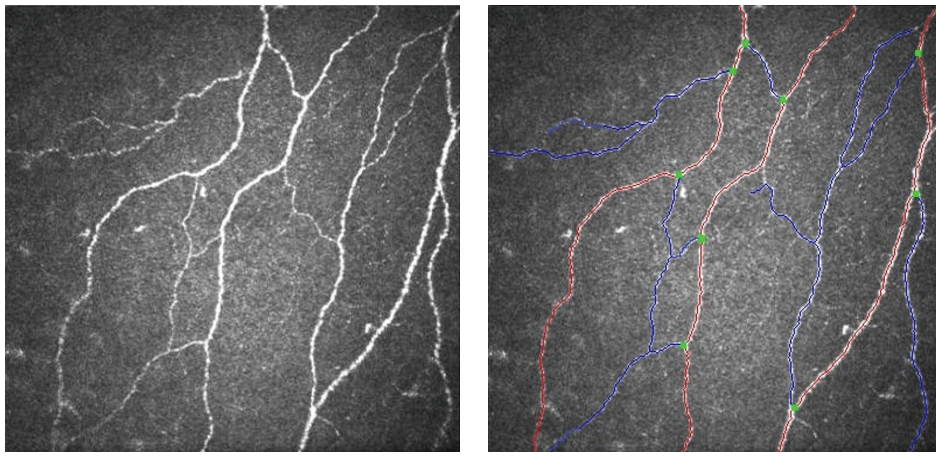

(a) (b)

Figure 1: In vivo confocal microscopy image (a) of the subbasal plexus of nerves in a patient of keratoconus and the same image after analysis by the automated CCmetrics software (b).

Table 2: The mean of subbasal nerve plexus parameters with the standard deviation. Group 3a is centered cones and group 3b is decentered cones.

	Centered ($n = 18$)	Decentered ($n = 15$)	p value
CNFD	21.6 ± 9.1	26.4 ± 5.6	0.09
CNBD	29.6 ± 18.9	47.1 ± 16.7	**<0.01**
CNFL	13.8 ± 4.3	15.9 ± 1.9	0.08
CTBD	46.9 ± 29.0	63.9 ± 22.1	0.07
CNFA	$5 \times 10^{-3} \pm 2 \times 10^{-3}$	$6 \times 10^{-3} \pm 1 \times 10^{-3}$	0.08
CNFW	$2 \times 10^{-2} \pm 2 \times 10^{-3}$	$2 \times 10^{-2} \pm 1 \times 10^{-3}$	1.0

layer thickness. The Bowman's ectasia index (BEI) has been proposed as a sensitive qualitative and quantitative diagnostic tool [19]. However, all these indices are reliable only in established cases of KC. In cases of a unilateral KC, more than half of the normal fellow eyes develop KC within 16 years with majority of them manifesting in the first six years of followup [20]. Currently, there are no devices or investigative modalities that are capable of predicting this change [5]. With a varying degree of progression, the need for better and sensitive tools is warranted.

Microstructure and in vitro studies with light and electron microscope have shown changes in all layers of the cornea in KC [20, 21]. In vivo studies suffer from a limitation of inadequate resolution. With the introduction of the IVCM, it has now become possible to visualize all the layers of the cornea down to the resolution of a few microns, at various depths and at the cellular level [11, 22]. It has previously been used to study the normal corneal architecture [11, 16, 22], alterations in various diseases such as corneal infections caused by viruses [23], acanthamoeba [24], or fungi [25] and in inflammatory conditions like dry eye [26]. Studies on corneal nerves in chronic migraine patients with symptoms of dry eye have shown a reduced fiber density on IVCM [27]. It has also been used to detect nerve damage and the reparative process in diabetics [28].

This in vivo imaging technique has recently been exploited to study the structural changes occurring in KC [29]. Morphological changes in the epithelium, the Bowman's layer, the subbasal, subepithelial, and stromal nerve plexus, keratocytes, collagen fibers, and the endothelial cells have been studied [29–31]. Fleischer ring and Vogt's striae are classically seen on the IVCM as hyper reflective structures [30]. Thus, it is also possible to study the specific morphological changes seen in the different layers of cornea in KC [31].

The subbasal nerve plexus has been mapped using the IVCM in KC with gross abnormal morphological changes even in patients with subclinical KC [9]. The plexus of nerves in KC shows a reduced nerve fiber density and increased tortuosity as compared to controls [32]. The functional effect of these changes has been established in a clinical study [33] where the authors have demonstrated reduced corneal sensitivity to different types of stimuli in patients with keratoconus. This suggests that though the impact of the disease process on the corneal nerves structurally and functionally has been described it has not been quantified as yet. Hence, we evaluated the subbasal plexus of nerves in a unique cohort of unilateral keratoconus where the differences between unaffected fellow eyes and affected keratoconic eyes were quantified and compared with controls. The utility of quantitatively detecting a subtle or early change to predict the disease onset or severity in the unaffected fellow eye is highlighted.

The quantification of the subbasal nerves was done by an automated software which extracts the nerve fiber data from a raw image thereby giving a "response" image which provides automated quantitative data regarding the CNFD, CNFL, CNBD, CTBD, CNFA, and CNFW. The analysis is objective, quick, and more reliable with negligible inter/intraobserver variability [34]. In our study, the quantitative analysis between the affected eye of unilateral KC (Group 2) and controls (Group 1) revealed a significant reduction in CNFD, CNBD, and CNFL, which is in accordance with previous reports [9]. In addition, there was a significant difference between the unaffected and affected eyes of the same individual. The values in the unaffected eyes were not similar to that in controls. This demonstrates the influence of the disease on topographically and clinically normal eyes. The subbasal nerve fiber quantitative changes might therefore help in establishing a diagnosis of KC in these eyes on follow-up even before it is manifested clinically. Besides serving as a disease marker it can also aid in monitoring disease progression.

There have been reports of subbasal nerve morphological changes at the base and apex of cones in KC. Subbasal nerves exhibit increased tortuosity with the branches running concentrically while following the contour of the topographic base of cone while the subbasal nerve fiber bundles at the apex have the most abnormal configurations which correlates well with ex vivo studies demonstrating that the greatest destruction of normal corneal architecture occurs at the apex of the cone [14]. We therefore also looked at the influence of the cone location in the KC group with 18 patients having a centered cone (Group 3a) and 15 patients with decentered cones (Group 3b). On analyzing the images taken at the apex of the cones in both subgroups, we found that all the parameters were increased in the decentered group with only the CNBD showing a statistically significant increase. Since we analyzed IVCM images taken only at the apex of the cornea, we hypothesize that the increased parameters in the decentered cone might be as a result of the base of cones being in the center of the cornea in contrast to central cones wherein the center of the cornea roughly corresponds to the apex of the cone. A quantification of the subbasal plexus of nerves and the correlation between parameters like CNFD, CNFL, and CNBD and grades of KC has also been reported [9].

At a cellular level, studies have implied that the abnormalities in keratoconus include the degeneration of epithelial basal cells and breaks in Bowman's layer, as well as the release of catabolic, proteolytic enzymes, and cytokines. This can potentially damage the corneal nerves and more particularly the Schwann cells passing between the acellular Bowman's layer and corneal epithelium [11, 12]. This is possibly the mechanism of morphological changes in the subbasal nerve plexus in established KC cases.

Currently there are no diagnostic modalities that can predict early changes prior to clinical manifestations or topographical changes. In our study we provide a quantitative analysis of the corneal subbasal nerve plexus in cases with unilateral KC with other risk factors for KC remaining constant for both eyes, allowing for a more objective comparison. In vivo confocal microscopy could be an extreme tool to provide insights into the pathogenesis of the disease and thereby influence the management strategy for each patient. Alterations in corneal nerve morphology can be used as an imaging marker for early diagnosis, for monitoring of progression, and for prognostication of keratoconus.

Conflict of Interests

The authors declare that there is no conflict of interests regarding the publication of this paper.

References

[1] J. H. Krachmer, R. S. Feder, and M. W. Belin, "Keratoconus and related noninflammatory corneal thinning disorders," *Survey of Ophthalmology*, vol. 28, no. 4, pp. 293–322, 1984.

[2] G. H. Bae, J. R. Kim, C. H. Kim, D. H. Lim, E. S. Chung, and T.-Y. Chung, "Corneal topographic and tomographic analysis of fellow eyes in unilateral keratoconus patients using pentacam," *American Journal of Ophthalmology*, vol. 157, no. 1, pp. 103–109.e1, 2014.

[3] R. H. Kennedy, W. M. Bourne, and J. A. Dyer, "A 48-year clinical and epidemiologic study of keratoconus," *American Journal of Ophthalmology*, vol. 101, no. 3, pp. 267–273, 1986.

[4] D. R. Holland, N. Maeda, S. B. Hannush et al., "Unilateral keratoconus. Incidence and quantitative topographic analysis," *Ophthalmology*, vol. 104, no. 9, pp. 1409–1413, 1997.

[5] X. Li, Y. S. Rabinowitz, K. Rasheed, and H. Yang, "Longitudinal study of the normal eyes in unilateral keratoconus patients," *Ophthalmology*, vol. 111, no. 3, pp. 440–446, 2004.

[6] F. Raiskup-Wolf, A. Hoyer, E. Spoerl, and L. E. Pillunat, "Collagen crosslinking with riboflavin and ultraviolet-A light in keratoconus: long-term results," *Journal of Cataract and Refractive Surgery*, vol. 34, no. 5, pp. 796–801, 2008.

[7] C. Wittig-Silva, M. Whiting, E. Lamoureux, R. G. Lindsay, L. J. Sullivan, and G. R. Snibson, "A randomized controlled trial of corneal collagen cross-linking in progressive keratoconus: preliminary results," *Journal of Refractive Surgery*, vol. 24, no. 7, pp. S720–S725, 2008.

[8] R. Shetty, L. Kaweri, N. Pahuja et al., "Current review and a simplified 'five-point management algorithm' for keratoconus," *Indian Journal of Ophthalmology*, vol. 63, no. 1, pp. 46–53, 2015.

[9] G. Bitirgen, A. Ozkagnici, B. Bozkurt, and R. A. Malik, "*In vivo* corneal confocal microscopic analysis in patients with keratoconus," *International Journal of Ophthalmology*, vol. 8, no. 3, pp. 534–539, 2015.

[10] R. L. Niederer, D. Perumal, T. Sherwin, and C. N. J. McGhee, "Laser scanning in vivo confocal microscopy reveals reduced innervation and reduction in cell density in all layers of the keratoconic cornea," *Investigative Ophthalmology and Visual Science*, vol. 49, no. 7, pp. 2964–2970, 2008.

[11] B. S. Shaheen, M. Bakir, and S. Jain, "Corneal nerves in health and disease," *Survey of Ophthalmology*, vol. 59, no. 3, pp. 263–285, 2014.

[12] L. J. Müller, G. F. J. M. Vrensen, L. Pels, B. N. Cardozo, and B. Willekens, "Architecture of human corneal nerves," *Investigative Ophthalmology and Visual Science*, vol. 38, no. 5, pp. 985–994, 1997.

[13] C. W. Morgan, I. Nadelhaft, and W. C. de Groat, "Anatomical localization of corneal afferent cells in the trigeminal ganglion," *Neurosurgery*, vol. 2, no. 3, pp. 252–258, 1978.

[14] D. V. Patel and C. N. J. McGhee, "Mapping of the normal human corneal sub-basal nerve plexus by in vivo laser scanning confocal microscopy," *Investigative Ophthalmology & Visual Science*, vol. 46, no. 12, pp. 4485–4488, 2005.

[15] J. H. Mathew, J. D. Goosey, and J. P. G. Bergmanson, "Quantified histopathology of the keratoconic cornea," *Optometry and Vision Science*, vol. 88, no. 8, pp. 988–997, 2011.

[16] D. V. Patel and C. N. J. McGhee, "In vivo confocal microscopy of human corneal nerves in health, in ocular and systemic disease, and following corneal surgery: a review," *British Journal of Ophthalmology*, vol. 93, no. 7, pp. 853–860, 2009.

[17] R. Shetty, R. M. M. A. Nuijts, M. Nicholson et al., "Cone location–dependent outcomes after combined topography-guided photorefractive keratectomy and collagen cross-linking," *American Journal of Ophthalmology*, vol. 159, no. 3, pp. 419–425, 2015.

[18] R. Shetty, S. D'Souza, S. Srivastava, and R. Ashwini, "Topography-guided custom ablation treatment for treatment of keratoconus," *Indian Journal of Ophthalmology*, vol. 61, no. 8, pp. 445–450, 2013.

[19] M. Abou Shousha, V. L. Perez, A. P. Fraga Santini Canto et al., "The use of Bowman's layer vertical topographic thickness map in the diagnosis of keratoconus," *Ophthalmology*, vol. 121, no. 5, pp. 988–993, 2014.

[20] E. Sykakis, F. Carley, L. Irion, J. Denton, and M. C. Hillarby, "An in depth analysis of histopathological characteristics found in keratoconus," *Pathology*, vol. 44, no. 3, pp. 234–239, 2012.

[21] S. Sawaguchi, T. Fukuchi, H. Abe, T. Kaiya, J. Sugar, and B. V. J. T. Yue, "Three-dimensional scanning electron microscopic study of keratoconus corneas," *Archives of Ophthalmology*, vol. 116, no. 1, pp. 62–68, 1998.

[22] D. V. Patel and C. N. J. McGhee, "Contemporary in vivo confocal microscopy of the living human cornea using white light and laser scanning techniques: a major review," *Clinical and Experimental Ophthalmology*, vol. 35, no. 1, pp. 71–88, 2007.

[23] T. R. Porzukowiak and K. Ly, "In vivo confocal microscopy use in endotheliitis," *Optometry and Vision Science*, vol. 92, no. 12, pp. e431–e436, 2015.

[24] D. N. Parmar, S. T. Awwad, W. M. Petroll, R. W. Bowman, J. P. McCulley, and H. D. Cavanagh, "Tandem scanning confocal corneal microscopy in the diagnosis of suspected acanthamoeba keratitis," *Ophthalmology*, vol. 113, no. 4, pp. 538–547, 2006.

[25] E. Brasnu, T. Bourcier, B. Dupas et al., "In vivo confocal microscopy in fungal keratitis," *British Journal of Ophthalmology*, vol. 91, no. 5, pp. 588–591, 2007.

[26] A. Kheirkhah, R. R. Darabad, A. Cruzat et al., "Corneal epithelial immune dendritic cell alterations in subtypes of dry eye disease: a pilot in vivo confocal microscopic study," *Investigative Opthalmology & Visual Science*, vol. 56, no. 12, pp. 7179–7185, 2015.

[27] K. I. Kinard, A. G. Smith, J. R. Singleton et al., "Chronic migraine is associated with reduced corneal nerve fiber density and symptoms of dry eye," *Headache*, vol. 55, no. 4, pp. 543–549, 2015.

[28] R. A. Malik, P. Kallinikos, C. A. Abbott et al., "Corneal confocal microscopy: a non-invasive surrogate of nerve fibre damage and repair in diabetic patients," *Diabetologia*, vol. 46, no. 5, pp. 683–688, 2003.

[29] N. Efron and J. G. Hollingsworth, "New perspectives on keratoconus as revealed by corneal confocal microscopy," *Clinical and Experimental Optometry*, vol. 91, no. 1, pp. 34–55, 2008.

[30] Ö. Ö. Uçakhan, A. Kanpolat, N. Ylmaz, and M. Özkan, "In vivo confocal microscopy findings in keratoconus," *Eye and Contact Lens*, vol. 32, no. 4, pp. 183–191, 2006.

[31] K. H. Weed, C. J. MacEwen, A. Cox, and C. N. J. McGhee, "Quantitative analysis of corneal microstructure in keratoconus utilising in vivo confocal microscopy," *Eye*, vol. 21, no. 5, pp. 614–623, 2007.

[32] L. S. Mannion, C. Tromans, and C. O'Donnell, "An evaluation of corneal nerve morphology and function in moderate keratoconus," *Contact Lens and Anterior Eye*, vol. 28, no. 4, pp. 185–192, 2005.

[33] L. Dienes, H. J. Kiss, K. Perényi et al., "Corneal sensitivity and dry eye symptoms in patients with keratoconus," *PLoS ONE*, vol. 10, no. 10, Article ID e0141621, 2015.

[34] M. A. Dabbah, J. Graham, I. N. Petropoulos, M. Tavakoli, and R. A. Malik, "Automatic analysis of diabetic peripheral neuropathy using multi-scale quantitative morphology of nerve fibres in corneal confocal microscopy imaging," *Medical Image Analysis*, vol. 15, no. 5, pp. 738–747, 2011.

Hindawi Publishing Corporation
BioMed Research International
Volume 2016, Article ID 7092938, 10 pages
http://dx.doi.org/10.1155/2016/7092938

Research Article

The Superficial Stromal Scar Formation Mechanism in Keratoconus: A Study Using Laser Scanning In Vivo Confocal Microscopy

Peng Song, Shuting Wang, Peicheng Zhang, Wenjie Sui, Yangyang Zhang, Ting Liu, and Hua Gao

Shandong Eye Hospital, Shandong Eye Institute, Shandong Academy of Medical Sciences, Jinan 250021, China

Correspondence should be addressed to Hua Gao; gaohua100@126.com

Received 16 October 2015; Revised 5 December 2015; Accepted 13 December 2015

Academic Editor: Dipika V. Patel

To investigate the mechanism of superficial stromal scarring in advanced keratoconus using confocal microscopy, the keratocyte density, distribution, micromorphology of corneal stroma, and SNP in three groups were observed. Eight corneal buttons of advanced keratoconus were examined by immunohistochemistry. The keratocyte densities in the sub-Bowman's stroma, anterior stroma, and posterior stroma and the mean SNP density were significantly different among the three groups. In the mild-to-moderate keratoconus group, activated keratocyte nuclei and comparatively highly reflective ECM were seen in the sub-Bowman's stroma, while fibrotic structures with comparatively high reflection were visible in the anterior stroma in advanced keratoconus. The alternating dark and light bands in the anterior stroma of the mild-to-moderate keratoconus group showed great variability in width and direction. The wide bands were localized mostly in the posterior stroma that corresponded to the Vogt striae in keratoconus and involved the anterior stroma only in advanced keratoconus. Histopathologically, high immunogenicity of α-SMA, vimentin, and FAP was expressed in the region of superficial stromal scarring. In vivo confocal microscopy revealed microstructural changes in the keratoconic cone. The activation of superficial keratocytes and abnormal remodeling of ECM may both play a key role in the superficial stromal scar formation in advanced keratoconus.

1. Introduction

Keratoconus is an ectatic corneal disorder characterized by progressive, central, or paracentral corneal thinning, which results in apical corneal protrusion, irregular astigmatism, superficial scar formation, and significantly decreased vision [1, 2]. Previous pathologic studies concluded that underlying abnormalities in the stromal repair and reactive species-linked activities and the interaction between these phenomena were implicated in the development of keratoconus [3, 4].

Corneal scarring is a commonly occurring consequence of several forms of trauma, wounds, chemical burns, infections, and refractive surgery; however, keratoconic patients do not have corneal trauma, epithelial defects, or any inflammatory diseases. Instead, altered expression of wound healing and stress-related proteins has been found in keratoconic corneas [5]. Previous reports have demonstrated that regions with stromal scarring and fibrotic deposits have comparatively high expressions of laminin-5, proteoglycans, fibrillin-1, tenascin-C, and types IV, VII, and VIII collagen [5–7]. Little information is available regarding this superficial scar formation although there have been a few confocal microscopic or histopathological findings [3, 8, 9]. A histopathological examination of patients with advanced keratoconus showed that the posterior stroma remained undisturbed in keratoconus, but tissue (lamellae) debris was detected in the anterior stroma [3]. Moreover, confocal microscopy revealed significant microstructural alterations and a decrease in keratocytes in the anterior and posterior stroma in patients with advanced keratoconus [9, 10].

Studies of superficial stromal scar formation ex vivo in keratoconus are subject to certain restrictions. The managements of mild-to-moderate keratoconus include rigid gas

permeable contact lens fitting, corneal collagen crosslinking, and intrastromal corneal ring segments [11, 12]. As keratoplasty is not considered as a treatment option for mild-to-moderate keratoconus, it is difficult to collect mild-to-moderate keratoconus buttons for investigation ex vivo. Confocal microscopy allows a noninvasive view of the living human cornea at magnifications of up to 800x. We hypothesized that microstructural abnormalities may occur in the stroma and lamellae during corneal protrusion in mild-to-moderate keratoconus and thus contribute to the progression of keratoconus and superficial scar formation. The aim of the present study was to investigate the corneal microstructural and histopathological changes in keratoconus, which may be the important proofs of mechanical failure, and relate these to the superficial stromal scar in keratoconus.

Table 1: The classification of keratoconus.

Stage	Characteristics
Mild-to-moderate keratoconus	Eccentric corneal steepening
	Induced myopia and/or astigmatism ≤ 8 D
	Corneal radii ≤ 53 D
	Vogt striae, no scars
	Corneal thickness ≥ 400 μm
Advanced keratoconus	Induced myopia and/or astigmatism > 8 D, even refraction not measurable
	Corneal radii > 53 D
	Corneal thickness < 400 μm
	No acute corneal hydrops or perforation

2. Materials and Methods

2.1. Subjects and Design. This prospective and cross-sectional comparative study was approved by the Ethics Committee of the Shandong Eye Institute and followed the tenets of the Declaration of Helsinki. Written informed consent was obtained from each participant.

All patients were diagnosed with keratoconus by clinical examinations, which included slit-lamp biomicroscopy, keratometry, A-scan ultrasonography, corneal topography, and in vivo laser scanning confocal microscopy. A positive diagnosis of keratoconus was based on the presence of at least one keratoconic feature (centric or eccentric corneal stromal thinning, Vogt striae, Fleischer ring, or Munson's sign) and topographic findings (an increased area of corneal power surrounded by concentric areas of decreasing power, inferior-superior power asymmetry, an inferior-superior dioptric asymmetry difference greater than 1.4 diopters, and skewing of the steepest radial axes above and below the horizontal meridian). Keratoconic eyes were divided into two groups based on the Keratoconus Severity Score (KSS) and modified Krumeich classification of keratoconus (Table 1) [12, 13]. The control group consisted of healthy individuals without risk factors for keratoconus. The diagnosis of keratoconus was made by Peng Song and Hua Gao, and the two doctors' agreement rate was 100%.

The exclusion criteria were as follows: a history of ocular trauma, any previous ocular surgery, the use of any systemic or ocular medications, coexisting corneal pathology, keratoconic eyes with acute corneal hydrops or perforation, contact lens wear, or the presence of systemic disease that may affect the cornea.

2.2. In Vivo Confocal Microscopy. The primary laser scanning in vivo confocal microscope was the Heidelberg Retina Tomograph HRT-2 (Heidelberg Engineering GmbH, Heidelberg, Germany); the addition of the Rostock Cornea Module (RCM) converted it into an in vivo confocal microscope of the eye surface. Before the measurement, 1 drop of topical anesthetic (0.5% proparacaine, Alcon, Fort Worth, TX) and 1 drop of carbomer eye gel (Bausch & Lomb, Rochester, New York, NY) were applied. A sterile and disposable polymethylmethacrylate cap was placed onto the head of the objective. The patient's chin was placed on the related part of the apparatus. The objective was zoomed onto the central cornea using the joystick. To ensure that only measurements in the central cornea were taken, the patient was instructed to fixate on a small red light with the contralateral eye. Centered and pressure-free contact of the HRT-2 with the cornea was monitored optically using a swivel color camera. The full thickness of the central cornea or the center of the keratoconic cone (within the central 2 mm diameter) was scanned using the "section mode" of the device. This mode enables instantaneous imaging of a single area of the cornea at a desired depth. All the confocal microscopic examinations were performed by the same investigator (Shuting Wang).

The following corneal layers were subjected to in vivo confocal microscopy: (1) the subbasal nerve plexus (SNP); (2) sub-Bowman's stroma (the layers of the stroma below Bowman's membrane); (3) the anterior stroma (the layers comprising one-third of the stroma); and (4) the posterior stroma (the layers comprising two-thirds of the stroma). The keratocytes were counted by a semiautomated cell counter. The focused layers of the anteroposterior keratocytes were recorded. Three randomly chosen images of three desired stromal layers per subject were analyzed, statistically compared, and averaged. Within the counting frame, the truncated cells of the left and lower edges were considered. The results were extrapolated up to an area of 1 mm^2. The SNP density was evaluated using NeuronJ, a free semiautomatic image analysis program, and a plug-in to the program, ImageJ (http://www.imagescience.org/meijering/software/neuronj/; accessed November 2012). Three randomly chosen images of the SNP per subject were analyzed, statistically compared, and averaged. The measurement of keratocyte density and SNP density was performed by two masked examiners (Peng Song and Peicheng Zhang).

2.3. Immunohistochemistry. The significance of FAP and vimentin was the major morphological characteristic of the fibroblasts, and the expression of vimentin corresponded to the expression of FAP. At least three 4 mm sections were obtained from the paraffin-embedded corneal buttons. The antigens were recovered by microwaving for 15 min

Table 2: Demographic and clinical data.

	Control	Mild-to-moderate	Advanced	P value
Number of eyes	20	35	35	
Gender (male/female)	10/10	20/15	19/16	>0.05[a]
Age, years	23.2 ± 2.5	21.0 ± 4.2	21.5 ± 4.1	0.129[b]
CCT, μm	553.3 ± 23.4	505.8 ± 25.1	390.6 ± 72.4	<0.001[c]
Cornea front				
K1, D	42.0 ± 1.3	43.7 ± 2.2	55.5 ± 7.4	<0.001[c]
K2, D	43.4 ± 1.3	45.3 ± 2.1	62.3 ± 8.8	<0.001[c]
Km, D	42.7 ± 1.3	44.5 ± 2.0	58.6 ± 7.8	<0.001[c]
Cornea back				
K1, D	−6.0 ± 0.2	−6.3 ± 0.4	−8.8 ± 1.8	<0.001[c]
K2, D	−6.4 ± 0.2	−6.9 ± 0.5	−10.1 ± 2.1	<0.001[c]
Km, D	−6.2 ± 0.2	−6.6 ± 0.4	−9.4 ± 1.8	<0.001[c]
KPD	1.2 ± 0.16	1.6 ± 0.5	4.3 ± 2.1	<0.001[c]

CCT: central corneal thickness; D: diopter; K: keratometry; KPD: keratometric power deviation.
[a]χ^2 test; [b]one-way ANOVA test; [c]Kruskal-Wallis test.

in an EDTA solution. Endogenous peroxidase activity was quenched by incubating the sections in 3% hydrogen peroxide for 5 min. Normal goat serum was used to block nonspecific staining. The sections were subsequently incubated with mouse antifibroblast activation protein (Abcam, Hong Kong, China), mouse anti-Vimentin (Abcam), and mouse anti-α-smooth muscle actin (Maxim, Fujian, China) for 60 min at 37°C, a reinforcing agent (Maxim) for 15 min at 37°C, and HRP-conjugated goat anti-mouse IgG for 30 min at 37°C. Peroxidase activity was visualized by incubating the sections in a diaminobenzidine (DAB) solution (Maxim). Negative controls were performed in the absence of primary antibodies. Finally, the samples were mounted and examined with a microscope (Nikon Eclipse E800, Nikon, Tokyo, Japan).

2.4. Statistical Analysis. Statistical analyses were performed using SPSS 19.0 (IBM). The Kolmogorov-Smirnov test was used to evaluate the distribution characteristics of the variables. The one-way ANOVA test and Kruskal-Wallis test were used to compare the variables between the groups. The Bonferroni method was used for adjustment so as to make multiple comparisons. Differences were considered statistically significant for P values less than 0.05.

3. Results

3.1. Demographic Profiles and Baseline Clinical Characteristics. Seventy eyes of 44 patients with keratoconus were selected from patients who were diagnosed with keratoconus at the Shandong Eye Institute from March 2012 to October 2014 and divided into groups of mild-to-moderate keratoconus (35 eyes) and advanced keratoconus (35 eyes). The control group comprised 20 healthy eyes of 20 volunteers recruited from the hospital staff and their relatives. The demographic and topographic features of the three groups are shown in Table 2. No statistically significant difference was observed in the age and gender distribution among the three groups.

Using slit-lamp microscopy, Vogt striae were found in 6 (17.1%) of 35 eyes with mild-to-moderate keratoconus and 29 (82.9%) of 35 eyes with advanced keratoconus. The Fleischer ring was found in 13 eyes (37.1%) with mild-to-moderate keratoconus and 33 eyes (94.3%) with advanced keratoconus. Superficial stromal scarring was detected in 8 eyes (22.9%) with advanced keratoconus (Figure 1) but not in any eye with mild-to-moderate keratoconus. None of the above was observed in the controls.

3.2. Clinical Examination with In Vivo Scanning Confocal Microscopy. The confocal microscopy findings are shown in Table 3. The mean densities of sub-Bowman's stromal keratocytes, anterior stromal keratocytes, posterior stromal keratocytes, and subbasal nerve plexus were significantly different among the three groups ($P = 0.008$, $P < 0.001$, $P < 0.001$, and $P < 0.001$, resp.). The mean sub-Bowman's stromal keratocyte density was significantly lower in the advanced keratoconus group but not in the mild-to-moderate keratoconus group when compared with the control group ($P = 0.036$ and $P < 0.001$, resp.) (Figure 2(a)). The mean anterior stromal keratocyte density was significantly lower in both the mild-to-moderate keratoconus group and the advanced keratoconus group when compared with the control group ($P = 0.002$ and $P < 0.001$, resp.) (Figure 2(b)). The mean posterior stromal keratocyte density was significantly lower in both the mild-to-moderate keratoconus group and the advanced keratoconus group when compared with the control group ($P = 0.003$ and $P < 0.001$, resp.) (Figure 2(c)). The mean subbasal nerve plexus density was significantly lower in the advanced keratoconus group but not in the mild-to-moderate keratoconus group when compared with the control group ($P < 0.001$ and $P = 0.095$, resp.) (Figure 2(d)).

Confocal microscopic images revealed the extent of the variation in density and micromorphology of the keratocytes and SNP in the three groups (Figure 3). The keratocyte density in sub-Bowman's stroma was higher than the anterior

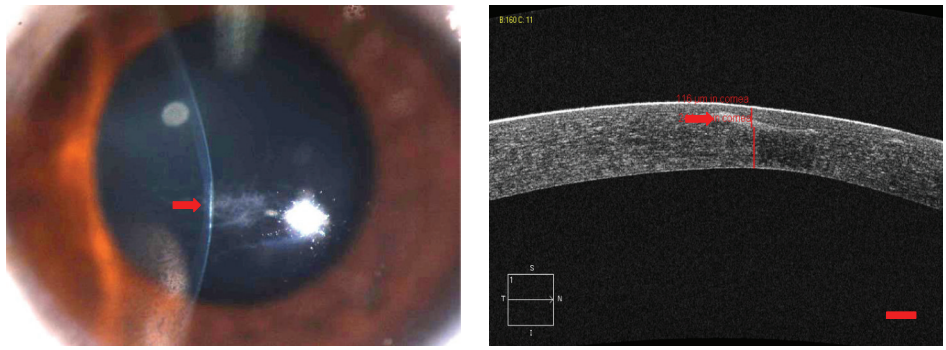

(a) (b)

Figure 1: Advanced keratoconus. (a) The appearance of superficial stromal scarring during the slit-lamp examination with a narrow-band light. (b) Stromal scarring was visible in the superficial stroma during the OCT examination. Scale bar: 200 μm.

Table 3: The density of the keratocytes and SNP.

	Controls	Mild-to-moderate	Advanced	F	P value
SBS keratocytes (cells/mm^2)	608.9 ± 102.1	610.2 ± 149.3	508.4 ± 137.0	5.198	0.008[a]
P value		1.000[b]	0.036[c]		
AS keratocytes (cells/mm^2)	409.9 ± 55.9	365.1 ± 47.6	301.4 ± 50.8	22.734	<0.001[a]
P value		0.002[b]	<0.001[c]		
PS keratocytes (cells/mm^2)	374.5 ± 36.2	322.3 ± 41.3	254.3 ± 58.7	31.302	<0.001[a]
P value		0.003[b]	<0.001[c]		
SNP density, mm/mm^2	15.9 ± 3.8	13.4 ± 3.9	8.5 ± 3.9	18.922	<0.001[a]
P value		0.284[b]	<0.001[c]		

SBS: sub-Bowman's stromal; AS: anterior stromal; PS: posterior stromal; SNP: subbasal nerve plexus.
[a]One-way ANOVA test; [b]Bonferroni test between controls and mild-to-moderate keratoconus.
[c]Bonferroni test between controls and advanced keratoconus.

and posterior stroma in all the groups. There was no significant difference in sub-Bowman's stromal keratocyte density between the controls and the mild-to-moderate keratoconus group, but an obvious decrease of keratocytes in the advanced keratoconus group (Figure 3(C1)) was visible compared with the other groups (Figures 3(A1) and 3(B1)). Highly reflective, sharply demarcated, and closely arranged cell nuclei of keratocytes were visualized in sub-Bowman's stroma in the controls, and the cytoplasm of this fibroblast subpopulation and the collagen fibers produced by them were not detectable (Figure 3(A1)). In the mild-to-moderate keratoconus group, keratocytes with activated nuclei and cytoplasmic processes produced a network appearance in sub-Bowman's stroma. The activated nuclei were branched and less readily identifiable individually, and the cytoplasm processes were also more than normal keratocytes (Figure 3(B1)). Moreover, the keratocytes had fewer cytoplasm processes and activated nuclei had reduced branches in the advanced keratoconus group (Figure 3(C1)).

In the anterior stroma, an obvious decrease in keratocytes was visible in the mild-to-moderate and advanced keratoconus groups when compared with the controls (Figures 3(A2), 3(B2), and 3(C2)). The anterior keratocytes in the mild-to-moderate keratoconus group had the same appearance as sub-Bowman's keratocytes, and a lower keratocyte density and more highly reflective cytoplasm and extracellular matrix (ECM) were detected compared with the controls (Figure 3(B2)). In the anterior stroma of the advanced keratoconus group, there were hyperreflective deposits, which corresponded with the superficial corneal scarring. In this zone, the keratocyte nuclei were not clearly visible (Figure 3(C2)).

In the posterior stroma, a decreasing trend of keratocyte density was found (Figures 3(A3), 3(B3), and 3(C3)). Alternating dark and light bands were visible in the anterior and posterior stroma of the eyes with keratoconus. In the anterior stroma, wider and more regular bands were presented in the advanced keratoconus group than in the mild-to-moderate keratoconus group (Figures 3(B2) and 3(C2)). The number and variation of striae in the posterior stroma were greater in the advanced keratoconus group than in the mild-to-moderate keratoconus group (Figures 3(B3) and 3(C3)). The direction of the bands was variable among the patients, mostly in an approximately vertical direction in the posterior stroma.

Examples of confocal microscopy images of the SNP in the control, mild-to-moderate keratoconus, and advanced keratoconus groups are shown in Figure 4. The normal nerve fibers in the controls mostly had thick, usually stretched, highly reflective structures, and some nerves were ramified into several fine branchlets (Figure 4(a)). In the patients

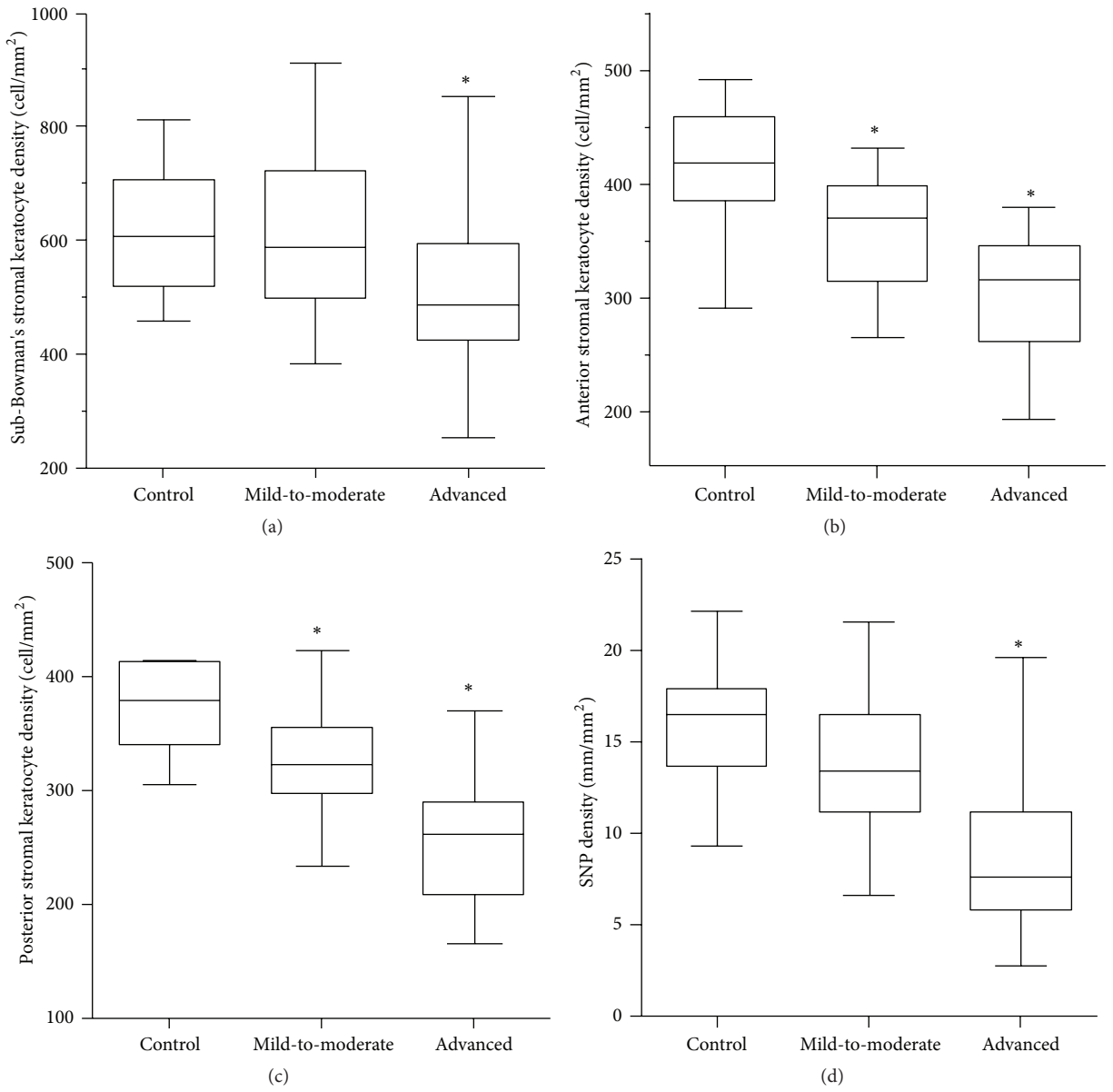

Figure 2: Box plots of keratocytes and nerve plexus densities measured by in vivo confocal microscopy. (a) Sub-Bowman's stromal keratocyte density in advanced keratoconus, (b) the anterior stromal keratocyte density in mild-to-moderate and advanced keratoconus, (c) the posterior stromal keratocyte density in mild-to-moderate and advanced keratoconus, and (d) the SNP density in advanced keratoconus were significantly lower than in the control subjects ($*$. all $P < 0.05$).

with mild-to-moderate keratoconus, the nerve fibers had a thickened, prominent appearance, such as excessive branching, curling, and even closed loops, but had no significant difference in SNP density compared with the controls (Figure 4(b)). The SNP density in the advanced keratoconus group was significantly lower than that of the control and mild-to-moderate keratoconus groups. The nerve fibers appeared short, interrupted, and disbranched (Figure 4(c)).

3.3. Immunohistochemistry. Eight keratoconic corneal buttons harvested from the 8 advanced keratoconus patients with superficial stromal scarring underwent immunohistochemistry staining, and the scar regions expressed high immunogenicity of fibroblast activation proteins (FAP), vimentin, and α-smooth muscle actin (α-SMA) (Figures 5 and 6). Decentralized expression of FAP and vimentin was visible throughout the corneas of the patients with keratoconus, and in the superficial stroma, excessive expression of FAP and vimentin was observed (Figure 5). The significance of the α-SMA expression was that it was the major morphological characteristic of the myofibroblasts; however, there was high expression of α-SMA only in the superficial stroma (Figures 5 and 6).

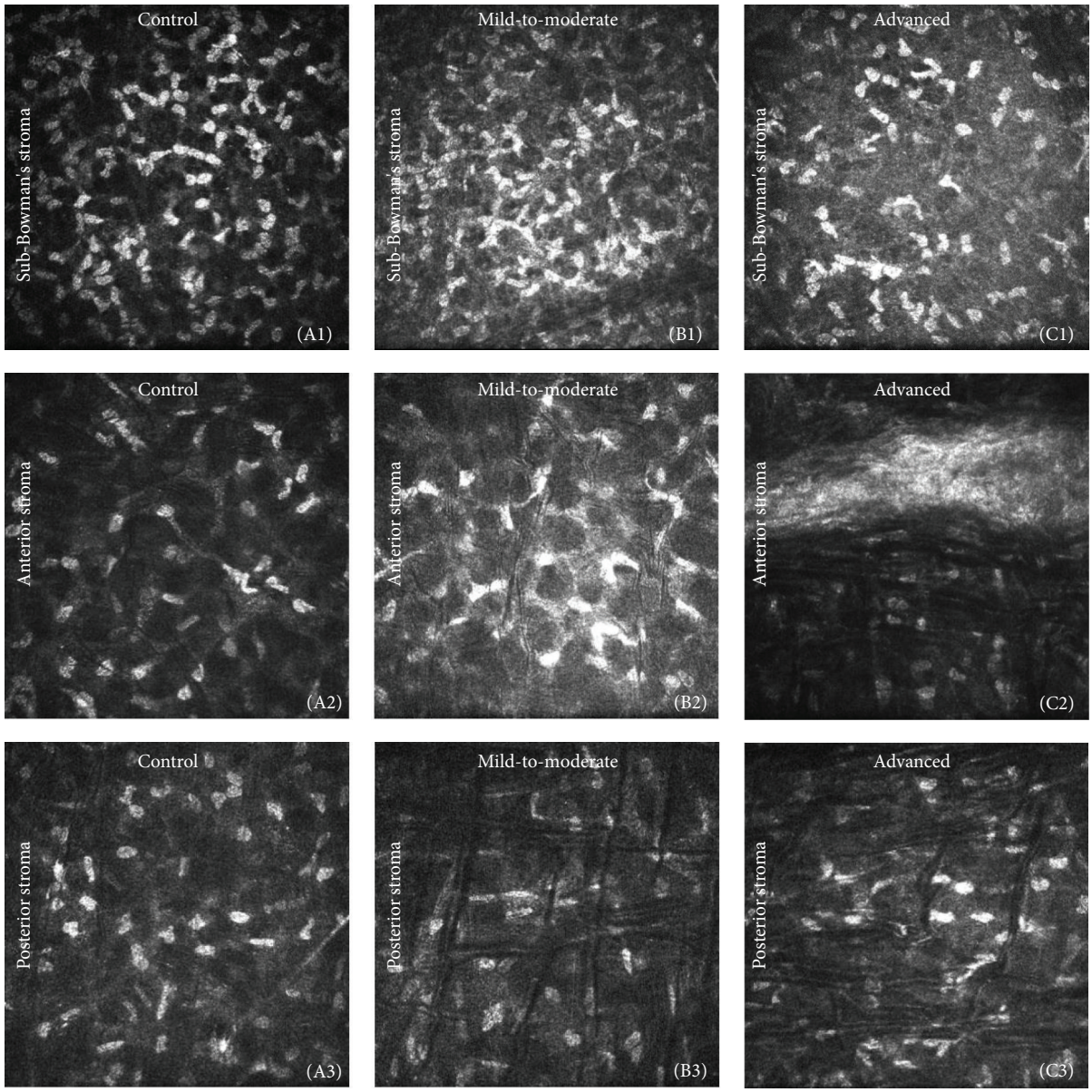

Figure 3: In vivo confocal microscopy images of the stroma in sub-Bowman's (top row) and anterior (middle row) and posterior stroma (bottom row) in the healthy controls, the mild-to-moderate keratoconus group, and the advanced keratoconus group, respectively. Image size: 400×400 μm. (A1) Normal keratocytes. Clearly demarcated, highly reflective, oval keratocyte nuclei. (B1) Activated nuclei with variable morphology that are unidentifiable individually. Highly reflective extracellular matrix (ECM). (C1) Lower keratocyte density and higher ECM reflectivity than (A1) and (B1). Hyperreflective keratocytes with activated nuclei and fewer cytoplasmic processes. (A2) Normal keratocytes. Lower keratocyte density than sub-Bowman's stromal keratocyte density. (B2) Activated keratocytes, thin and varied-orientation bands, and highly reflective ECM. (C2) Wider and regular bands and hyperreflective deposits were visible. (A3) Normal keratocytes in the posterior stroma. (B3) Wider and orthorhombic bands, rare keratocyte nuclei located in the bands. (C3) The number of bands was greater than those in the mild-to-moderate keratoconus group, and the arrangement of striae was more disordered.

4. Discussion

Superficial stromal scarring is usually observed in advanced keratoconus, and it affects vision severely, increases irregular astigmatism, and even leads to the failure of treatment with rigid gas permeable contact lenses [14]. According to previous pathologic studies, tenascin, laminin-5, perlecan, and type VII collagen are expressed to a greater extent in clinically and histologically scarred keratoconus [6], but there have been few investigations regarding the mechanism of superficial stromal scarring [5, 7]. With the help of in vivo confocal microscopy, we performed this study to investigate the consecutive microstructural changes in keratoconus and the potential mechanism for superficial stroma scarring in patients with healthy corneas, mild-to-moderate keratoconus, and advanced keratoconus.

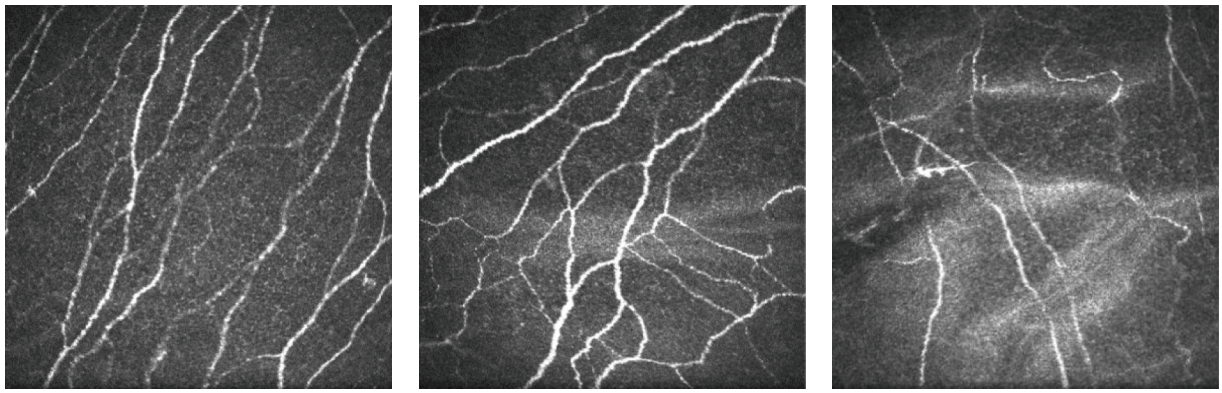

(a) (b) (c)

Figure 4: Subbasal nerve plexus images obtained by scanning slit confocal microscopy. Image size: 400 × 400 μm. (a) Normal nerves in the controls. Parallel nerve fiber bundles with bunches. (b) The SNP in mild-to-moderate keratoconus. There was a tortuous network of nerve fiber bundles. (c) The SNP in advanced keratoconus. Short, interrupted, and disbranched nerve fibers were visible.

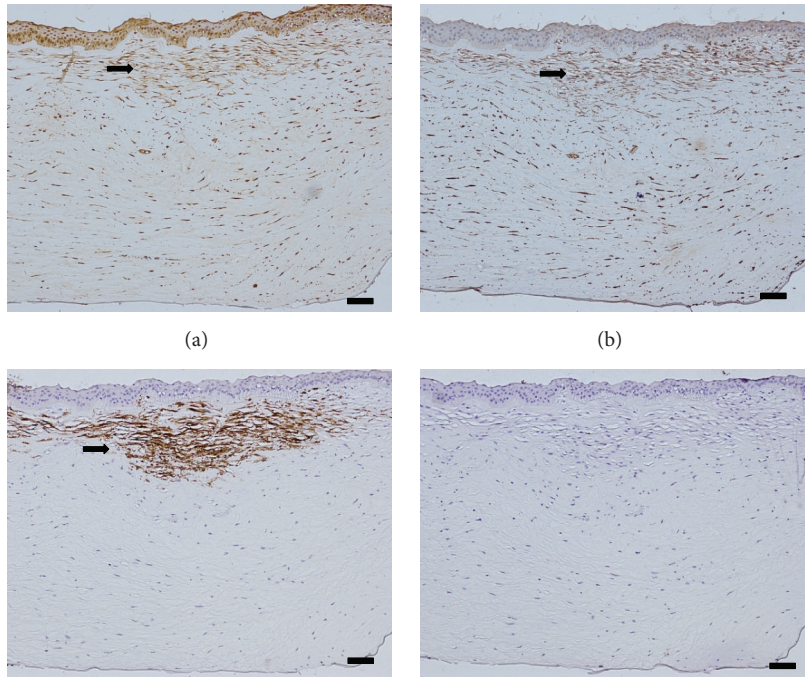

(a) (b) (c) (d)

Figure 5: A patient with advanced keratoconus. (a) High FAP expression in the superficial stroma (black arrow) and decentralized expression in the posterior stroma. (b) Vimentin expression in the superficial stroma (black arrow) and decentralized expression in the posterior stroma. (c) α-SMA expression in the superficial stroma (black arrow). (d) Negative controls in the absence of primary antibodies. Scale bar: 100 μm.

As keratoconus progresses, keratocytes undergo significant changes. A keratocyte is a pinacocyte located in the gap of the parallel arrangement lamellae and is responsible for the synthesis and maintenance of the collagen fibrils and extracellular matrix. As an inactive mesenchymal cell, keratocytes usually preform a quiescent phenotype without abnormal stimulation, so the reflective and sharply demarcated cell nuclei of keratocytes are visible by scanning with in vivo confocal microscopy. In several confocal microscopy studies, the keratocyte density in patients with keratoconus was found to be significantly lower than in the normal controls, and decreases in anterior stromal keratocytes correlated with indices of disease severity [8, 10, 15]. Our study had different findings compared with previous research however. We found no difference in the density of sub-Bowman's stromal keratocytes between patients with mild-to-moderate keratoconus and the controls, but there was significant difference in the morphologic changes of sub-Bowman's stromal keratocytes, branched cell nuclei, and increased cytoplasm processes, indicating that these keratocytes had

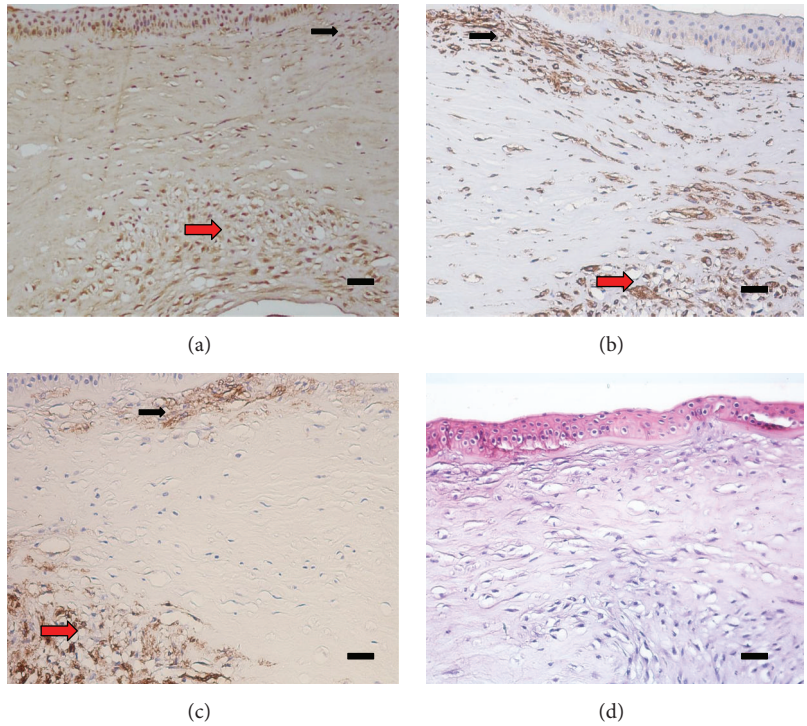

(a) (b) (c) (d)

Figure 6: A patient with advanced keratoconus suffered from superficial corneal scarring and posterior corneal scarring due to rupture of Descemet's membrane. (a) High FAP expression in the superficial stroma (black arrow) and posterior stroma (red arrow). (b) Vimentin expression in the superficial stroma (black arrow) and posterior stroma (red arrow). (c) α-SMA expression in the superficial stroma (black arrow). (d) Negative controls in the absence of primary antibodies. Scale bar: 50 μm.

been activated. Contrary to quiescent keratocytes, the active keratocyte nuclei were less readily identified individually. The activated appearance of keratocytes suggested that an undetermined damage may stimulate fibrocytes to translate into fibroblasts and induce the mitosis of fibroblasts.

Previous studies suggested that the decrease in keratocytes and the imbalance of keratocyte synthesis in keratoconus resulted in a loss of stroma and a decrease in corneal biomechanics [8–10, 16]. Keratoconic cone may be related to an undetermined abnormality in corneal mechanical properties [17], such as corneal thinning and ectasia, caused by the loss of stromal lamellae [3, 18]. Through cohesive tensile strength testing, Dawson et al. found that the anterior 40% of the central corneal stroma was the strongest region of a normal cornea, and the posterior 20% was the weakest region [19]. Therefore, we conclude that the posterior cornea is the weakest region and may endure much smaller tension than anterior cornea. Clinically, the outstanding manifestation of mild keratoconus is that the posterior corneal surface often protrudes forward significantly more than the anterior corneal surface when viewed using corneal topography [20]. In our study, wide alternating dark and light bands were first detected in the posterior stroma of patients with mild-to-moderate keratoconus using confocal microscopy and were finally detected in both the anterior and posterior stroma of patients with advanced keratoconus. These findings may be related to the corneal biomechanic distribution and significant reduction in corneal biomechanics in advanced keratoconus. As reported previously, alternating dark and light bands represented folds of stromal lamellae [21], so alterations in the location and stage of the bands' distribution support the assertion that the abnormalities of the biomechanical properties first occur in the posterior stroma.

Meek et al. [22], through synchrotron X-ray scattering, detected systematic realignment of fibrils. This indicated a high degree of inter- and probably intralamellar displacement and slippage, which may be promoted by a loss of cohesive forces and mechanical failure and lead to thinning of the central cornea and associated changes in corneal curvature. Together with the protrusion of the posterior corneal surface, the anterior collagen withstands increasing tension, and this abnormal tension may lead to the slippage, folding, or even rupture of the anterior collagen lamellae. We hypothesize that this damage to the anterior collagen lamellae could cause the activation of keratocytes, and that is closely related to the formation of superficial stromal scarring. The collagen fibers produced by keratocytes were not visible with in vivo confocal microscopy, so we were unable to detect direct evidence of the slippage or rupture of the anterior collagen lamellae. Nevertheless, one important finding about the alteration of SNP in our study indirectly supported our hypothesis. We found that the nerve fibers had a thickened, prominent appearance, such as excessive branching and curling, and were even interrupted, which may be attributable to alterations in the corneal biomechanics in keratoconus, such as folds and rupturing of the stromal lamellae. Parissi

et al. [23] reported that keratoconus was characterized by a progressive decreasing nerve density and altered nerve morphology, despite CXL treatment. In addition, it was reported that the anterior collagen lamellae were disturbed as observed by histopathology and X-ray scattering techniques [4, 17, 24]. The slippage of the lamellae, especially the anterior stromal lamellae, may stimulate the quiescent keratocytes to change and activate fibroblasts, thus corresponding with the higher reflective image of sub-Bowman's keratocytes in keratoconus. In this progression, mechanical failure stimulation may be a key regulator in keratocyte activation.

Changes in collagen fibers and lamellae can promote the transformation of quiescent keratocytes into fibroblasts and myofibroblasts, a repair phenotype of keratocytes [25]. To verify whether the keratocytes had been activated in accordance with our hypothesis, we evaluated the properties of fibrosis in scarred keratoconus using immunohistochemistry. Vimentin and FAP provide signs of keratocyte activation, and α-SMA is a sign of scar formation. We found that α-SMA, vimentin, and FAP were prominently expressed, with α-SMA only being highly expressed in the superficial stroma. These findings indicated that the keratocytes in keratoconus had been activated widely, and the formation of fibrosis was derived from myofibroblasts in the superficial stroma. Activated keratocytes may result in abnormal remodeling in keratoconus, contributing to the formation of superficial stromal scarring in advanced keratoconus.

The current study involved different stages of keratoconus, so we had an approximate horizon of the microstructure alterations in the development of keratoconus, except in patients who wear contact lenses. The semiautomated cell and nerve counter may have had unspecified measurement errors, which could be minimized with repeated and single-blind measurements. We observed keratocyte activation in keratoconus and verified it via the histopathological examination, but we had no idea of the initiation factor of keratocyte activation. A previous study [7] reported that growth factors from the epithelium may induce a fibrotic wound healing response following the rupture of Bowman's layer. To exclude the disturbance of epithelial-stromal interactions, longitudinal investigations on keratocyte functions under mechanical stimulation in keratoconus are needed, and these may reveal more insights into this putative association.

5. Conclusion

Abnormal microstructures detected in the keratoconic cone showed the slippage, folding, and even rupture of the anterior lamellae and a decrease in biomechanical strength in the development of keratoconus. All these abnormal alterations further encourage keratocyte activation and converting into fibroblasts, and even myofibroblasts, leading to the abnormal remodeling of ECM and the presence of superficial stromal scarring.

Conflict of Interests

The authors declare that there is no conflict of interests regarding the publication of this paper.

Acknowledgments

This study was supported by National Natural Science Foundation of China (81370989 and 81570821), National Basic Research Program of China (2013CB967004), Science & Technology Program of Qingdao (13-1-4-169-jch), Taishan Scholar Program, and Shandong Provincial Excellent Innovation Team Program. The authors thank Ping Lin for her editorial assistance.

References

[1] Y. S. Rabinowitz, "Keratoconus," *Survey of Ophthalmology*, vol. 42, no. 4, pp. 297–319, 1998.

[2] J. H. Krachmer, R. S. Feder, and M. W. Belin, "Keratoconus and related noninflammatory corneal thinning disorders," *Survey of Ophthalmology*, vol. 28, no. 4, pp. 293–322, 1984.

[3] J. H. Mathew, J. D. Goosey, and J. P. G. Bergmanson, "Quantified histopathology of the keratoconic cornea," *Optometry and Vision Science*, vol. 88, no. 8, pp. 988–997, 2011.

[4] I. M. Y. Cheung, C. N. J. McGhee, and T. Sherwin, "A new perspective on the pathobiology of keratoconus: interplay of stromal wound healing and reactive species-associated processes," *Clinical & Experimental Optometry*, vol. 96, no. 2, pp. 188–196, 2013.

[5] L. Zhou, B. Y. J. T. Yue, S. S. Twining, J. Sugar, and R. S. Feder, "Expression of wound healing and stress-related proteins in keratoconus corneas," *Current Eye Research*, vol. 15, no. 11, pp. 1124–1131, 1996.

[6] M. C. Kenney, A. B. Nesburn, R. E. Burgeson, R. J. Butkowski, and A. V. Ljubimov, "Abnormalities of the extracellular matrix in keratoconus corneas," *Cornea*, vol. 16, no. 3, pp. 345–351, 1997.

[7] A. Tuori, I. Virtanen, E. Aine, and H. Uusitalo, "The expression of tenascin and fibronectin in keratoconus, scarred and normal human cornea," *Graefe's Archive for Clinical and Experimental Ophthalmology*, vol. 235, no. 4, pp. 222–229, 1997.

[8] J. Y. F. Ku, R. L. Niederer, D. V. Patel, T. Sherwin, and C. N. J. McGhee, "Laser scanning in vivo confocal analysis of keratocyte density in keratoconus," *Ophthalmology*, vol. 115, no. 5, pp. 845–850, 2008.

[9] J. G. Hollingsworth, N. Efron, and A. B. Tullo, "In vivo corneal confocal microscopy in keratoconus," *Ophthalmic & Physiological Optics*, vol. 25, no. 3, pp. 254–260, 2005.

[10] R. L. Niederer, D. Perumal, T. Sherwin, and C. N. J. McGhee, "Laser scanning in vivo confocal microscopy reveals reduced innervation and reduction in cell density in all layers of the keratoconic cornea," *Investigative Ophthalmology & Visual Science*, vol. 49, no. 7, pp. 2964–2970, 2008.

[11] D. M. Gore, A. J. Shortt, and B. D. Allan, "New clinical pathways for keratoconus," *Eye*, vol. 27, no. 3, pp. 329–339, 2013.

[12] J. Colin and S. Velou, "Current surgical options for keratoconus," *Journal of Cataract and Refractive Surgery*, vol. 29, no. 2, pp. 379–386, 2003.

[13] T. T. McMahon, L. Szczotka-Flynn, J. T. Barr et al., "A new method for grading the severity of keratoconus: the Keratoconus Severity Score (KSS)," *Cornea*, vol. 25, no. 7, pp. 794–800, 2006.

[14] J. T. Barr, B. S. Wilson, M. O. Gordon et al., "Estimation of the incidence and factors predictive of corneal scarring in the collaborative longitudinal evaluation of keratoconus (clek) study," *Cornea*, vol. 25, no. 1, pp. 16–25, 2006.

[15] E. B. Ozgurhan, N. Kara, A. Yildirim, E. Bozkurt, H. Uslu, and A. Demirok, "Evaluation of corneal microstructure in keratoconus: a confocal microscopy study," *American Journal of Ophthalmology*, vol. 156, no. 5, pp. 885.e2–893.e2, 2013.

[16] V. Hurmeric, A. Sahin, G. Ozge, and A. Bayer, "The relationship between corneal biomechanical properties and confocal microscopy findings in normal and keratoconic eyes," *Cornea*, vol. 29, no. 6, pp. 641–649, 2010.

[17] S. Hayes, C. Boote, S. J. Tuft, A. J. Quantock, and K. M. Meek, "A study of corneal thickness, shape and collagen organisation in keratoconus using videokeratography and X-ray scattering techniques," *Experimental Eye Research*, vol. 84, no. 3, pp. 423–434, 2007.

[18] N. Morishige, A. J. Wahlert, M. C. Kenney et al., "Second-harmonic imaging microscopy of normal human and keratoconus cornea," *Investigative Ophthalmology & Visual Science*, vol. 48, no. 3, pp. 1087–1094, 2007.

[19] D. G. Dawson, H. E. Grossniklaus, B. E. McCarey, and H. F. Edelhauser, "Biomechanical and wound healing characteristics of corneas after excimer laser keratorefractive surgery: is there a difference between advanced surface ablation and sub-Bowman's keratomileusis?" *Journal of Refractive Surgery*, vol. 24, no. 1, pp. S90–S96, 2008.

[20] R. Ishii, K. Kamiya, A. Igarashi, K. Shimizu, Y. Utsumi, and T. Kumanomido, "Correlation of corneal elevation with severity of keratoconus by means of anterior and posterior topographic analysis," *Cornea*, vol. 31, no. 3, pp. 253–258, 2012.

[21] J. G. Hollingsworth and N. Efron, "Observations of banding patterns (vogt striae) in keratoconus: a confocal microscopy study," *Cornea*, vol. 24, no. 2, pp. 162–166, 2005.

[22] K. M. Meek, S. J. Tuft, Y. Huang et al., "Changes in collagen orientation and distribution in keratoconus corneas," *Investigative Ophthalmology & Visual Science*, vol. 46, no. 6, pp. 1948–1956, 2005.

[23] M. Parissi, S. Randjelovic, E. Poletti et al., "Corneal nerve regeneration after collagen cross-linking treatment of keratoconus: a 5-year longitudinal study," *JAMA Ophthalmology*, 2015.

[24] N. J. Fullwood, S. J. Tuft, N. S. Malik, K. M. Meek, A. E. A. Ridgway, and R. J. Harrison, "Synchrotron x-ray diffraction studies of keratoconus corneal stroma," *Investigative Ophthalmology & Visual Science*, vol. 33, no. 5, pp. 1734–1741, 1992.

[25] L. Muthusubramaniam, L. Peng, T. Zaitseva, M. Paukshto, G. R. Martin, and T. A. Desai, "Collagen fibril diameter and alignment promote the quiescent keratocyte phenotype," *Journal of Biomedical Materials Research—Part A*, vol. 100, no. 3, pp. 613–621, 2012.

Hindawi Publishing Corporation
BioMed Research International
Volume 2015, Article ID 951081, 11 pages
http://dx.doi.org/10.1155/2015/951081

Review Article

In Vivo Confocal Microscopy of the Human Cornea in the Assessment of Peripheral Neuropathy and Systemic Diseases

Ellen F. Wang, Stuti L. Misra, and Dipika V. Patel

Department of Ophthalmology, New Zealand National Eye Centre, Faculty of Medical and Health Sciences, The University of Auckland, Auckland 1142, New Zealand

Correspondence should be addressed to Dipika V. Patel; dipika.patel@auckland.ac.nz

Received 29 October 2015; Accepted 22 November 2015

Academic Editor: Paolo Nucci

In vivo confocal microscopy (IVCM) of the living human cornea offers the ability to perform repeated imaging without tissue damage. Studies using corneal IVCM have led to significant contributions to scientific and clinical knowledge of the living cornea in health and pathological states. Recently the application of corneal IVCM beyond ophthalmology to wider clinical and research fields has been demonstrated. Abnormalities of the corneal subbasal nerve plexus have been associated with many forms of peripheral neuropathy and Langerhans cells correlate with systemic inflammatory states. There is a rapidly growing evidence base investigating the use of corneal IVCM in many systemic conditions and a well-established evidence base for IVCM imaging of the corneal subbasal plexus in diabetic peripheral neuropathy. This paper reviews the potential use of corneal IVCM in general clinical practice as a noninvasive method of assessing peripheral neuropathies, monitoring inflammatory states and clinical therapeutic response.

1. Introduction

The cornea is the most densely innervated tissue in the body [1]. The cranial nerves, with the exception of the optic nerve, are considered to be a part of the peripheral nervous system, with all the sensory nerves being derived from neural crest cells during embryology [2]. Therefore corneal nerves, arising from the ophthalmic branch of the trigeminal nerve, are considered a part of the peripheral nervous system [2]. The nerves enter the midstroma to track anteriorly from the periphery into the centre in a radial pattern, losing their myelin sheath within 1 mm of the limbus to aid corneal transparency [1, 3, 4]. Corneal nerves are comprised of large, myelinated Aδ fibres that run parallel to Bowman's layer and small, unmyelinated C-fibres that run parallel to Bowman's layer for a short course and then penetrate the epithelium to terminate in invaginations within the superficial cells [1, 3, 4].

Living human corneal nerves can be imaged noninvasively using in vivo confocal microscopy (IVCM) (Figure 1) [3–6]. Three different modes of IVCM have been developed: laser scanning confocal microscopy, slit-scanning confocal microscopy, and tandem scanning confocal microscopy [3–5]. These modes vary in terms of light emission, magnification, contrast, and resolution but all offer the ability to repeatedly examine the same cornea without tissue damage.

IVCM has been widely utilized in clinical practice in corneal and ocular surface imaging. It is used as an aid in the diagnosis of *Acanthamoeba* keratitis, in the assessment of keratoconus, dry eyes, and contact lens wear [5]. Repeated examination of the same cornea allows for detection of changes that are used to monitor response to therapy and recovery after corneal surgery [5]. As well as enabling imaging of corneal pathology, IVCM is increasingly being investigated for its potential to evaluate systemic disease. Studies using this technique have demonstrated corneal subbasal nerve changes that correlate with peripheral neuropathies such as diabetic peripheral neuropathy, idiopathic small fibre neuropathy, Fabry disease, and HIV associated peripheral neuropathy (Table 1) [7–13]. IVCM has also been used to evaluate the ocular effects of neurodegenerative conditions, rheumatological conditions (Table 2), genetic diseases, and chemotherapy.

The current review discusses the contribution of IVCM in the diagnosis and assessment of these systemic diseases and its ability to overcome limitations in current clinical methods

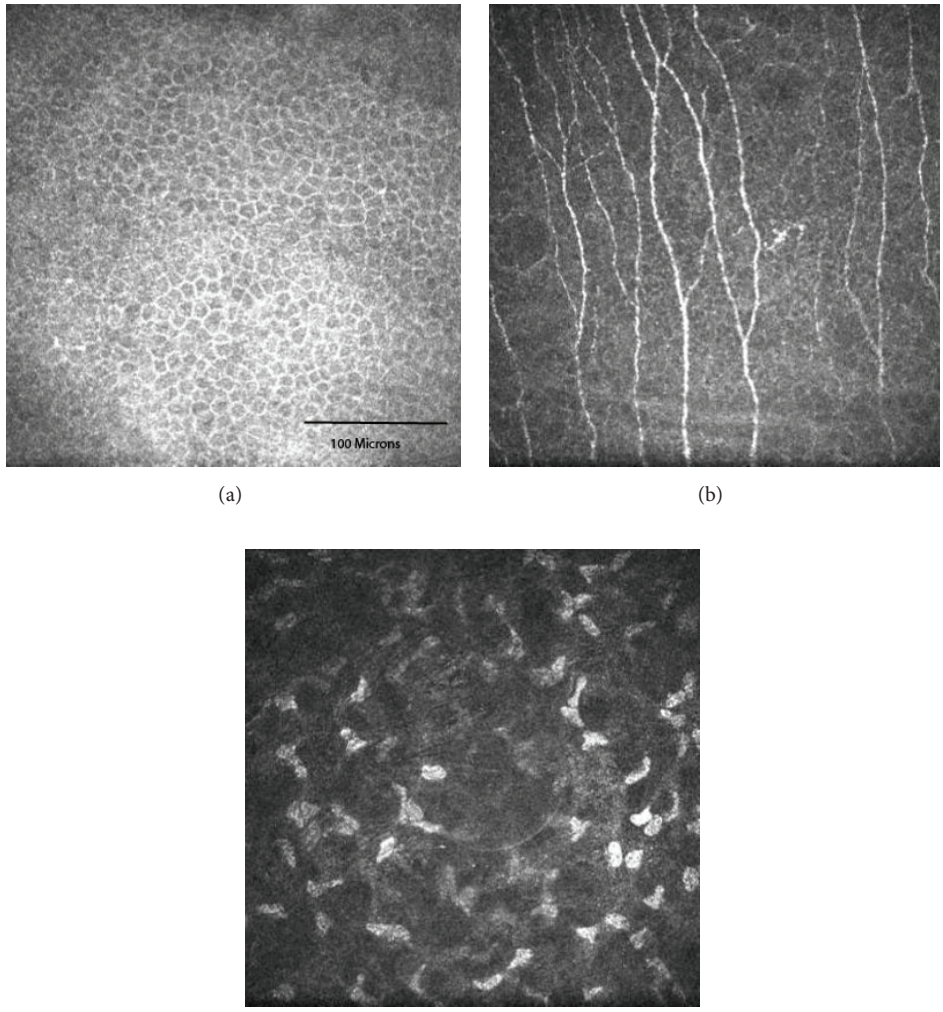

Figure 1: In vivo confocal microscopy images showing the normal corneal basal epithelium (a), central corneal subbasal plexus (b), and stroma (c) from a healthy 24-year-old female.

of assessing these conditions. This review also aims to explore IVCM's potential use in clinical diagnosis, monitoring disease progression, and therapeutic response in current standard clinical practice and in clinical trials of novel treatments, thereby contributing to clinical knowledge and informed clinical decision making.

2. Diabetes

Diabetes is a disease that is of growing global significance, now affecting over 366 million people worldwide [14]. It affects multiple organ systems with its microvascular complications causing the well-known clinical triad of nephropathy, retinopathy, and neuropathy, with diabetic peripheral neuropathy being the most common [15]. These complications lead to decreased quality of life for patients and an increasing burden on global healthcare systems and can result in debilitating long term sequelae such as foot ulceration, amputations, blindness, and renal failure.

Current methods of detecting diabetic peripheral neuropathy include taking a medical history and an examination that involves a clinical peripheral nervous examination, bioesthesiometry, and invasive nerve conduction studies [16–18]. These methods often detect diabetic peripheral neuropathy when the neuropathy becomes well established and have limited sensitivity for detecting early diabetic peripheral neuropathy [7, 16, 18, 19]. While tight glycaemic control is a known key factor in the clinical management of diabetes, it limits the progression of neuropathy in type 1 diabetes, but not type 2 [1]. There is no pharmacological method of preventing or reversing diabetic peripheral neuropathy [1, 16, 20]. Current methods of detecting peripheral neuropathy have several disadvantages including their subjective and variable nature and while electrophysiology and nerve biopsies are reliable, they are expensive and invasive [1, 15, 21].

IVCM is a rapid, noninvasive, and accurate method that enables quantitative analysis of the corneal subbasal nerve plexus and could potentially provide a surrogate marker for

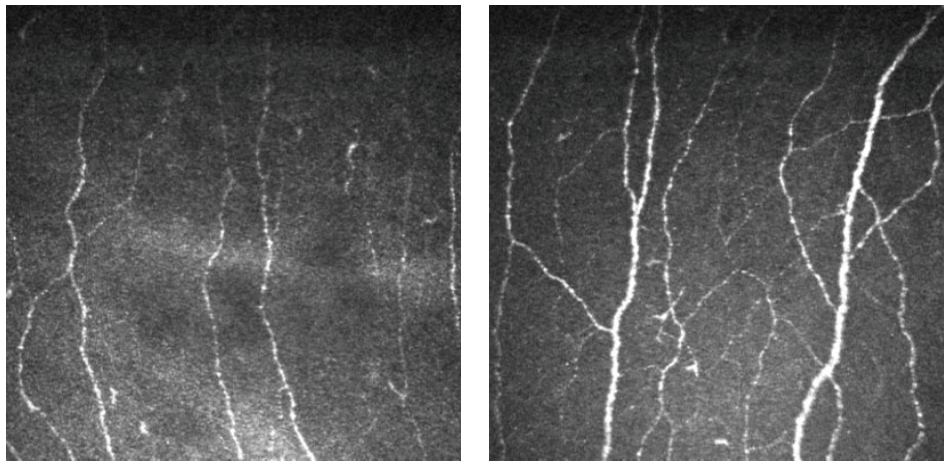

(a) (b)

Figure 2: In vivo confocal microscopy images showing the corneal subbasal plexus of a 33-year-old female with a 14-year history of type 1 diabetes (a) and a healthy 32-year-old healthy female (frame size represents 400 μm × 400 μm).

diabetic peripheral neuropathy [1, 14, 19]. The total length of corneal nerves per unit area is reported to be the most reproducible measure of corneal subbasal nerve density in patients with diabetes [22]. Studies have also shown that patients with type 1 or type 2 diabetes exhibit a marked reduction in subbasal nerve density compared to healthy corneas (Figure 2, Table 3) [8, 14]. Importantly, 50% of patients with diabetes who had no clinical signs of neuropathy were shown to have abnormal corneal subbasal nerve plexus changes, demonstrating corneal changes precede clinically detected peripheral nerve changes [19].

Corneal subbasal nerve density correlates with clinical and electrophysiological assessment of the severity of diabetic peripheral neuropathy [14, 16, 23]. Decreased subbasal nerve density is associated with symptoms of peripheral neuropathy and decreased intraepidermal nerve density [16, 23]. Interestingly, these changes in corneal nerve density precede any clinical signs or symptoms of neuropathy, retinopathy, and microalbuminuria and are also seen in patients with impaired glucose tolerance, without meeting clinical criteria for type 2 diabetes mellitus [7, 8, 14, 16, 24, 25].

IVCM has also been used to assess the recovery of type 1 diabetic patients that undergo pancreas and kidney transplantation [26, 27]. In these studies the focus of IVCM imaging was to detect a therapeutic response to transplantation [26, 28]. Patients receiving simultaneous pancreas and kidney transplantation suffer from severe diabetic consequences, including neuropathy [26–28]. Introducing functioning islet β-cells via pancreas transplantation into patients with type 1 diabetes reverses some of the end organ damage caused and although slow to improve diabetic nephropathy it reportedly improves diabetic neuropathy within one year of receiving the transplant [27]. Regeneration of the intraepidermal nerve fibre layer is an important outcome measure of transplant success and can only be assessed by performing skin biopsies. The correlation of corneal subbasal plexus density with intraepidermal nerve fibre density suggests the potential use of IVCM for monitoring therapeutic response [26, 28]. This could open the door to further studies in this application to other systemic conditions, including the conditions mentioned in this review.

Table 1: Corneal subbasal nerve densities on in vivo confocal microscopy in a range of systemic diseases.

	Corneal subbasal nerve density in patients (mm/mm^2)	Corneal subbasal nerve density in controls (mm/mm^2)
Diabetes type 1 [14]	20.6 ± 1.5	27.7 ± 1.1
Diabetes type 2 [24]	4.3 ± 1.5	13.5 ± 0.3
Parkinson's disease [32]	15.0 ± 8.0	13.5 ± 5.0
Progressive supranuclear palsy [32]	15.0 ± 6.0	13.5 ± 5.0
Amyotrophic lateral sclerosis [36]	1.8 ± 0.4	2.3 ± 0.4
Idiopathic small fibre neuropathy [38]	4.4 ± 0.6	9.3 ± 0.6
Charcot-Marie-Tooth type 1A [41]	15.8 ± 1.5	26.7 ± 1.3
Chronic inflammatory demyelinating polyneuropathy [62]	18.1 ± 3.4	23.5 ± 3.6
Chemotherapy induced peripheral neuropathy [9]	6.8 ± 2.4	10.8 ± 3.8

3. Neurodegenerative Diseases

3.1. Parkinson's Disease and Progressive Supranuclear Palsy. Parkinson's disease (PD) and progressive supranuclear palsy (PSP) are neurodegenerative movement disorders that have similar clinical presentations [29]. Both PD and PSP patients

Table 2: Langerhans cell density on in vivo confocal microscopy in the central and peripheral cornea in rheumatological conditions.

	Central Langerhans cell density in patients (cell/mm^2)	Central Langerhans cell density in controls (cell/mm^2)	Peripheral Langerhans cell density in patients (cell/mm^2)	Peripheral Langerhans cell density in patients (cell/mm^2)
Systemic lupus erythematosus [45]	43.08 ± 48.67	20.57 ± 21.04	124.78 ± 165.39	78.00 ± 39.51
*Ankylosing spondylitis [49]	75.50 (51.18–112.6)	14.50 (0.00–35.10)	131.0 (80.33–168.4)	65.50 (46.75–88.00)
Rheumatoid arthritis [52]	68.15 ± 71.27	23.85 ± 33.81	126.8 ± 104.6	69.29 ± 33.26

*Figures for ankylosing spondylitis are expressed as median with interquartile range and others as a mean with standard deviation.

Table 3: Corneal subbasal nerve densities on in vivo confocal microscopy in diabetes mellitus.

	Corneal subbasal nerve density in patients (mm/mm^2)	Corneal subbasal nerve density in controls (mm/mm^2)
Petropoulos et al. [14], type 1 diabetes		
No retinopathy	20.6 ± 1.5	27.7 ± 1.1
Retinopathy	17.4 ± 0.9	27.7 ± 1.1
No microalbuminuria	19.9 ± 1.7	27.7 ± 1.1
Microalbuminuria	14.3 ± 1.4	27.7 ± 1.1
Misra et al. [19], type 1 diabetes	11.0 ± 3.8	21.17 ± 4.2
Malik et al. [24], type 2 diabetes		
Mild	10.8 ± 0.9	13.5 ± 0.3
Moderate	7.5 ± 1.1	13.5 ± 0.3
Severe	4.3 ± 1.5	13.5 ± 0.3
Tavakoli et al. [23], type 2 diabetes		
Mild	5.48 ± 0.45	11.21 ± 0.88
Moderate	3.01 ± 0.39	11.21 ± 0.88
Severe	2.99 ± 0.34	11.21 ± 0.88

are noted to have ocular surface disease in the form of dry eye syndrome, exacerbated by the decreased blink rate associated with these movement disorders [30]. This is thought to occur due to a denervation of the cornea, leading to reduced corneal sensitivity and reduced blink rate, resulting in asymptomatic surface disease [30]. A study of a small group of patients with a diagnosis of either PD (4 patients) or PSP (7 patients) reported significantly reduced corneal sensitivity and blink rate compared to healthy age-matched controls. However, there was no difference in corneal subbasal nerve density between the three groups despite reduced corneal sensitivity [30]. This observation suggests that the ocular effects of Parkinson's disease and PSP may be due to neural dysfunction rather than denervation but require further investigation due to the small numbers of patients studied [30].

Peripheral neuropathy associated with PD is common and reported to affect 38–55% of patients and the risk of developing peripheral neuropathy in PD may be greater in those treated with levodopa [31]. A study investigating the relationship between corneal nerve density and Parkinson's related peripheral neuropathy examined 25 patients with Parkinson's disease and 25 healthy control subjects. All underwent corneal sensitivity testing with a Cochet-Bonnet aesthesiometer and IVCM. Patients with Parkinson's disease were reported to have significantly decreased corneal sensation, lower corneal nerve density, and greater nerve tortuosity compared with control subjects. The parameters measured were also noted to be related to exposure to dopaminergic medication, inferring the potential use of IVCM to monitor patients receiving dopaminergic medication although the nature of this relationship was not specified [32].

3.2. Amyotrophic Lateral Sclerosis. Amyotrophic lateral sclerosis (ALS) or Lou Gehrig's disease is the most common degenerative disease of motor neurons [33]. Progressive degeneration of upper and lower motor neurons in the brain and spinal cord leads to decreased coordination, speech or voice changes, and cognitive changes that eventually result in muscle atrophy and spasticity, and ultimately death [33]. Most cases are sporadic and the exact aetiology is unknown although several gene mutations have been identified in cases of both familial and sporadic ALS [33]. While ALS largely is a disease of motor neurones, the sensory nervous system is also known to be involved,

causing a decrease in intraepidermal nerve fibre density [34–36].

Subclinical sensory neuron involvement has been demonstrated with pathological evidence on sural nerve biopsies taken from ALS patients [35, 37]. A study of 8 sporadic ALS patients demonstrated that although none of the patients had any signs or symptoms of sensory neuropathy, there was a clear reduction in corneal subbasal nerve density compared with age-matched healthy control subjects [37]. Disease burden was assessed using the ALS Severity Score and the revised ALS Functional Rating Scale [37]. Severity was assessed with 4 outcome measures based on function: speech, swallowing, lower extremities, and upper extremities with speech and swallowing comprising the "bulbar subscore" and the lower and upper extremities comprising the "spinal subscore" [38]. Interestingly, corneal nerve damage correlated with bulbar disability scores but not with spinal disability [37]. In this case series, IVCM has revealed the possibility that ALS is associated with a small fibre neuropathy and further IVCM studies may bring us closer to understanding the mechanisms behind the poorly understood aetiology of ALS.

3.3. Idiopathic Small Fibre Neuropathy. Idiopathic small fibre neuropathy (ISFN) is a subset of small fibre neuropathy that occurs due to damage of the small unmyelinated peripheral nerves, known as C-fibres. The neuropathy is sensory in nature but symptoms are highly variable in location and severity. Typically the symptoms begin in the extremities and while impaired glucose tolerance has been a suggested risk factor, it is not present in all cases and symptoms do not seem to be related to nerve damage. Idiopathic small fibre neuropathy is therefore more difficult to diagnose than other neuropathies [39], particularly since nerve conduction studies evaluate large myelinated fibres and do not test the small unmyelinated fibres. Quantitative sensory testing is subjective and unreliable, meaning clinicians are increasingly turning to skin biopsies for a conclusive diagnosis.

A pioneering IVCM study of 24 patients with idiopathic small fibre neuropathy showed a significant decrease in corneal subbasal nerve density and increased nerve fibre tortuosity [39]. Corneal subbasal nerve changes were not correlated with impaired glucose tolerance, body mass index (BMI), lipid levels, or blood pressure [39]. This is an interesting observation given that all the patients in this study had significant neuropathy symptoms but normal electrophysiology and quantitative sensory testing [39]. Another small case series of three patients with ISFN also demonstrated significantly decreased corneal subbasal nerve density compared with normal controls, correlating with intraepidermal nerve fibre density from skin punch biopsies [40]. Whilst these studies are too small to draw concrete conclusions, they point to the fact that the mechanism behind ISFN is still poorly understood and thus far only associations with metabolic risk factors can be made without any causal relationships.

3.4. Charcot-Marie-Tooth Disease. Charcot-Marie-Tooth (CMT) disease is the most common hereditary motor and sensory neuropathy that causes progressive loss of muscle tissue and sensation [41, 42]. CMT is categorised into subtypes based on the gene mutation that is present with the most common subtype being type 1A, accounting for 70–80% of all cases [42]. The diagnosis is based on history and genetic testing, clinical examination, and nerve conduction testing [41, 42]. Although disease progression is attributed to demyelination and axonal degeneration of large myelinated fibres, there is no correlation between motor or sensory nerve conduction testing and neurological disability scores in CMT1A [41, 43].

CMT is associated with a small fibre neuropathy (C-fibres) but this has been difficult to assess and quantify. Electrophysiology does not test the small unmyelinated fibres involved in this neuropathy and therefore patients with CMT are traditionally investigated with subjective quantitative sensory testing and with invasive skin or sural nerve biopsies [42]. In a study 12 patients with CMT1A were recruited with 12 age-matched healthy subjects and all underwent a detailed neurological examination including bioesthesiometry, nerve conduction studies and symptoms of neuropathy, corneal sensitivity measured using a noncontact corneal aesthesiometer, and IVCM [42]. Patients with CMT1A were reported to have significantly decreased corneal subbasal nerve density, correlating strongly with symptoms of painful neuropathy and reduced nerve conduction testing scores [42].

IVCM has an emerging role in enabling clinicians to quantify the small fibre pathology in CMT1A. IVCM offers a rapid, noninvasive evaluation of CMT1A, offering an advantage over quantitative sensory testing and biopsies.

4. Rheumatology

4.1. Systemic Lupus Erythematosus. Systemic lupus erythematosus (SLE) is a chronic inflammatory autoimmune condition of varying severity that can affect any organ system. It is of unknown aetiology and its pathogenesis involves the production of autoantibodies due to loss of T-cell regulatory ability and results in complement activation that triggers the inflammatory cascade [44]. It has a variety of ocular manifestations including optic neuropathy, retinal vasculitis, and keratoconjunctivitis sicca with keratoconjunctivitis sicca being the most common [44].

SLE related keratoconjunctivitis sicca demonstrates a marked increase in the density of Langerhans cells within the central cornea, with over half of these cells exhibiting dendritic features, as imaged by IVCM (Figure 3) [45]. Langerhans cells are a subset of the population of antigen presenting dendritic cells within the cornea, mainly located in the epithelium of the peripheral cornea [46]. They activate T-cells as part of the corneal immune system [46]. In pathological states Langerhans cells mature, form dendritic processes, and migrate from the periphery into the central cornea [46].

Interestingly, IVCM has been used to assess a case of bilateral deep keratitis associated with SLE induced iridocyclitis [47]. The patient presented with decreased visual acuity during a flare-up of SLE and examination revealed deep stromal opacities spread throughout the central and

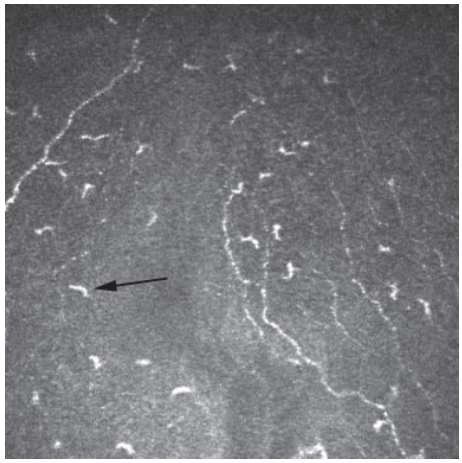

Figure 3: In vivo confocal microscopy image at the level of Bowman's layer showing Langerhans cells (arrow) (frame size represents 400 μm × 400 μm).

peripheral cornea. IVCM was used to further assess the nature of these opacities and subsequently demonstrated deposition of refringent crystals within the corneal stroma [47]. These deposits mirror the deposition of immune complexes in systemic tissues in patients with SLE. The crystalline deposits are located in the deep stroma and are believed to occur as a result of dilation of perilimbal vessels during inflammatory episodes [47–49].

While rare, corneal manifestations can be the initial presentation of SLE and in these cases IVCM of corneal deposits may contribute towards diagnosis. However, further studies are needed to clarify its role in diagnosis and to investigate the potential of using IVCM to monitor the progression of deep keratitis as a biomarker for disease severity [47]. IVCM may also aid in the assessment of keratoconjunctivitis sicca, the most common ocular manifestation of SLE [44]. Further studies of IVCM imagining of Langerhans cells in the central cornea in SLE could help establish a relationship between this and disease progression and systemic inflammation, potentially providing another biomarker for clinical monitoring of SLE.

4.2. Ankylosing Spondylitis. Ankylosing spondylitis (AS) is a seronegative chronic inflammatory condition primarily of the axial skeleton, with variable involvement of the peripheral skeleton [50]. AS typically affects young males with the most common presenting complaint being lower back pain due to sacroiliac joint inflammation [50]. Progression of the disease leads to bone formation in the spine which results in fusion of the joints [51].

The association between AS and uveitis is well known [52]. AS is also associated with corneal changes; the most common is keratoconjunctivitis sicca due to secondary Sjögren's syndrome, occurring in 10% of patients [50].

As in SLE, Langerhans cells play an important role in AS related keratoconjunctivitis sicca. There is also increasing evidence to suggest that Langerhans cells in the cornea play an important role in the immunoregulatory processes [50]. Studies investigating the role of these cells in the cornea have noted that Langerhans cells in the cornea tend to be activated [44, 46, 53]. Langerhans cells then migrate from their usual location in the peripheral cornea, into the central cornea during an inflammatory state [44, 46, 50, 53].

An increased number and activation of Langerhans cells were not associated with articular disease symptom severity but correlated with patients with higher systemic inflammatory levels [i.e., higher serum C-reactive protein (CRP) and erythrocyte sedimentation rate (ESR)] [50]. Due to the small numbers in this study (24 patients) associations between Langerhans cell density and HLA B27 could not be made [50]. Patients with an active systemic inflammatory disease state (elevated serum CRP and ESR) had significantly decreased tear production compared with healthy control subjects and AS patients with low systemic inflammation [50]. This suggests that corneal changes are associated with systemic inflammation rather than dry eye and poses the possibility that IVCM of Langerhans cells, much like SLE, can be used to monitor disease progression and therapeutic response [44].

4.3. Rheumatoid Arthritis. Rheumatoid arthritis (RA) is a chronic, inflammatory disorder affecting the joints, leading to progressive deformation and loss of function [54]. The inflammation affects the joint capsule and cartilage, causing fibrosis, stiffness, and pain. Systemically RA can cause diffuse inflammation of the pleura, pericardium, and ocular surfaces [54]. Ocular manifestations of RA include scleritis, keratitis, and keratoconjunctivitis, with sicca symptoms being the most common [53]. IVCM allows for direct visualisation of the ocular tissues, especially the Langerhans cells that play a key role in regulation of the corneal immune response [53].

The maturation process by which Langerhans cells develop dendrites and migrate to the central cornea is induced by inflammatory cytokines including IL-1α, IL-6, IL-8, IL-12, and TNF-α [53]. As with systemic lupus erythematosus and ankylosing spondylitis, IVCM of the central cornea in 52 RA patients and 24 age-matched controls revealed an increase in dendritic, activated Langerhans cells in the central cornea of those with RA [53]. Langerhans cell density at the central cornea was 68.15 ± 71.27 cells/mm^2 in RA patients and 23.85 ± 33.81 cells/mm^2 in healthy control subjects [53]. This remains a significant increase even after patients with overlapping Sjögren's syndrome and eye symptoms were excluded [53]. IVCM allows for an integrated, whole body approach to assessment of rheumatoid arthritis where disease severity can be measured in terms of not only systemic inflammatory markers, but also clinical ocular signs of keratoconjunctivitis sicca and Langerhans cell density.

4.4. Sjögren's Syndrome. Sjögren's syndrome is a chronic autoimmune disorder in which the exocrine glands are affected by inflammation leading to xerostomia and keratoconjunctivitis sicca. The syndrome can be primary or may occur secondary to another connective tissue disorder [54]. Previously, keratoconjunctivitis sicca associated with Sjögren's syndrome was thought to be due to a deficiency

in the secretion of the aqueous component of the tear film, but now it is recognised to be a complex interaction between aqueous deficiency, lacrimal gland inflammation, and evaporative dry eye [55].

Sjögren's disease shows an increased density of dendritic Langerhans cells in the central cornea, as imaged by IVCM. This increase is observed in several other systemic diseases, previously mentioned in this review [46, 50, 53]. Langerhans cell density could possibly be a useful marker of disease status in Sjögren's syndrome.

Another biomarker investigated in Sjögren's disease is conjunctival goblet cell density and meibomian gland density [55, 56]. Both primary and secondary Sjögren's patients demonstrated lower meibomian gland density. However, Sjögren's syndrome shows less acinar dilation, lower secretion reflectivity, and decreased gland opening diameters in contrast to patients with meibomian gland disease [55]. A decrease in conjunctival goblet cell density is reported to be an accurate marker of ocular surface disease [56]. This is due to the role of the goblet cells in secreting the mucin needed for tear film stability and a reduction in the number of goblet cells is associated with ocular surface disease [56]. Traditionally assessment of goblet cells is made by impression cytology [56]. IVCM enables imaging of goblet cells in vivo and a significant decrease in goblet cell density has been demonstrated in Sjögren's syndrome patients noninvasively [56]. However it is of note that goblet cell density measured by IVCM was higher than the density measured by impression cytology [56]. Examination of goblet cell density allows for not only diagnosis of Sjögren's syndrome, but also evaluation of the efficacy of therapeutic interventions and monitoring of disease progression [56].

5. Genetic Diseases: Fabry Disease

Fabry disease is a rare genetic, X-linked lysosomal storage disease characterised by a deficiency or absence of the alpha-galactosidase A enzyme. This deficiency results in the accumulation of a metabolic by-product known as globotriaosylceramide (Gb3), a glycosphingolipid. The accumulation of glycosphingolipid in vasculature, tissues, and end organs produced a clinical myriad of symptoms that can include renal failure, hypertension, cardiomyopathy, neuropathy, anhidrosis, and angiokeratomas [57]. Presentation of Fabry disease varies and includes cardiomyopathies, renal impairment, unexplained pain throughout the whole body or localised in the extremities, within the abdomen and thoracic cavity, and gastrointestinal and cerebrovascular symptoms [58]. The variability in clinical presentation makes Fabry disease an often elusive diagnosis. A review of Fabry disease demonstrated that the delay in diagnosis can be as long as 10 years, a significant delay in a potentially life-threatening disease [57]. Corneal verticillata is a characteristic ocular sign of Fabry disease, occurring in 88% of all female and 95% of all male patients and are thought to occur due to glycosphingolipid deposition within the cornea at the level of Bowman's layer [57].

Corneal verticillata can be caused by a variety of agents, usually long term therapy with a wide variety of medications (e.g., amiodarone), or can occur secondary to environmental exposure to silica dust [57]. Verticillata is hyperreflective intracellular inclusions, and their appearance on IVCM as an irregular surface on Bowman's layer helps to differentiate Fabry disease from other causes such as amiodarone-induced keratopathy [12, 58]. IVCM also reveals generalised deposition of a reflective substance throughout the corneal stroma [12]. In addition to IVCM's diagnostic merit, it has also been demonstrated to be useful in monitoring the regression of the hyperreflective inclusions in patients being treated with enzyme replacement therapy [10].

Fabry disease is associated with a small fibre neuropathy, a key factor in the diagnosis and monitoring of disease progression [18]. Electrophysiology and quantitative sensory testing have been employed for monitoring purposes but are known to be less accurate than the more invasive techniques of sural nerve or skin biopsies [18]. Symptom severity, electrophysiology, and quantitative sensory testing (QST) all correlated significantly with a decrease in subbasal corneal nerve density on IVCM, making IVCM a potentially accurate and noninvasive monitoring tool in this disease [18].

6. Immunology

6.1. HIV. Human immunodeficiency virus (HIV) associated peripheral neuropathy is the most common neurological effect of the virus and affects most HIV patients to varying degrees [59]. As with small fibre neuropathies of other causes, HIV peripheral neuropathy is associated with a significant decrease in intraepidermal nerve fibre density [60]. HIV neuropathy can be assessed through reported symptoms, quantitative sensory testing, and skin biopsies of intraepidermal nerve fibre density, each with their own limitations. Patient reported symptoms are subjective, and often symptoms of mild neuropathy are not reported [60, 61]. Quantitative sensory testing of vibration, warm and cool sensation are able to detect individuals with the greatest degree of peripheral nerve dysfunction when correlated with invasive skin punch biopsies [61]. While these methods are able to identify those with HIV associated neuropathy, they are not sensitive enough to detect mild neuropathy [61].

A key study investigating simian immunodeficiency virus (SIV), the simian variant of HIV, has shown that SIV leads to significant corneal subbasal nerve loss in Macaque monkeys [62]. The study involved *in vitro* immunolabeling of corneal tissue from Macaque monkeys infected with SIV followed by manual and automated analysis of nerve density [62]. Corneal nerve density was directly correlated with epidermal nerve fibre length, measurement of the degree of RNA viral replication, and cellular immune activation in the trigeminal ganglia [62]. In addition to these correlations, corneal nerve fibre density was reported to be lower in the group with faster progression of neuropathy, signalling the potential to use IVCM as a monitoring tool for the progression of disease [62].

This study has been heralded as a cornerstone development in the study of HIV neuropathy. If this is also demonstrated in human patients, IVCM could provide effective diagnosis of HIV neuropathy and be a valuable clinical

tool in monitoring the progression of HIV neuropathy [62].

6.2. Peripheral Autoimmune Neuropathy. Peripheral autoimmune neuropathy is a group of syndromes involving an acquired, chronic inflammatory process that results in peripheral nerve damage. Several different immune pathways have been implicated but the process is still poorly understood. Chronic inflammatory demyelinating polyneuropathy (CIDP) is one such syndrome and while it mainly affects large myelinated nerves, skin biopsies of CIDP patients have also demonstrated small nerve fibre involvement [63].

IVCM demonstrated significantly reduced corneal subbasal nerve density in CIDP patients [63]. Despite this, subbasal nerve density did not correlate with nerve conduction studies, trigeminal somatosensory evoked potentials, or any other clinical measurement. This lack of correlation points towards the multifocal nerve fibre involvement hypothesis in a poorly understood condition [63].

Another case noted normal subbasal nerves but significantly thickened and tortuous stromal nerves that returned to normal appearances after treatment with rituximab and corticosteroids [11]. These corneal nerve changes correlated with clinical symptoms and nerve conduction studies [11]. The observation of decreased subbasal nerve density in CIDP could contribute to overall medical knowledge and understanding of the underlying pathogenesis of this condition. The application of IVCM to this condition requires further investigation. Larger prospective studies are needed to explore the relationship between corneal subbasal nerve density and the pathogenesis and progression of CIDP. Its ability to simultaneously assess small fibre damage and the immune response in dendritic, maturing Langerhans cells makes IVCM an attractive potential tool in the diagnosis and monitoring of CIDP.

7. Chemotherapy Induced Peripheral Neuropathy

Chemotherapy with platinum based agents such as oxaliplatin is considered the standard of care in treatment of gastrointestinal cancers [64]. Unfortunately the drug may cause sensory neuropathy in up to 80% of patients, a neuropathy sufficiently severe to limit the dose of chemotherapy delivered or terminate treatment altogether [64]. Recently, corneal IVCM has been shown to be a sensitive clinical tool in early diabetic peripheral neuropathy and may be clinically used to diagnose and monitor progression of neuropathy. Therefore, it may be possible to use corneal IVCM as a surrogate or even prognostic marker for chemotherapy induced peripheral neuropathy.

In the largest case series in the literature, fifteen patients receiving oxaliplatin chemotherapy for colorectal adenocarcinoma were assessed prior to commencement of chemotherapy, after four cycles in those undergoing more than four cycles, and again after completion of chemotherapy [9]. Out of the fifteen oxaliplatin patients, ten had worsened subjective neuropathy symptoms at the end of the study and eight had clinically detected signs of peripheral neuropathy. IVCM revealed corneal subbasal nerve plexus abnormalities in ten patients, with a decreased nerve density and increased tortuosity (Figure 4). Seven of these patients had worsened symptoms of neuropathy and abnormal neurophysiology; the remaining three had worsened symptoms and normal neurophysiology. Of the five patients with stable symptom scores, four had IVCM changes. IVCM changes were present after four cycles and persisted until completion [9].

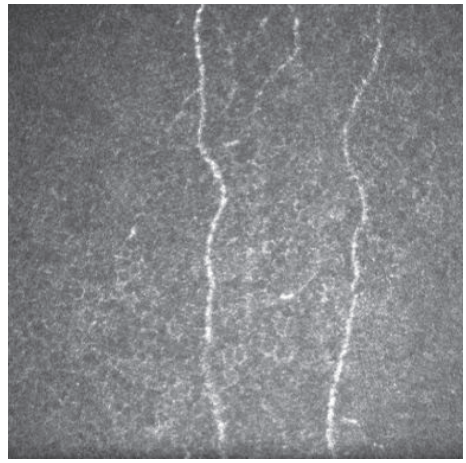

Figure 4: In vivo confocal microscopy image of the central corneal subbasal plexus of a 72-year-old male who completed nine courses of oxaliplatin chemotherapy, showing a low subbasal nerve density (frame size represents 400 μm × 400 μm).

This case series highlighted the potential role IVCM may play in oxaliplatin-induced peripheral neuropathy and how it may be used to identify at-risk patients. Future studies investigating the use of IVCM in oxaliplatin-induced peripheral neuropathy are needed to fully assess the correlation between corneal subbasal nerve density and peripheral neuropathy. Further assessment may reveal corneal IVCM to be a cost-effective, rapid screening tool for detecting or predicting oxaliplatin-induced peripheral neuropathy and monitoring its development during chemotherapy treatment.

8. Conclusion

IVCM allows for repeated, noninvasive, direct visualisation of these nerves, enabling detection of damage, making it a powerful clinical and research tool [4, 5]. Recently there is increasing interest in applying this technique to the assessment of systemic conditions and peripheral neuropathies with hopes that its advantages will provide a rapid, cost-effective method of assessing and managing patients.

Peripheral neuropathies are currently evaluated using several methods such as electrophysiology, assessment of neurological disability via various validated questionnaires, and quantitative sensory testing [15, 21, 24, 65]. These clinical parameters have several limitations when assessed in a clinical setting. Questionnaires are subjective, and while electrophysiology and quantitative sensory testing methods are objective, they are often not sensitive enough to detect

the early stages of neuropathy. Only the gold standard of an invasive nerve or skin biopsy will permit clinicians to directly examine nerve fibre damage. IVCM is able to overcome these limitations and most importantly allows for repeated examinations without causing tissue damage.

There is growing evidence regarding the use of IVCM in patients with diabetes and correlating corneal nerve density with peripheral neuropathy. However, only a handful of clinical studies have investigated the use IVCM in other systemic conditions, and most of the studies involved are small case series. While providing interesting results that suggest IVCM could be clinically useful in these conditions, further research is needed to fully explore its diagnostic and monitoring potential.

There is an increasing body of research investigating the use of IVCM of the cornea in patients with systemic diseases. However, while being promising much of the research in this field involves small numbers of patients. Despite showing statistically significant correlations, further work is needed to evaluate its potential use in the diagnosis and management of systemic disease.

Conflict of Interests

The authors declare that there is no conflict of interests regarding the publication of this paper.

References

[1] M. Tavakoli, I. N. Petropoulos, and R. A. Malik, "Corneal confocal microscopy to assess diabetic neuropathy: an eye on the foot," *Journal of Diabetes Science and Technology*, vol. 7, no. 5, pp. 1179–1189, 2013.

[2] B. Pansky, "The peripheral nervous system and cranial nerves," in *Review of Medical Embryology*, p. 152, Macmillan Publishers, New York, NY, USA, 1st edition, 1982.

[3] L. Oliveira-Soto and N. Efron, "Morphology of corneal nerves using confocal microscopy," *Cornea*, vol. 20, no. 4, pp. 374–384, 2001.

[4] D. V. Patel and C. N. J. McGhee, "Mapping of the normal human corneal sub-basal nerve plexus by in vivo laser scanning confocal microscopy," *Investigative Ophthalmology & Visual Science*, vol. 46, no. 12, pp. 4485–4488, 2005.

[5] D. V. Patel and C. N. J. McGhee, "In vivo confocal microscopy of human corneal nerves in health, in ocular and systemic disease, and following corneal surgery: a review," *British Journal of Ophthalmology*, vol. 93, no. 7, pp. 853–860, 2009.

[6] C. N. Grupcheva, T. Wong, A. F. Riley, and C. N. J. McGhee, "Assessing the sub-basal nerve plexus of the living healthy human cornea by in vivo confocal microscopy," *Clinical and Experimental Ophthalmology*, vol. 30, no. 3, pp. 187–190, 2002.

[7] O. Asghar, I. N. Petropoulos, U. Alam et al., "Corneal confocal microscopy detects neuropathy in subjects with impaired glucose tolerance," *Diabetes Care*, vol. 37, no. 9, pp. 2643–2646, 2014.

[8] G. Bitirgen, A. Ozkagnici, R. A. Malik, and H. Kerimoglu, "Corneal nerve fibre damage precedes diabetic retinopathy in patients with Type 2 diabetes mellitus," *Diabetic Medicine*, vol. 31, no. 4, pp. 431–438, 2014.

[9] M. Campagnolo, D. Lazzarini, I. Fregona et al., "Corneal confocal microscopy in patients with oxaliplatin-induced peripheral neuropathy," *Journal of the Peripheral Nervous System*, vol. 18, no. 3, pp. 269–271, 2013.

[10] K. Falke, A. Büttner, M. Schittkowski et al., "The microstructure of cornea verticillata in Fabry disease and amiodarone-induced keratopathy: a confocal laser-scanning microscopy study," *Graefe's Archive for Clinical and Experimental Ophthalmology*, vol. 247, no. 4, pp. 523–534, 2009.

[11] P. H. Lalive, A. Truffert, M. R. Magistris, T. Landis, and A. Dosso, "Peripheral autoimmune neuropathy assessed using corneal in vivo confocal microscopy," *Archives of Neurology*, vol. 66, no. 3, pp. 403–405, 2009.

[12] L. Mastropasqua, M. Nubile, M. Lanzini, P. Carpineto, L. Toto, and M. Ciancaglini, "Corneal and conjunctival manifestations in Fabry disease: in vivo confocal microscopy study," *American Journal of Ophthalmology*, vol. 141, no. 4, pp. 709–709.e11, 2006.

[13] I. N. Petropoulos, U. Alam, H. Fadavi et al., "Rapid automated diagnosis of diabetic peripheral neuropathy with in vivo corneal confocal microscopy," *Investigative Ophthalmology & Visual Science*, vol. 55, no. 4, pp. 2071–2078, 2014.

[14] I. N. Petropoulos, P. Green, A. W. Chan et al., "Corneal confocal microscopy detects neuropathy in patients with type 1 diabetes without retinopathy or microalbuminuria," *PLoS ONE*, vol. 10, no. 4, Article ID e0123517, 2015.

[15] P. J. Dyck, C. J. Overland, P. A. Low et al., "Signs and symptoms versus nerve conduction studies to diagnose diabetic sensorimotor polyneuropathy: CI vs. NPhys trial," *Muscle and Nerve*, vol. 42, no. 2, pp. 157–164, 2010.

[16] C. Quattrini, M. Tavakoli, M. Jeziorska et al., "Surrogate markers of small fiber damage in human diabetic neuropathy," *Diabetes*, vol. 56, no. 8, pp. 2148–2154, 2007.

[17] N. Pritchard, K. Edwards, A. M. Shahidi et al., "Corneal markers of diabetic neuropathy," *Ocular Surface*, vol. 9, no. 1, pp. 17–28, 2011.

[18] M. Tavakoli, A. Marshall, L. Thompson et al., "Corneal confocal microscopy: a novel noninvasive means to diagnose neuropathy in patients with Fabry disease," *Muscle and Nerve*, vol. 40, no. 6, pp. 976–984, 2009.

[19] S. L. Misra, J. P. Craig, D. V. Patel et al., "In vivo confocal microscopy of corneal nerves: an ocular biomarker for peripheral and cardiac autonomic neuropathy in type 1 diabetes mellitus," *Investigative Opthalmology & Visual Science*, vol. 56, no. 9, pp. 5060–5065, 2015.

[20] G. Bitirgen, A. Ozkagnici, R. A. Malik, and H. Kerimoglu, "Corneal nerve fibre damage precedes diabetic retinopathy in patients with type 2 diabetes mellitus," *Diabetic Medicine*, vol. 31, no. 4, pp. 431–438, 2014.

[21] R. Freeman, K. P. Chase, and M. R. Risk, "Quantitative sensory testing cannot differentiate simulated sensory loss from sensory neuropathy," *Neurology*, vol. 60, no. 3, pp. 465–470, 2003.

[22] P. Hertz, V. Bril, A. Orszag et al., "Reproducibility of in vivo corneal confocal microscopy as a novel screening test for early diabetic sensorimotor polyneuropathy," *Diabetic Medicine*, vol. 28, no. 10, pp. 1253–1260, 2011.

[23] M. Tavakoli, C. Quattrini, C. Abbott et al., "Corneal confocal microscopy: a novel noninvasive test to diagnose and stratify the severity of human diabetic neuropathy," *Diabetes Care*, vol. 33, no. 8, pp. 1792–1797, 2010.

[24] R. A. Malik, P. Kallinikos, C. A. Abbott et al., "Corneal confocal microscopy: a non-invasive surrogate of nerve fibre damage and

repair in diabetic patients," *Diabetologia*, vol. 46, no. 5, pp. 683–688, 2003.

[25] A. M. Shahidi, G. P. Sampson, N. Pritchard et al., "Retinal nerve fibre layer thinning associated with diabetic peripheral neuropathy," *Diabetic Medicine*, vol. 29, no. 7, pp. e106–e111, 2012.

[26] S. Mehra, M. Tavakoli, P. A. Kallinikos et al., "Corneal confocal microscopy detects early nerve regeneration after pancreas transplantation in patients with type 1 diabetes," *Diabetes Care*, vol. 30, no. 10, pp. 2608–2612, 2007.

[27] X. Navarro, D. E. R. Sutherland, and W. R. Kennedy, "Long-term effects of pancreatic transplantation on diabetic neuropathy," *Annals of Neurology*, vol. 42, no. 5, pp. 727–736, 1997.

[28] M. Tavakoli, M. Mitu-Pretorian, I. N. Petropoulos et al., "Corneal confocal microscopy detects early nerve regeneration in diabetic neuropathy after simultaneous pancreas and kidney transplantation," *Diabetes*, vol. 62, no. 1, pp. 254–260, 2013.

[29] R. G. Burciu, E. Ofori, P. Shukla et al., "Distinct patterns of brain activity in progressive supranuclear palsy and Parkinson's disease," *Movement Disorders*, vol. 30, no. 9, pp. 1248–1258, 2015.

[30] V. C. Reddy, S. V. Patel, D. O. Hodge, and J. A. Leavitt, "Corneal sensitivity, blink rate, and corneal nerve density in progressive supranuclear palsy and parkinson disease," *Cornea*, vol. 32, no. 5, pp. 631–635, 2013.

[31] F. Mancini, C. Comi, G. D. Oggioni et al., "Prevalence and features of peripheral neuropathy in Parkinson's disease patients under different therapeutic regimens," *Parkinsonism and Related Disorders*, vol. 20, no. 1, pp. 27–31, 2014.

[32] R. Anjos, L. Vieira, A. Sousa, V. Maduro, N. Alves, and P. Candelaria, "Peripheral neuropathy in Parkinson disease: an in vivo confocal microscopy study," *Acta Ophthalmologica*, vol. 92, supplement 253, 2014.

[33] R. Mancuso and X. Navarro, "Amyotrophic lateral sclerosis: current perspectives from basic research to the clinic," *Progress in Neurobiology*, vol. 133, pp. 1–26, 2015.

[34] G. Amoiridis, D. Tsimoulis, and I. Ameridou, "Clinical, electrophysiologic, and pathologic evidence for sensory abnormalities in ALS," *Neurology*, vol. 71, no. 10, p. 779, 2008.

[35] M. Hammad, A. Silva, J. Glass, J. T. Sladky, and M. Benatar, "Clinical, electrophysiologic, and pathologic evidence for sensory abnormalities in ALS," *Neurology*, vol. 69, no. 24, pp. 2236–2242, 2007.

[36] J. Weis, I. Katona, G. Müller-Newen et al., "Small-fiber neuropathy in patients with ALS," *Neurology*, vol. 76, no. 23, pp. 2024–2029, 2011.

[37] G. Ferrari, E. Grisan, F. Scarpa et al., "Corneal confocal microscopy reveals trigeminal small sensory fiber neuropathy in amyotrophic lateral sclerosis," *Frontiers in Aging Neuroscience*, vol. 6, article 278, 2014.

[38] A. D. Hillel, R. M. Miller, K. Yorkston, E. McDonald, F. H. Norris, and N. Konikow, "Amyotrophic lateral sclerosis severity scale," *Neuroepidemiology*, vol. 8, no. 3, pp. 142–150, 1989.

[39] M. Tavakoli, A. Marshall, R. Pitceathly et al., "Corneal confocal microscopy: a novel means to detect nerve fibre damage in idiopathic small fibre neuropathy," *Experimental Neurology*, vol. 223, no. 1, pp. 245–250, 2010.

[40] F. Gemignani, G. Ferrari, F. Vitetta, M. Giovanelli, C. Macaluso, and A. Marbini, "Non-length-dependent small fibre neuropathy. Confocal microscopy study of the corneal innervation," *Journal of Neurology, Neurosurgery and Psychiatry*, vol. 81, no. 7, pp. 731–733, 2010.

[41] K. M. Krajewski, R. A. Lewis, D. R. Fuerst et al., "Neurological dysfunction and axonal degeneration in Charcot-Marie-Tooth disease type 1A," *Brain*, vol. 123, no. 7, pp. 1516–1527, 2000.

[42] M. Tavakoli, A. Marshall, S. Banka et al., "Corneal confocal microscopy detects small-fiber neuropathy in Charcot-Marie-Tooth disease type 1A patients," *Muscle and Nerve*, vol. 46, no. 5, pp. 698–704, 2012.

[43] P. J. Dyck, P. J. Thomas, J. W. Griffin, P. A. Low, and J. F. Poduslo, Eds., *Peripheral Neuropathy*, W.B. Saunders Company, Philadelphia, Pa, USA, 3rd edition, 1993.

[44] N. V. Palejwala, H. S. Walia, and S. Yeh, "Ocular manifestations of systemic lupus erythematosus: a review of the literature," *Autoimmune Diseases*, vol. 2012, Article ID 290898, 9 pages, 2012.

[45] A. Zhivov, J. Stave, B. Vollmar, and R. Guthoff, "In vivo confocal microscopic evaluation of langerhans cell density and distribution in the corneal epithelium of healthy volunteers and contact lens wearers," *Cornea*, vol. 26, no. 1, pp. 47–54, 2007.

[46] M. D. Resch, L. Marsovszky, J. Németh, M. Bocskai, L. Kovács, and A. Balog, "Dry eye and corneal langerhans cells in systemic lupus erythematosus," *Journal of Ophthalmology*, vol. 2015, Article ID 543835, 8 pages, 2015.

[47] C. B. D. Adan, V. F. M. Trevisani, M. Vasconcellos, D. de Freitas, L. B. de Souza, and M. Mannis, "Bilateral deep keratitis caused by systemic lupus erythematosus," *Cornea*, vol. 23, no. 2, pp. 207–209, 2004.

[48] O. Halmay and K. Ludwig, "Bilateral band-shaped deep keratitis and iridocyclitis in systemic lupus erythematosus," *British Journal of Ophthalmology*, vol. 48, no. 10, pp. 558–562, 1964.

[49] J. A. Reeves, "Keratopathy associated with systemic lupus erythematosus," *Archives of ophthalmology*, vol. 74, pp. 159–160, 1965.

[50] L. Marsovszky, J. Németh, M. D. Resch et al., "Corneal Langerhans cell and dry eye examinations in ankylosing spondylitis," *Innate Immunity*, vol. 20, no. 5, pp. 471–477, 2013.

[51] A. van Tubergen, P. M. Black, and G. Coteur, "Are patient-reported outcome instruments for ankylosing spondylitis fit for purpose for the axial spondyloarthritis patient? A qualitative and psychometric analysis," *Rheumatology*, vol. 54, no. 10, pp. 1842–1851, 2015.

[52] M. A. Khan, M. Haroon, and J. T. Rosenbaum, "Acute anterior uveitis and spondyloarthritis: more than meets the eye," *Current Rheumatology Reports*, vol. 17, article 59, 2015.

[53] L. Marsovszky, M. D. Resch, J. Németh et al., "In vivo confocal microscopic evaluation of corneal Langerhans cell density, and distribution and evaluation of dry eye in rheumatoid arthritis," *Innate Immunity*, vol. 19, no. 4, pp. 348–354, 2013.

[54] A. Mohsenin and J. J. Huang, "Ocular manifestations of systemic inflammatory diseases," *Connecticut Medicine*, vol. 76, no. 9, pp. 533–544, 2012.

[55] E. Villani, S. Beretta, M. De Capitani, D. Galimberti, F. Viola, and R. Ratiglia, "In vivo confocal microscopy of meibomian glands in Sjögren's syndrome," *Investigative Ophthalmology & Visual Science*, vol. 52, no. 2, pp. 933–939, 2011.

[56] J. Hong, W. Zhu, H. Zhuang et al., "In vivo confocal microscopy of conjunctival goblet cells in patients with Sjögren's syndrome dry eye," *British Journal of Ophthalmology*, vol. 94, no. 11, pp. 1454–1458, 2010.

[57] N. Samiy, "Ocular features of Fabry disease: diagnosis of a treatable life-threatening disorder," *Survey of Ophthalmology*, vol. 53, no. 4, pp. 416–423, 2008.

[58] J. Wasielica-Poslednik, N. Pfeiffer, J. Reinke, and S. Pitz, "Confocal laser-scanning microscopy allows differentiation between Fabry disease and amiodarone-induced keratopathy," *Graefe's Archive for Clinical and Experimental Ophthalmology*, vol. 249, no. 11, pp. 1689–1696, 2011.

[59] T. J. C. Phillips, M. Brown, J. D. Ramirez et al., "Sensory, psychological, and metabolic dysfunction in HIV-associated peripheral neuropathy: a cross-sectional deep profiling study," *Pain*, vol. 155, no. 9, pp. 1846–1860, 2014.

[60] M. Polydefkis, C. T. Yiannoutsos, B. A. Cohen et al., "Reduced intraepidermal nerve fiber density in HIV-associated sensory neuropathy," *Neurology*, vol. 58, no. 1, pp. 115–119, 2002.

[61] C. L. Cherry, S. L. Wesselingh, L. Lal, and J. C. McArthur, "Evaluation of a clinical screening tool for HIV-associated sensory neuropathies," *Neurology*, vol. 65, no. 11, pp. 1778–1781, 2005.

[62] J. L. Dorsey, L. M. Mangus, J. D. Oakley et al., "Loss of corneal sensory nerve fibers in SIV-infected macaques: an alternate approach to investigate HIV-induced PNS damage," *The American Journal of Pathology*, vol. 184, no. 6, pp. 1652–1659, 2014.

[63] C. Schneider, F. Bucher, C. Cursiefen, G. R. Fink, L. M. Heindl, and H. C. Lehmann, "Corneal confocal microscopy detects small fiber damage in chronic inflammatory demyelinating polyneuropathy (CIDP)," *Journal of the Peripheral Nervous System*, vol. 19, no. 4, pp. 322–327, 2014.

[64] A. A. Argyriou, A. P. Kyritsis, T. Makatsoris, and H. P. Kalofonos, "Chemotherapy-induced peripheral neuropathy in adults: a comprehensive update of the literature," *Cancer Management and Research*, vol. 6, no. 1, pp. 135–147, 2014.

[65] G. Ferrari, N. Nalassamy, H. Downs, R. Dana, and A. L. Oaklander, "Corneal innervation as a window to peripheral neuropathies," *Experimental Eye Research*, vol. 113, pp. 148–150, 2013.